Role of Hedgehog Signaling in Olfactory Epithelium Regeneration

by

Anna Shirazyan

A dissertation submitted in partial fulfillment
of the requirements for the degree of
Doctor of Philosophy
(Cell and Developmental Biology)
in the University of Michigan
2022

Doctoral Committee:

Professor Sunny Y. Wong, Chair
Associate Professor Benjamin L. Allen
Professor Andrzej A. Dlugosz
Associate Professor Bradley Goldstein
Professor Charlotte M. Mistretta

Anna Shirazyan

shiraza@umich.edu

ORCID iD: 0000-0001-5711-0487

Dedication

To my family.

Acknowledgements

I could not have completed this dissertation without the support of the following people.

First, I would like to thank my mentor Dr. Ben Allen. Thank you for always taking the time to meet with me one-on-one, for your positive support, and for your encouragement. I appreciate your enthusiasm every time I brought an exciting new piece of data and your advice whenever some experiments inevitably went wrong. I can attribute my scientific and professional growth to the way you teach all your students – to think critically about the data, to question everything, and expect the unexpected result. I also would like to thank all the current and past Allen lab members – Nicole Franks, Bridget Waas, Tyler Hoard, Haeyoung Park, and Hannah Schrader. Thank you all for always lending an ear whether its scientific advice or personal support. Special thanks to Nicole for maintaining the reporter alleles used in Chapter 2 of this dissertation. Another special thanks to Haeyoung who will take over as the resident olfactory expert in the lab and contributed to Chapter 2 of this dissertation. I would also like to thank my undergraduate students Melissa Kim, who validated some of the antibodies used in Chapter 2, and Justine Ra, for her help in maintaining my mouse colonies. I would like to thank past Allen lab members: Drs. Michael Scales and Martha Echevarria-Andino for your support throughout my PhD and being some of the first to train me in the lab as a rotation student. I would also like Dr. Ariell Joiner without whom this project would have never existed. Thank you, Ariell, for the foundational work you did on the olfactory epithelium!

I would also like to thank all my committee members. Thank you, Dr. Sunny Wong, for chairing my committee and your technical expertise and advice regarding the experiments in this dissertation. Thank you, Dr. Charlotte Mistretta, for introducing me to the chemosensory field, your expert technical advice, and your continued support for my professional development. Thank you, Dr. Andrzej Dlugosz, for providing many of the mouse models used in Chapter 2, your assistance in this project, and your support in my career endeavors. Lastly, thank you to Dr. Bradley Goldstein for taking the time to serve on my committee as an external member and your expertise in the field of olfactory regeneration, without which some experiments in Chapter 2 would not be possible.

Lastly, I would like to thank all my friends and family, in Michigan, in California, and importantly, in Armenia. I could not do it without all your love and support. Thank you!

Table of Contents

List of Tables

List of Figures

Abstract

The olfactory epithelium (OE) lines the nasal cavities and is responsible for smell (odorant) sensation. Specialized neurons called olfactory sensory neurons (OSNs) bind to odorant molecules and transduce the smell signal to brain circuits for olfactory perception. Due to the constant contact of the OE with the air, which contains environmental stressors and pathogens, the cells of the OE must be constantly replenished. This makes the OE one of the few sites of adult neurogenesis. Two presumed stem cell populations can proliferate and differentiate into OE cells – the mitotically active globose basal cells (GBCs) and relatively quiescent horizontal basal cells (HBCs). The signaling pathways that coordinate stem cell mediated turnover, homeostasis, and regeneration of the OE remain understudied.

The Hedgehog (HH) signaling pathway is an attractive candidate for study in the context of OE regeneration. Previous work from our lab demonstrated that HBCs have functional primary cilia that are necessary for HBC-mediated regeneration of the OE. Importantly, primary cilia are also necessary for proper HH signaling and processing of downstream HH transcription factors called GLIs. Therefore, we hypothesized that GLI transcription factors could be functioning in the OE. In this dissertation I investigate 1) the expression of GLI transcription factors in the OE, 2) the consequence of driving GLI activator in HBCs, and 3) the consequence of depletion of GLIs in HBCs on OE regeneration.

Furthermore, I describe a novel role for HH transcription factors GLI2 and GLI3 in OE regeneration. Specifically, I demonstrate that driving overactive GLI2 in HBCs results in

aberrant cell identity and loss of OSN lineages following injury. Additionally, I show that loss of both GLI2 and GLI3 in HBCs results in defects in OE regeneration following injury. My data suggest that proper levels of both GLI2 and GLI3 in HBCs are necessary for the OE to be able to recover from acute injury. My work can be a springboard for future studies in HH signaling in the OE and further expand our understanding of this unique, neuroregenerative epithelium.

Chapter 1 The Olfactory Epithelium and Hedgehog Signaling

1.1 Abstract

The olfactory epithelium (OE) is a unique regenerative neuroepithelium that is necessary for olfaction, the sensation and perception of smell. It is one of the few tissues that undergoes continual neurogenesis throughout the lifespan of an organism. Ongoing neurogenesis is necessary due to constant contact of the OE with air, which contains environmental toxins, chemical agents, and pathogenic particles. These stressors can result in death of post-mitotic olfactory sensory neurons (OSNs). Fortuitously, two presumed stem cell populations, globose basal cells (GBCs) and horizontal basal cells (HBCs), can proliferate and differentiate into OSNs in the OE. Although previous work has examined how GBCs and HBCs function to replenish the OE, the signaling pathways that govern HBC-specific regeneration of the OE remain understudied.

Hedgehog (HH) signaling is an important evolutionarily conserved signaling pathway necessary for early developmental patterning and organogenesis. HH signaling is also important in the maintenance and regeneration of multiple epithelial tissues, including lingual epithelia, skin, and respiratory epithelia. Notably, HH signaling relies on the primary cilium, a microtubule-based signaling organelle, for proper signal transduction. Previous collaborative work from our lab demonstrated that HBCs assemble primary cilia and that abrogation of primary cilia formation in HBCs results in defective OE regeneration. This study makes the HH pathway an attractive candidate for study in HBC-mediated OE regeneration.

In this chapter I will discuss the olfactory epithelium and how it functions, with a specific focus on HBC-mediated OE regeneration. I will also summarize the mechanisms of HH signaling, with an emphasis on GLI proteins, the transcriptional effectors of the HH pathway. Further, I will provide an overview of HH signaling in regenerative epithelia, with a focus on the the skin, respiratory epithelium, and lingual epithelium. Finally, I will discuss the rationale for examining potential roles for HH signaling in the context of HBC-mediated OE regeneration.

1.2 Olfaction – An Ancient and Evolutionarily Conserved Sense

1.2.1 Evolution of Olfaction

The chemical senses are the oldest, most evolutionarily conserved senses amongst all animals (Hoover, 2010; Young et al., 2002). These senses are taste, smell, and chemistheses (touch and pain). Our sense of smell is especially key to our survival and function. Early vertebrates relied on smell to find a food source that was unspoiled or attract mates with pheromones (Hoover, 2010). Similarly, smell signaled danger, whether it was a toxicant, a scent of a predator, or smoke from a nearby fire (Hoover, 2010). Prior to our evolution to land-dwelling animals, our aquatic ancient ancestors were able to detect water soluble odorants. Fishes, amphibians, and mammals all share ancestral olfactory genes though fish retain the most (Hoover, 2010).

Mammals, unlike fish, detect smells through odorant molecules that are present in the air using their nose (Shepherd, 2004). The nose contains specialized structures called turbinates which help move odorant molecules into the nasal cavity (Shepherd, 2004). As humans developed as a species, so did our sense of smell. Our eyes moved to the center of the face and as a result our noses decreased in size and scope (Sarafoleanu et al., 2009; Shepherd, 2004). Interestingly, the number of functional human olfactory receptor (OR) genes also decreased. In fact, compared to mice which have 1,100 functional OR genes out of 1,300-1,500 total, humans have approximately 350 functional OR genes out of 1,000 total (Mombaerts, 2004; Nei et al., 2008). Despite this evolutionary decrease in ORs, humans are still able to discern complex odors due to higher brain processing (Sarafoleanu *et al.*, 2009). Our ability to smell is essential not only for proper olfaction, but also for flavor perception when we eat. Our quality of life depends on this chemical sense that we often take for granted. In the following sections, I will highlight

how the olfactory system functions, how it is maintained, how it can be impaired, and what the current gaps in knowledge are in olfactory regeneration.

1.2.2 The Olfactory Epithelium

The olfactory epithelium (OE) resides at the turbinates of the nose and is responsible for perception of odorant molecules (Graziadei, 1973). The OE is a pseudostratified neuroepithelium with several distinct cell types (Figure 1.1). The olfactory sensory neurons (OSNs) are the most abundant cell type in the OE (Kawagishi et al., 2014; Moran et al., 1982b) (Figure 1.1). Mature OSNs (mOSNs) are responsible for transducing odorant signals and transmission to the olfactory bulb (OB) (DeMaria and Ngai, 2010). They are bipolar neurons that project a single dendrite into the nasal cavity and a single axon to the OB (DeMaria and Ngai, 2010). Due to continuous contact with the air, OSNs are constantly exposed to environmental toxins and pathogens (Graziadei and Graziadei, 1979). In the event of bacterial or viral infection, supporting glial-like cells known as sustentacular cells (Sus) have enzymes that can break up these pathogens (Chen et al., 1992) (Figure 1.1). If either Sus cells or OSNs die, two presumed stem cell populations known as the Horizontal Basal Cells (HBCs) and Globose Basal Cells (GBCs) can differentiate and replenish the OE (Schwob et al., 2017) (Figure 1.1). GBCs are more proliferative and contribute to daily maintenance of the OE (Schwob *et al.*, 2017). Opposingly, HBCs are more quiescent and divide only in the presence of severe injury to the OE (Schwob *et al.*, 2017). In the following sub sections I will describe in detail the cell types in the OE and their individual roles in transducing and maintaining olfaction.

OSNs

OSNs are the most abundant cell type in the adult mammalian OE, with approximately 5.2 million OSNs present in the mouse OE (Kawagishi *et al.*, 2014) and 6 million in the human

OE (Moran *et al.*, 1982b). OSNs are the primary transducers of olfactory signals to the brain. The dendrites of OSNs project from the cell body to the nasal cavity. At the tip of each dendrite is a knob that projects approximately 20-35 non-motile cilia into the nasal cavity (McClintock et al., 2020). These cilia have a 9 + 2 microtubule structure but are non-motile due to the lack of dynein arms necessary for movement, making OSNs an attractive cell type for study of ciliary dynamics (Menco, 1984). Recent studies indicate the lengths of these cilia vary from 2 to 100 µm, making them longer than most primary cilia in the brain (Williams et al., 2014). The multiciliated nature of OSNs makes them uniquely primed for their purpose: odorant reception, smell transduction and transmission to the OB.

Olfactory receptors (ORs) are enriched at the primary cilia of OSNs. Fascinatingly, OSNs express only one OR gene per neuron, and further only one OR allele per OSN (Chess et al., 1994; Malnic et al., 1999). Of even greater interest, the axons of OSNs expressing the same ORs converge also at the same glomerulus at the OB (Mombaerts et al., 1996). Upon binding of an odorant molecule to an OR, a signaling cascade is initiated, leading to the depolarization of the OSN membrane and change in action potential, eventually resulting in release of neurotransmitters at the synaptic terminal in the OB (DeMaria and Ngai, 2010).

Sus Cells, MVCs, and Bowman's Glands

Sustentacular (Sus) cells are the supporting glial-like cells in the OE. Apically, Sus cells project microvilli into the air cavity, and basally they contact the basal lamina with structures known as endfeet (Doyle et al., 2001). Sus cells are identifiable with cytokeratin 18 staining in the cytoplasm (Holbrook et al., 2011). Apical expression of transcription factor SOX2 identifies nuclei of Sus cells (Guo et al., 2010). Sus cells express cytochromes P450 (Chen *et al.*, 1992; Ding et al., 1991), enzymes that metabolize xenobiotic compounds, making Sus cells some of the

first cells to respond to respiratory infections (McDonnell and Dang, 2013). Sus cells also provide structural support and enwrap OSNs and their dendritic knobs that project into the air cavity (Liang, 2020). In addition to Sus cells, there are other supporting-cell types known as microvillar cells (MVCs) and the Bowman's Gland (BG). Microvillar cells are a heterogeneous cell type and thought to function in regeneration (Asan and Drenckhahn, 2005; Jia et al., 2013; Moran et al., 1982a). Bowman's glands span the OE and rest in the lamina propria (Moran *et al.*, 1982b). They secrete mucus and their acinar and duct cells secrete xenobiotic compounds. Cells of the Bowman's glands can be labelled with SOX9 staining (Holbrook *et al.*, 2011).

GBCs

Globose Basal Cells (GBCs) are a rapidly dividing stem cell population in the OE. They regularly proliferate and differentiate to replenish all cell types in the OE (Graziadei, 1973; Graziadei and Graziadei, 1979). GBCs are a heterogenous cell type, expressing various transcription factors that indicate their lineage potential (Schwob *et al.*, 2017). Notably, GBCs ubiquitously express SEC8 which will be used in later chapters to identify GBCs (Joiner et al., 2015). GBCs have the potential to differentiate either into neuronal or non-neuronal lineages, or self-renew (Schwob *et al.*, 2017). Several studies have described PAX6- and SOX2-expressing GBCs as being the earliest in the differentiation cascade and thus with the most pluripotency (Guo *et al.*, 2010; Li et al., 2022; Lin et al., 2017). For GBCs to differentiate into neurons there is downregulation of PAX6 and SOX2, and upregulation of *Ascl1*/MASH1that specifies GBCs to a neuronal cell fate (Cau et al., 1997; Gordon et al., 1995). Neuronal differentiating GBCs then completely downregulate PAX6/SOX2, and upregulate expression of Neurog1 and NeuroD1, which cements their differentiation into OSNs (Cau et al., 2002) (Manglapus et al., 2004). The

rapidly dividing nature of GBCs allows for constant replenishment of OSNs that may die due to age or environmental influences (Huard and Schwob, 1995).

HBCs

Horizontal basal cells (HBCs) are a quiescent, mitotically inactive stem cell population in the OE (Carter et al., 2004; Holbrook et al., 1995). Unlike GBCs, HBCs are thought to be homogenous and identifiable by positive cytokeratin 5 and 14, ICAM-1/CD54, and NP63 staining (Schwob *et al.*, 2017). HBCs adhere to the basal lamina of the OE and are established late in mouse OE development (Packard et al., 2011). HBC proliferation is directed by NP63, where NP63 maintains the quiescence of HBCs and is transiently downregulated when HBCs are active (Packard *et al.*, 2011). Additionally, genetic ablation of NP63 from HBCs has resulted in spontaneous differentiation of HBCs into OE cell types (Fletcher et al., 2011). Other signaling pathways such as Notch have been implicated in HBCs which will be discussed in later sections (Herrick et al., 2018; Herrick et al., 2017). Since HBCs are a quiescent stem cell population, most informative studies use various OE lesion models in order to activate HBCs and examine their effects on the OE (Iwai et al., 2008; Leung et al., 2007). In the following section, I will highlight how the OE regenerates and what lesion models are used to study OE regeneration.

1.2.3 Regeneration of the Olfactory Epithelium

The OE undergoes continuous regeneration throughout the lifetime of an organism (Graziadei and Graziadei, 1979; Morrison and Costanzo, 1989). In homeostatic conditions, retroviral injections to the OE label only GBCs and OSNs, illustrating that GBCs mainly replenish OSNs as needed (Schwob et al., 1994) (Figure 1.2). To illustrate the regenerative capacities of the OE, many in the field utilize various lesion models that injure the OE and then examine the recovery of the OE post-injury (Figure 1.2). Several such models exist, the most

used being bulbectomies, surgical removal of one of the lobes of the olfactory bulb, and chemical lesions, such as exposure to methyl bromide gas or injection of methimazole(Schwob *et al.*, 2017) (Figure 1.2). Coupled with genetic lineage tracing methods, these studies helped define the stem cell populations of the OE and their roles in regeneration.

Removal of one of the olfactory bulbs (bulbectomy) results in severance of OSN axonal projections and OSN cell death in the OE (Costanzo and Graziadei, 1983). Following bulbectomy, retrovirally labelled GBCs were able to give rise to OSNs, but not HBCs or Sus cells since those remained uninjured (Caggiano et al., 1994). Further studies used more severe chemical lesion models that destroyed the majority of the OE– methyl bromide gas and methimazole (Brittebo, 1995; Hurtt et al., 1987). Chemical lesions also have the advantage of being temporary– most of the OE completely heals 8 weeks following injury (Schwob et al., 1995). Additional studies using methyl bromide lesions hinted at the existence HBCs and their ability to give rise to both OSNs and Sus cells (Schwob *et al.*, 1994).

Several lineage tracing studies using an HBC-specific *Cre* driver illustrated the contribution of HBCs to the OE (Iwai *et al.*, 2008; Leung *et al.*, 2007). HBCs were labelled using a tamoxifen inducible *Keratin5Cre*^{ER} and crossed with a BGAL lineage tracing allele and examined prior to and following injury (Iwai *et al.*, 2008; Leung *et al.*, 2007). Importantly, under homeostatic conditions there were little to no HBC-derived cells in the OE, confirming that HBCs are quiescent in the absence of injury (Iwai *et al.*, 2008; Leung *et al.*, 2007). These studies also demonstrated that methyl bromide or methimazole were both sufficient to drive high levels of HBC proliferation and differentiation, while bulbectomy was not (Leung *et al.*, 2007). Thus, many following studies used methimazole or methyl bromide to study the effects of HBCs on

OE regeneration. Furthering our understanding of OE regeneration can help further treatments for patients suffering from olfactory dysfunction.

Olfactory dysfunction can result in either complete (anosmia) or partial (hyposmia) loss of smell. Olfactory dysfunction can arise from physical injury, inflammation from infections, aging, exposure to chemicals, and medical procedures (Doty, 1979). Aging is one of the most common reasons for olfactory dysfunction, with increasing prevalence correlating with increase in age (Murphy et al., 2002). Importantly, prior respiratory infections also increase the risk of olfactory dysfunction in aged people (Murphy *et al.*, 2002). Aging in the rodent model has also shown a decrease in OSN number with an increase in age (Conley et al., 2003). Importantly, aging has also shown a decrease in HBC and GBC proliferation, suggesting that depletion of stem cells that can impair OE regeneration (Ducray et al., 2002). Understanding how the OE regenerates can help treat patients suffering from age-related OE dysfunction.

The OE utilizes various enzymes for breakdown of xenobiotic compounds in order to protect OSNs from cell death (Reed, 1993). However, sometimes these systems fail resulting in OSN death and loss of smell. In fact, upper respiratory infections can cause smell dysfunction (Potter et al., 2020). The recent onset of the COVID-19 pandemic has resulted in loss of smell in patients (Aziz et al., 2021). COVID-19 infects and destroys Sus cells, resulting in major damage to the OE in patients with anosmia (Butowt and von Bartheld, 2021). To more effectively treat OE disorders from infection we need to understand the signaling mechanisms governing regeneration.

1.2.4 Signaling Pathways in Olfactory Epithelium Regeneration

Several pathways of interest have been identified in the stem cells of the OE, and implicated in OE regeneration (Schwob *et al.*, 2017). One such pathway is Wnt signaling. LGR5,

a Wnt target gene that is present in stem cells, is expressed in GBCs in neonatal and adult OE (Chen et al., 2014). Additionally, LGR5+ GBCs contributed to all cell types following methimazole lesion (Chen *et al.*, 2014). Administration of Wnt signaling inhibitors also resulted in impaired OE regeneration following injury (Wang et al., 2011). While these studies demonstrated how Wnt functions in the OE *in vitro*, more rigorous *in vivo* studies are necessary to dissect how Wnt signaling drives GBC-mediated recovery of the OE in the context of regeneration.

Another pathway that has been examined in OE regeneration is Notch signaling. First discovered in *Drosophila*, Notch signaling was named after the distinct defects in neurogenesis of Notch mutants (Lehmann et al., 1983). Mammalian Notch ligands consist of Delta-like1, Delta-like2, Delta-like3, Jagged1, and Jagged2 (Lai, 2004). Through direct cell-cell interactions, these ligands bind to Notch receptors, Notch1-4 which contain epidermal growth factor (EGF) repeats (Rebay et al., 1991). Upon Notch receptor-ligand binding, the Notch receptor is proteolyzed and releases a soluble intracellular fragment of Notch (NICD) into the cytoplasm (Kopan et al., 1996; Schroeter et al., 1998; Struhl and Adachi, 1998). NICD cooperates with other cofactors such as mastermind-like molecule (MAML) and DNA binding proteins in the C-promoter binding factor (CSL) family of proteins (also known as RPB-J) (Jeffries et al., 2002; Kato et al., 1997; Tamura et al., 1995; Wu et al., 2002). The NICD-MAML-RPB-J complex translocates to the nucleus where RPB-J binds upstream of *Hes* promoters, the transcriptional effectors of the Notch signaling pathway (de la Pompa et al., 1997; Ohtsuka et al., 1999).

In the OE, genetic ablation of Notch2 results in death of Sus cells in post-natal OE (Rodriguez et al., 2008). Later studies further elucidated the expression of Notch signaling pathway components (Herrick *et al.*, 2017). Notch1, Notch2, and downstream Notch target Hes1

are all expressed in HBCs (Herrick *et al.*, 2017). Additional studies examined the genetic effect of overactive or inactive Notch signaling in the OE and consequences on regeneration (Herrick *et al.*, 2018). Overexpression of Notch1 intracellular domain resulted in HBCs giving rise to non-neuronal lineages following injury (Herrick *et al.*, 2018). Conversely, inactivation of Notch signaling in HBCs resulted in more neuronal lineages following injury (Herrick *et al.*, 2018). Taken together, these studies indicate Notch signaling can modulate the fate of HBCs following injury. It remains unclear what signals drive HBC-mediated regeneration of the OE and if they are solely Notch mediated.

Recent work from our lab demonstrated that HBCs have functional primary cilia, an organelle that is necessary for proper Hedgehog (HH) signal transduction (Joiner *et al.*, 2015). Importantly, abrogation of primary cilia in HBCs results in improper regeneration of the OE (Joiner *et al.*, 2015). HH signaling is an important early developmental pathway that has been proven to be necessary in many adult neural and regenerative tissues (Petrova and Joyner, 2014). Investigation of Hedgehog signaling in the OE could further elucidate what signals mediate OE regeneration. In the following section I will describe the Hedgehog signaling pathway in detail and how it pertains to adult tissue maintenance and regeneration.

1.3 Hedgehog Signaling in Adult Tissue Maintenance and Regeneration

The Hedgehog (HH) signaling pathway was initially described in a genetic screen of *Drosophila melanogaster* (fruit fly) larvae (Nusslein-Volhard and Wieschaus, 1980). The name "Hedgehog" was derived from the pattern of denticles spiking out of the HH mutant larvae, resembling a hedgehog (Nusslein-Volhard and Wieschaus, 1980). Additional HH pathway components were also discovered in Drosophila, such as the HH receptor *Patched*-1 (PTCH1) and the core signal transduction component *Smoothened* (SMO) (Alcedo et al., 1996; Nakano et

al., 1989). Since the initial discovery of HH in *Drosophila*, subsequent studies have shown that HH is conserved in different vertebrates (Echelard et al., 1993; Goodrich et al., 1996; Krauss et al., 1993; Riddle et al., 1993).

HH signaling has been studied extensively in the context of development and embryology. As our understanding of HH signaling furthered, many adult tissues were also shown to rely on HH signaling. Some such examples are the brain, the skin, the lung, and the tongue. In the following sections, I will highlight the mechanisms of HH signaling, focusing on HH transcription factors – the GLIs, and describe how adult tissues rely on HH signaling for their maintenance and regeneration.

1.3.1 Mechanisms of Canonical Hedgehog Signaling

Hedgehog refers to the gene encoding the ligand of the HH signaling pathway. The HH gene has three mammalian paralogues – *Sonic hedgehog* (SHH), *Indian hedgehog* (IHH), and *Desert hedgehog* (DHH) (Echelard *et al.*, 1993). The HH ligand is a secreted molecule, initially synthesized at 45kDa and then post-translationally modified to a 19kDa form (Briscoe and Therond, 2013). The modifications are as follows: cleavage of the C-terminal domain (Bumcrot et al., 1995), followed by covalent attachment of a cholesterol molecule to the C-terminus (Porter et al., 1996), and palmitoylation of the N-terminal domain (Chamoun et al., 2001). The secretion of HH ligand from HH-producing cells is mediated by the transmembrane protein Dispatched (DISP)(Burke et al., 1999) and the secreted protein Scube2 (Creanga et al., 2012). Secreted HH is essential for proper neural tube patterning and development in mammals (Dessaud et al., 2008).

Canonical HH signal transduction starts at the plasma membrane, where HH ligand binds to the twelve pass transmembrane protein Patched 1 (PTCH1), and in the absence of HH

signaling PTCH1 inhibits further downstream HH signal transduction (Chen and Struhl, 1996; Ingham et al., 1991; Marigo et al., 1996; Nakano *et al.*, 1989; Stone et al., 1996). This process can be mediated by several HH co-receptors, depending on the tissue and context. These are Growth arrest-specific gene 1 (GAS1) (Allen et al., 2007; Lee et al., 2001; Martinelli and Fan, 2007), Cell Adhesion Associated, Oncogene Regulated (CDON) (Tenzen et al., 2006), and Brother of CDON (BOC)(Tenzen *et al.*, 2006). Upon binding of HH to PTCH1, the PTCH1/HH complex is internalized and targeted for lysosomal degradation (Gallet and Therond, 2005). Degradation of this complex results in the removal of PTCH1 repression on Smoothened (SMO) (Chen and Struhl, 1996; Denef et al., 2000; Ingham et al., 2000) (Figure 1.3).

Following the removal of PTCH1 inhibition on SMO, SMO accumulates at the tip of the primary cilium (Corbit et al., 2005; Rohatgi et al., 2007). The primary cilium is a microtubule-based organelle that is essential for proper HH signaling (Huangfu et al., 2003). The primary cilium is also necessary for the processing of glioma associated oncogene (GLI) transcription factors, the downstream effectors of HH signaling (Haycraft et al., 2005; Liu et al., 2005) (Figure 1.3). In the following section I will detail this process and how GLIs are post-translationally modified in HH signaling.

1.3.2 Processing and Regulation of GLI Transcription Factors in HH Signaling

The GLI family of transcription factors are the primary effectors of downstream Hedgehog signaling in vertebrates and are evolutionarily conserved amongst many species (Wilson and Chuang, 2010). In *Drosophila*, the transcriptional transducer of HH signaling is known as Ci and structurally similar to the mammalian GLIs (Ingham et al., 2011). The GLI proteins in mammals are GLI1, GLI2, and GLI3. All GLIs share a Zinc-finger DNA-binding domain and bind to a specific sequence in the human genome (5'-GACCACCCA-3') (Kinzler et

al., 1988; Kinzler and Vogelstein, 1990). The three GLIs also share a C-terminal activator domain which is necessary for downstream HH signaling (Hui and Angers, 2011). GLI2 and GLI3 also contain an N-terminal repressor domain, which GLI1 lacks due to evolutionary divergence (Dai et al., 1999; Sasaki et al., 1999). GLI1 and GLI2 act primarily as an activator of HH signaling (GLI-A) while GLI3 acts primarily as a repressor (GLI-R) (Sasaki et al., 1997; Sasaki *et al.*, 1999). The GLI transcription factors are processed differently both in the absence and presence of HH ligand, detailed below.

In the absence of HH signaling, GLI1 is not expressed and thus unable to activate HH signaling (Bai et al., 2002). GLI2 and GLI3 are expressed but are post-translationally modified into a truncated repressor form (GLI-R) (Figure 1.4). This is accomplished by several biochemical processes. GLI2/GLI3 are bound in the cytoplasm by a kinesin-4 protein, KIF7, which is necessary for the proper processing of GLIs to repressor form (Cheung et al., 2009; Endoh-Yamagami et al., 2009; Liem et al., 2009). Additional binding to GLIs by Suppressor of fused homolog (SUFU) further facilitates the processing of GLI2 and GLI3 into repressors (Humke et al., 2010). Downstream of the GLI2 and GLI3 Zinc-finger binding domain are phosphorylation clusters containing conserved PKA, GSK3ß, and CK1 sites, which are phosphorylated in the absence of HH ligand (Pan et al., 2006; Wang et al., 2000; Wang and Li, 2006). This phosphorylation leads to ubiquitination of GLI2 and subsequent degradation, though some fraction of cleaved GLI2R remains (Pan *et al.*, 2006). GLI3 phosphorylation leads to proteolytic cleavage of the C-terminal activator domain, resulting in a truncated repressor form of GLI3, GLI3R (Dai *et al.*, 1999; Wang *et al.*, 2000). Following this, GLI3R translocates to the nucleus and suppresses HH target gene expression (Humke *et al.*, 2010). GLIR is then able to

modify HH-specific enhancers through deacetylation of Histone H3K27, and thereby turning "off" HH target gene expression (Lex et al., 2020).

In the presence of HH ligand, GLIs are processed into full length transcriptional activators (GLI-A) (Pan *et al.*, 2006; Wang *et al.*, 2000) (Figure 1.4). This process, like the processing of GLI2 and GLI3 to repressors, is also dependent on primary cilia. Following the removal of PTCH1 inhibition on SMO, SMO translocates to the cilium where it accumulates (Corbit *et al.*, 2005; Rohatgi *et al.*, 2007). Deletion of an important ciliary transport protein IFT88 results in perturbed SMO translocation and GLI processing, resulting in distinct HH phenotypes (Haycraft *et al.*, 2005; Huangfu and Anderson, 2005; Huangfu *et al.*, 2003). Also necessary for the trafficking of GLIs to the cilium is KIF7, since loss of KIF7 impairs ciliary tip accumulation of GLI2 and GLI3 (Endoh-Yamagami *et al.*, 2009). GLIs are then trafficked out of the cilium where they are phosphorylated in the cytoplasm at distinct activating cites, thus becoming full length activators (GLI-A) (Humke *et al.*, 2010; Niewiadomski et al., 2014). Following phosphorylation, GLIs can translocate to the nucleus and turn on HH signaling target gene expression (Humke *et al.*, 2010; Niewiadomski *et al.*, 2014).

1.3.3 HH Signaling in Adult Neurogenesis

HH signaling has been shown to be essential for proper neural tube development. A morphogenic gradient of SHH from the notochord ventralizes the neural tube and specifies various cell fates during embryonic development (Dessaud *et al.*, 2008; Echelard *et al.*, 1993; Riddle *et al.*, 1993). Similarly, GLIs are also present in neural tube development and play important roles. *Gli1* is expressed in the ventral neural tube but is expendable since *Gli1*$^{-/-}$ mice are viable and have no observable neural tube patterning defects (Bai *et al.*, 2002; Hui et al., 1994; Park et al., 2000; Sasaki *et al.*, 1997). *Gli2* expression, unlike *Gli1*, is expressed

throughout the neural tube; *Gli2*$^{-/-}$ mice have neural tube patterning defects (Bai *et al.*, 2002; Ding et al., 1998; Matise et al., 1998; Sasaki *et al.*, 1997). *Gli3* is expressed is the dorsal neural tube, opposite to the SHH morphogenic gradient, and *Gli3*$^{-/-}$ animals also display neural tube patterning defects (Bai et al., 2004; Sasaki *et al.*, 1997). In addition to neural tube development, GLIs are also important for adult neurogenesis and homeostasis.

There are several sites of adult neurogenesis in the brain (Petrova and Joyner, 2014). In the mammalian brain there are two sources of new neurons – the subventricular zone (SVZ) of the lateral ventricles and the subgranular zone (SGZ) of the hippocampal dentate gyrus (Fuentealba et al., 2012). These sources are comprised of neural stem cells (NSCs), which rely on HH signaling to be established. Genetic deletion of *Shh*, *Smo*, or *Kif3a*, a component necessary for primary cilia, all result in depletion of NSC progenitors and defects in the olfactory bulb and dentate gyrus (Balordi and Fishell, 2007a; Han et al., 2008; Machold et al., 2003). These findings demonstrate that HH signaling is necessary for the establishment of regenerative cells in the brain.

HH signaling is also necessary for proper maintenance and neurogenesis at the SVZ and SGZ. Lineage tracing studies of *Gli1* expressing cells indicated that a subset of neural stem cells are able to self-renew and differentiate in the SVZ and SGZ (Ahn and Joyner, 2005). Pharmacological studies using either HH agonists or inhibitors demonstrated that HH signaling stimulates proliferation of NSC in the SVZ and SGZ (Lai et al., 2003; Machold *et al.*, 2003; Palma et al., 2005). Inhibition of the HH signaling pathway by genetic deletion of *Smo* in the NSCs of the SVZ resulted in reduced neurogenesis in the SVZ (Balordi and Fishell, 2007b; Petrova et al., 2013). Conversely, overactivation of the pathway using *Ptch1* deletion in NSCs promoted self-renewal in NSCs and proliferation (Ferent et al., 2014). Interestingly, deletion of

either *Gli2* or *Gli3* in the NSCs of the SVZ does not result in any significant phenotypes (Petrova *et al.*, 2013), though recent work suggests *Gli3* is necessary for NSC differentiation to OLIG2+ progenitors (Embalabala et al., 2022). Taken together, these studies indicate that HH signaling is necessary for adult neurogenesis and neural stem cells in the brain.

1.3.4 HH Signaling in Adult Tissue Regeneration and Homeostasis

HH signaling is important for maintenance of several adult tissues. Interestingly, HH signaling has been shown to be crucial for maintenance of several regenerative epithelia: the skin, the lung, and the tongue (Petrova and Joyner, 2014). In this section I will focus on epithelial tissues and how HH signaling plays important functions in epithelial tissue homeostasis and regeneration.

The Skin and Hair Follicles

HH signaling is necessary for hair follicle development and morphogenesis (Chiang et al., 1999; St-Jacques et al., 1998). The skin continues to regenerate in adulthood and relies on a stem cell niche for maintenance of hair follicles (Bickenbach and Mackenzie, 1984; Morris et al., 1986). Similar to the brain, HH signaling also helps maintain stem cell populations in the dermis as well. SHH ligand is present in the skin, specifically in the lower bulb of hair follicles during the anagen phase of growth (Oro and Higgins, 2003). HH downstream targets *Gli1* and *Ptch1* are more broadly expressed in the hair follicle (Oro and Higgins, 2003). Conditional *Shh* deletion from the stem cell niche resulted in defects in hair bulb proliferation (Hsu et al., 2014). HH signaling is also sufficient to drive new hair follicle growth in adult skin (Sun et al., 2020). Taken together, these data indicate that HH signaling is essential for the epidermal stem cell niche and hair growth.

Mutations in the HH signaling pathway are common in basal cell carcinoma (BCC) patients (Hahn et al., 1996; Johnson et al., 1996; Reifenberger et al., 1998). Overexpression of *Gli1* induced BCC tumors in frog embryos and tadpoles (Dahmane et al., 1997). The majority of BCC mutations are attributed to PTCH1 or SMO, resulting in cancerous growths (Teglund and Toftgard, 2010). Further work in rodents has elucidated the mechanisms of HH signaling in BCC. Overexpression of GLI2 led to BCCs in mice and upregulation of HH target genes in tumors (Grachtchouk et al., 2000). Additional work with mice overexpressing GLI2 demonstrated that HH signaling is required for BCC proliferation and growth (Hutchin et al., 2005). Studies using a truncated form of GLI2 lacking the N-terminal repressor domain (GLI2ΔN) indicated BCCs arise from hair follicle stem cells and require high HH activity (Grachtchouk et al., 2011). These studies all demonstrate that HH signaling must be properly regulated in order to prevent BCC formation.

The Lung Epithelium

The respiratory epithelium is in constant contact with the air, and thus has mechanisms for alveolar maintenance and regeneration (Mason and Williams, 1977). Injury of the respiratory epithelium resulted in upregulation of *Shh* and *Gli1* in club cells (Watkins et al., 2003). Mice containing $Gli1^{lacZ/+}$ allele had more *Gli1* fibroblasts in the airway following lung injury, indicating that HH signaling may play a role in the fibrotic response in the lung (Liu et al., 2013b). Further work indicated that SHH ligand is present in the airway and signals to the surrounding GLI1+ mesenchyme (Peng et al., 2015). Genetic ablation of SHH ligand resulted in proliferation of mesenchymal cells and increase in epithelial cells in the airway (Peng *et al.*, 2015). Additionally, genetic expansion of HH signaling in the lung mesenchyme results in

emphysema- a chronic obstructive pulmonary disease (Wang et al., 2018). These data indicated that HH signaling maintains quiescence in the lung.

The Lingual Epithelium

The lingual epithelium regenerates frequently in response to environmental and physical stressors (Hamamichi et al., 2006; Perea-Martinez et al., 2013). Taste buds, the organs necessary for the perception of taste, turn over and regenerate throughout an organism's lifespan (Beidler and Smallman, 1965; Farbman, 1980). HH signaling is important for taste bud formation and development, making it an attractive candidate for investigation in adult tongue (Hall et al., 2003; Liu et al., 2004; Mistretta et al., 2003).

In adult mice lineage tracing studies using a *Gli1* reporter illustrated that SHH-responding cells were present in the taste bud, and that SHH ligand is also present in proliferative stem cells (Liu et al., 2013a). Overstimulation of the HH signaling pathway using a constitutively active GLI2 transgene (GLI2ΔN) in K5+ resulted in loss of taste buds and disrupted taste bud morphology (Liu *et al.*, 2013a). Similar studies genetically disrupting GLI expression in the taste epithelium also resulted in taste bud loss but some phenotypes were reversed upon removal of inhibition (Ermilov et al., 2016). Conversely, overexpression of SHH ligand in taste bud basal cells resulted in ectopic taste bud formation (Miura et al., 2014). These data indicated that HH signaling carefully regulates taste organ maintenance in the tongue.

An important insight into HH signaling in the tongue came from patients taking vismodegib, a potent HH inhibitor used to treat BCC. Importantly, many patients reported severe loss of taste and loss of quality of life (Fife et al., 2017). This prompted further studies examining HH signaling in the tongue with pharmacologic approaches. Pharmacologic inhibition of the HH pathway using LDE225 (sonidegib) resulted in loss of taste buds and disrupted taste

bud morphology (Kumari et al., 2015). Measurements of chorda tympani nerve responses to taste stimuli were also disrupted in mice treated with LDE225 (Kumari *et al.*, 2015). Interestingly, taste buds eventually regain their ability to respond to taste stimuli following removal of LDE225 (Kumari et al., 2017). Both genetic and pharmacologic data in the tongue support that HH signaling is essential for taste bud maintenance, regeneration, and taste chemoreception.

1.3.5 Conclusion

Proper regeneration of the olfactory epithelium (OE) is necessary for our continued ability to smell throughout our lifetime. This is due to the constant exposure of olfactory sensory neurons (OSNs) with the air, where they can encounter environmental stressors such as viruses and bacteria. Our ability to smell impacts our enjoyment of food and ability to smell dangers, things we take for granted until they are no longer available to us. The recent onset of the COVID19 pandemic illustrated how loss of smell was impacting the quality of life of those with anosmia (Coelho et al., 2021). Understanding the signaling mechanisms governing OE regeneration can provide therapeutic targets for patients with anosmia.

The Hedgehog (HH) signaling pathway, as detailed above, has been extensively studied in regenerative epithelia. Importantly, studies in the tongue, another chemosensory organ, illustrated that HH signaling is necessary for taste sensation and maintenance of proliferating basal cells. HH signaling is also reliant on primary cilia, which are present in the HBCs of the OE. Importantly, HBCs lacking primary cilia are unable to properly regenerate the OE (Joiner *et al.*, 2015). As I described above, primary cilia are necessary for the proper processing of the GLI transcription factors. GLI2 and GLI3 are dependent on primary cilia in order to be processed into transcriptional activators or repressors of the HH signaling pathway. This makes the GLI transcription factors an attractive candidate of study in the OE, and specifically in HBCs. In

Chapter 2, I will describe the expression of GLIs in the OE in homeostatic and injured conditions. Additionally, I will demonstrate that GLI2 and GLI3 are necessary for proper HBC mediated regeneration of the OE. In Chapter 3 I will summarize my findings and propose potential future directions for this work. It is important to note that prior to this work the HH signaling pathway was unexplored in the OE. Overall, my findings describe a novel role for GLIs in the OE and open many possible future studies for HH signaling in the OE.

1.4 Figures

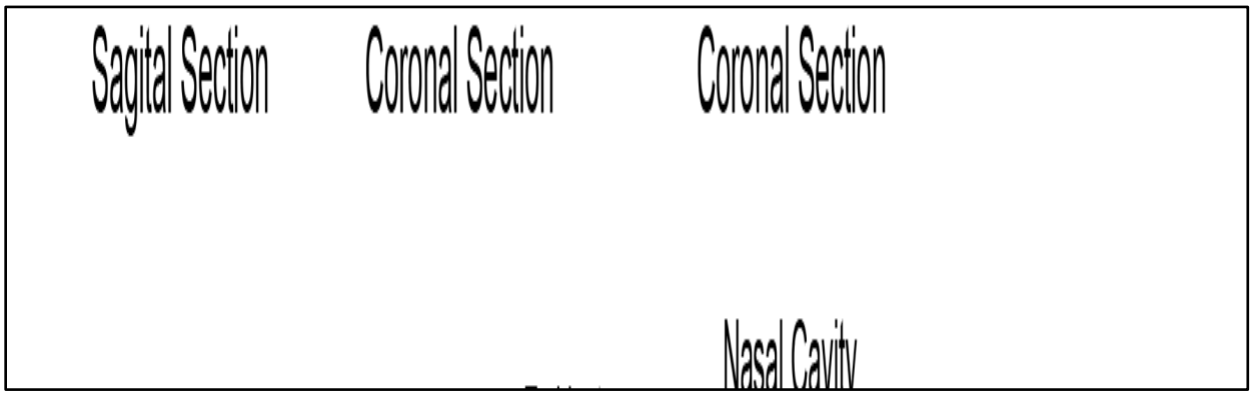

Figure 1.1 Cell Types of the Olfactory Epithelium

Schematic displaying a sagittal section through a rodent brain (far left), coronal section through the olfactory epithelium (middle), and cell types of the olfactory epithelium (far right). Cell types include microvillar cells (MVCs), sustentacular cells (Sus), mature olfactory sensory neurons (mOSNs), immature olfactory sensory neurons (iOSNs), globose basal cells (GBCs), and horizontal basal cells (HBCs).

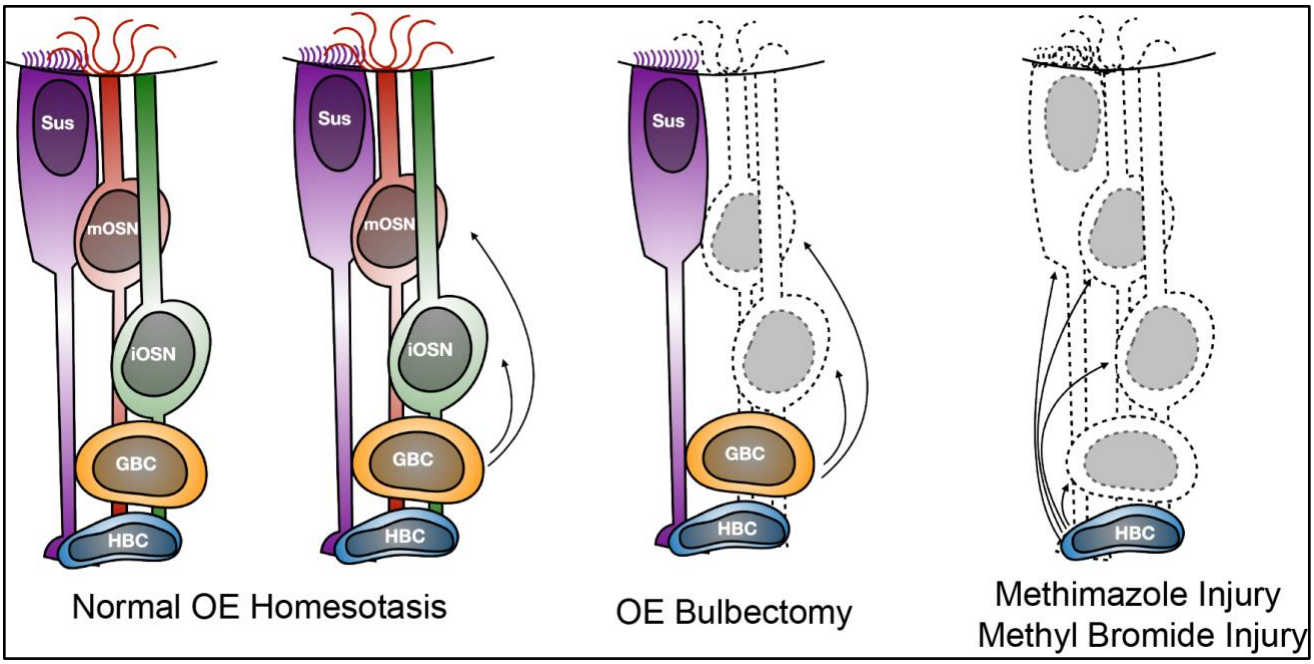

Figure 1.2 Lesion Models in the Olfactory Epithelium

Cartoon displaying normal OE homeostasis where primarily globose basal cells (GBCs) mediate recovery of olfactory sensory neurons (OSNs) (far left). Bulbectomy, removal of one of the olfactory bulbs, results in OSN cell death and primarily GBC-mediated recovery of the OE (middle).

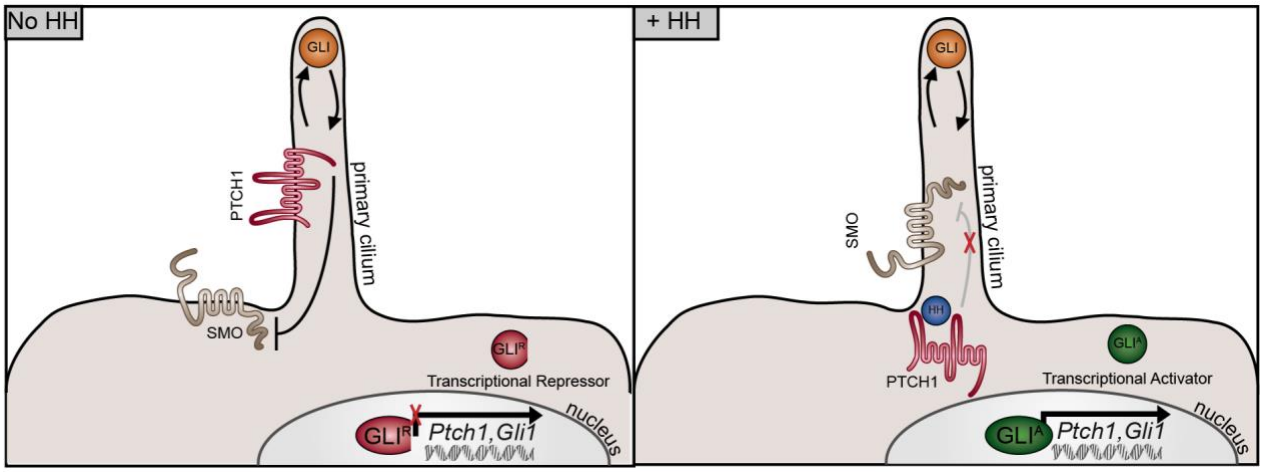

Figure 1.3 Schematic of Hedgehog Signaling

In the absence of HH ligand (No HH, left panel), PTCH1 inhibits SMO, SMO is unable to enter the primary cilium, and GLIs are processed into transcriptional repressors (GLI-R), causing repression of HH target genes *Ptch1*, *Gli1*. In the presence of HH ligand, HH binds to PTCH1 which is then internalized and degraded, removing inhibition of PTCH1 on SMO. SMO can then translocate to the cilium and accumulate at the tips along with full-length GLIs. GLIs are then processed to transcriptional activators (GLI-A), and translocate to the nucleus to turn on HH target genes *Ptch1*, *Gli1*.

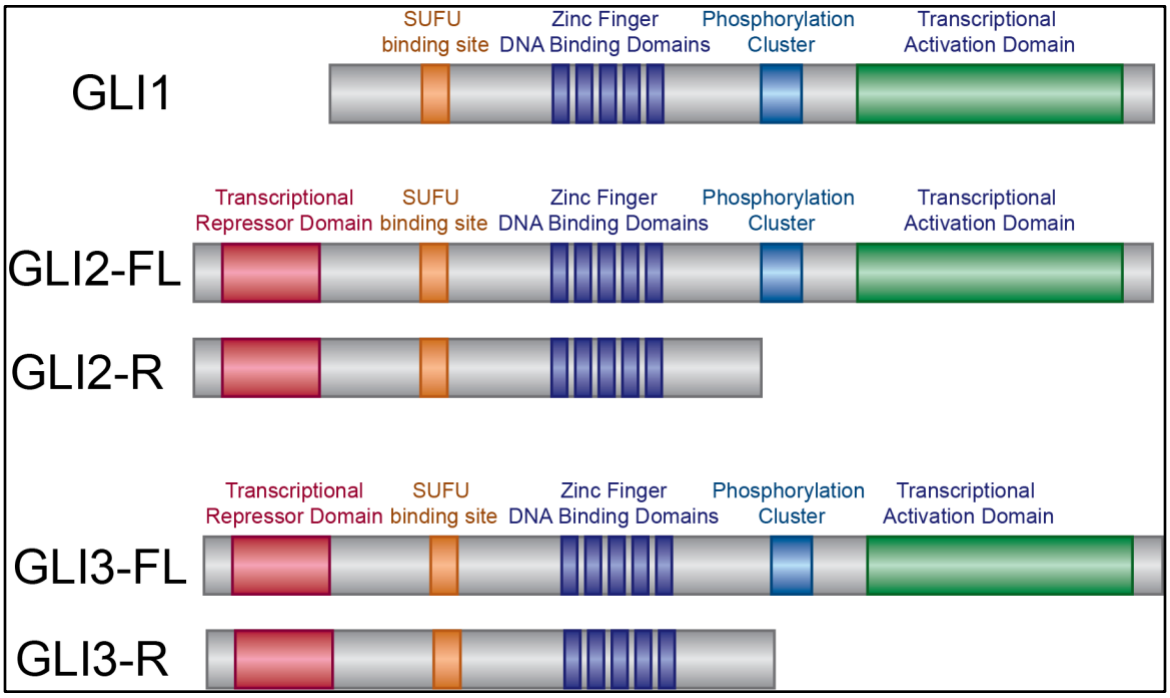

Figure 1.4 Schematics of GLI1-3 Transcription Factors

All GLIs contain a SUFU binding site, conserved zinc finger DNA binding domains, phosphorylation cluster, and a C-terminal transcriptional activation domain. GLI2 and GLI3 also contain an N-terminal repressor domain, which GLI1 does not have. GLI2 and GLI3 can also be post-translationally processed into truncated repressor forms following a proteolytic cleavage before the phosphorylation cluster.

1.5 References

Ahn, S., and Joyner, A.L. (2005). In vivo analysis of quiescent adult neural stem cells responding to Sonic hedgehog. Nature *437*, 894-897.

Alcedo, J., Ayzenzon, M., Von Ohlen, T., Noll, M., and Hooper, J.E. (1996). The Drosophila smoothened gene encodes a seven-pass membrane protein, a putative receptor for the hedgehog signal. Cell *86*, 221-232.

Allen, B.L., Tenzen, T., and McMahon, A.P. (2007). The Hedgehog-binding proteins Gas1 and Cdo cooperate to positively regulate Shh signaling during mouse development. Genes Dev *21*, 1244-1257.

Asan, E., and Drenckhahn, D. (2005). Immunocytochemical characterization of two types of microvillar cells in rodent olfactory epithelium. Histochem Cell Biol *123*, 157-168.

Aziz, M., Goyal, H., Haghbin, H., Lee-Smith, W.M., Gajendran, M., and Perisetti, A. (2021). The Association of "Loss of Smell" to COVID-19: A Systematic Review and Meta-Analysis. Am J Med Sci *361*, 216-225.

Bai, C.B., Auerbach, W., Lee, J.S., Stephen, D., and Joyner, A.L. (2002). Gli2, but not Gli1, is required for initial Shh signaling and ectopic activation of the Shh pathway. Development *129*, 4753-4761.

Bai, C.B., Stephen, D., and Joyner, A.L. (2004). All mouse ventral spinal cord patterning by hedgehog is Gli dependent and involves an activator function of Gli3. Dev Cell *6*, 103-115.

Balordi, F., and Fishell, G. (2007a). Hedgehog signaling in the subventricular zone is required for both the maintenance of stem cells and the migration of newborn neurons. J Neurosci *27*, 5936-5947.

Balordi, F., and Fishell, G. (2007b). Mosaic removal of hedgehog signaling in the adult SVZ reveals that the residual wild-type stem cells have a limited capacity for self-renewal. J Neurosci *27*, 14248-14259.

Beidler, L.M., and Smallman, R.L. (1965). Renewal of cells within taste buds. J Cell Biol *27*, 263-272.

Bickenbach, J.R., and Mackenzie, I.C. (1984). Identification and localization of label-retaining cells in hamster epithelia. J Invest Dermatol *82*, 618-622.

Briscoe, J., and Therond, P.P. (2013). The mechanisms of Hedgehog signalling and its roles in development and disease. Nat Rev Mol Cell Biol *14*, 416-429.

Brittebo, E.B. (1995). Metabolism-dependent toxicity of methimazole in the olfactory nasal mucosa. Pharmacol Toxicol *76*, 76-79.

Brownell, I., Guevara, E., Bai, C.B., Loomis, C.A., and Joyner, A.L. (2011). Nerve-derived sonic hedgehog defines a niche for hair follicle stem cells capable of becoming epidermal stem cells. Cell Stem Cell *8*, 552-565.

Bumcrot, D.A., Takada, R., and McMahon, A.P. (1995). Proteolytic processing yields two secreted forms of sonic hedgehog. Mol Cell Biol *15*, 2294-2303.

Burke, R., Nellen, D., Bellotto, M., Hafen, E., Senti, K.A., Dickson, B.J., and Basler, K. (1999). Dispatched, a novel sterol-sensing domain protein dedicated to the release of cholesterol-modified hedgehog from signaling cells. Cell *99*, 803-815.

Butowt, R., and von Bartheld, C.S. (2021). Anosmia in COVID-19: Underlying Mechanisms and Assessment of an Olfactory Route to Brain Infection. Neuroscientist *27*, 582-603.

Caggiano, M., Kauer, J.S., and Hunter, D.D. (1994). Globose basal cells are neuronal progenitors in the olfactory epithelium: a lineage analysis using a replication-incompetent retrovirus. Neuron *13*, 339-352.

Carter, L.A., MacDonald, J.L., and Roskams, A.J. (2004). Olfactory horizontal basal cells demonstrate a conserved multipotent progenitor phenotype. J Neurosci *24*, 5670-5683.

Cau, E., Casarosa, S., and Guillemot, F. (2002). Mash1 and Ngn1 control distinct steps of determination and differentiation in the olfactory sensory neuron lineage. Development *129*, 1871-1880.

Cau, E., Gradwohl, G., Fode, C., and Guillemot, F. (1997). Mash1 activates a cascade of bHLH regulators in olfactory neuron progenitors. Development *124*, 1611-1621.

Chamoun, Z., Mann, R.K., Nellen, D., von Kessler, D.P., Bellotto, M., Beachy, P.A., and Basler, K. (2001). Skinny hedgehog, an acyltransferase required for palmitoylation and activity of the hedgehog signal. Science *293*, 2080-2084.

Chen, M., Tian, S., Yang, X., Lane, A.P., Reed, R.R., and Liu, H. (2014). Wnt-responsive Lgr5(+) globose basal cells function as multipotent olfactory epithelium progenitor cells. J Neurosci *34*, 8268-8276.

Chen, Y., Getchell, M.L., Ding, X., and Getchell, T.V. (1992). Immunolocalization of two cytochrome P450 isozymes in rat nasal chemosensory tissue. Neuroreport *3*, 749-752.

Chen, Y., and Struhl, G. (1996). Dual roles for patched in sequestering and transducing Hedgehog. Cell *87*, 553-563.

Chess, A., Simon, I., Cedar, H., and Axel, R. (1994). Allelic inactivation regulates olfactory receptor gene expression. Cell *78*, 823-834.

Cheung, H.O., Zhang, X., Ribeiro, A., Mo, R., Makino, S., Puviindran, V., Law, K.K., Briscoe, J., and Hui, C.C. (2009). The kinesin protein Kif7 is a critical regulator of Gli transcription factors in mammalian hedgehog signaling. Sci Signal *2*, ra29.

Chiang, C., Swan, R.Z., Grachtchouk, M., Bolinger, M., Litingtung, Y., Robertson, E.K., Cooper, M.K., Gaffield, W., Westphal, H., Beachy, P.A., and Dlugosz, A.A. (1999). Essential role for Sonic hedgehog during hair follicle morphogenesis. Dev Biol *205*, 1-9.

Coelho, D.H., Reiter, E.R., Budd, S.G., Shin, Y., Kons, Z.A., and Costanzo, R.M. (2021). Quality of life and safety impact of COVID-19 associated smell and taste disturbances. Am J Otolaryngol *42*, 103001.

Conley, D.B., Robinson, A.M., Shinners, M.J., and Kern, R.C. (2003). Age-related olfactory dysfunction: cellular and molecular characterization in the rat. Am J Rhinol *17*, 169-175.

Corbit, K.C., Aanstad, P., Singla, V., Norman, A.R., Stainier, D.Y., and Reiter, J.F. (2005). Vertebrate Smoothened functions at the primary cilium. Nature *437*, 1018-1021.

Costanzo, R.M., and Graziadei, P.P. (1983). A quantitative analysis of changes in the olfactory epithelium following bulbectomy in hamster. J Comp Neurol *215*, 370-381.

Creanga, A., Glenn, T.D., Mann, R.K., Saunders, A.M., Talbot, W.S., and Beachy, P.A. (2012). Scube/You activity mediates release of dually lipid-modified Hedgehog signal in soluble form. Genes Dev *26*, 1312-1325.

Dahmane, N., Lee, J., Robins, P., Heller, P., and Ruiz i Altaba, A. (1997). Activation of the transcription factor Gli1 and the Sonic hedgehog signalling pathway in skin tumours. Nature *389*, 876-881.

Dai, P., Akimaru, H., Tanaka, Y., Maekawa, T., Nakafuku, M., and Ishii, S. (1999). Sonic Hedgehog-induced activation of the Gli1 promoter is mediated by GLI3. J Biol Chem *274*, 8143-8152.

de la Pompa, J.L., Wakeham, A., Correia, K.M., Samper, E., Brown, S., Aguilera, R.J., Nakano, T., Honjo, T., Mak, T.W., Rossant, J., and Conlon, R.A. (1997). Conservation of the Notch signalling pathway in mammalian neurogenesis. Development *124*, 1139-1148.

DeMaria, S., and Ngai, J. (2010). The cell biology of smell. J Cell Biol *191*, 443-452.

Denef, N., Neubuser, D., Perez, L., and Cohen, S.M. (2000). Hedgehog induces opposite changes in turnover and subcellular localization of patched and smoothened. Cell *102*, 521-531.

Dessaud, E., McMahon, A.P., and Briscoe, J. (2008). Pattern formation in the vertebrate neural tube: a sonic hedgehog morphogen-regulated transcriptional network. Development *135*, 2489-2503.

Ding, Q., Motoyama, J., Gasca, S., Mo, R., Sasaki, H., Rossant, J., and Hui, C.C. (1998). Diminished Sonic hedgehog signaling and lack of floor plate differentiation in Gli2 mutant mice. Development *125*, 2533-2543.

Ding, X.X., Porter, T.D., Peng, H.M., and Coon, M.J. (1991). cDNA and derived amino acid sequence of rabbit nasal cytochrome P450NMb (P450IIG1), a unique isozyme possibly involved in olfaction. Arch Biochem Biophys *285*, 120-125.

Doty, R.L. (1979). A review of olfactory dysfunctions in man. Am J Otolaryngol *1*, 57-79.

Doyle, K.L., Khan, M., and Cunningham, A.M. (2001). Expression of the intermediate filament protein nestin by sustentacular cells in mature olfactory neuroepithelium. J Comp Neurol *437*, 186-195.

Ducray, A., Bondier, J.R., Michel, G., Bon, K., Millot, J.L., Propper, A., and Kastner, A. (2002). Recovery following peripheral destruction of olfactory neurons in young and adult mice. Eur J Neurosci *15*, 1907-1917.

Echelard, Y., Epstein, D.J., St-Jacques, B., Shen, L., Mohler, J., McMahon, J.A., and McMahon, A.P. (1993). Sonic hedgehog, a member of a family of putative signaling molecules, is implicated in the regulation of CNS polarity. Cell *75*, 1417-1430.

Embalabala, R.J., Brockman, A.A., Jurewicz, A.R., Kong, J.A., Ryan, K., Guinto, C.D., Alvarez-Buylla, A., Chiang, C., and Ihrie, R.A. (2022). GLI3 Is Required for OLIG2+ Progeny Production in Adult Dorsal Neural Stem Cells. Cells *11*.

Endoh-Yamagami, S., Evangelista, M., Wilson, D., Wen, X., Theunissen, J.W., Phamluong, K., Davis, M., Scales, S.J., Solloway, M.J., de Sauvage, F.J., and Peterson, A.S. (2009). The mammalian Cos2 homolog Kif7 plays an essential role in modulating Hh signal transduction during development. Curr Biol *19*, 1320-1326.

Ermilov, A.N., Kumari, A., Li, L., Joiner, A.M., Grachtchouk, M.A., Allen, B.L., Dlugosz, A.A., and Mistretta, C.M. (2016). Maintenance of Taste Organs Is Strictly Dependent on Epithelial Hedgehog/GLI Signaling. PLoS Genet *12*, e1006442.

Farbman, A.I. (1980). Renewal of taste bud cells in rat circumvallate papillae. Cell Tissue Kinet *13*, 349-357.

Ferent, J., Cochard, L., Faure, H., Taddei, M., Hahn, H., Ruat, M., and Traiffort, E. (2014). Genetic activation of Hedgehog signaling unbalances the rate of neural stem cell renewal by increasing symmetric divisions. Stem Cell Reports *3*, 312-323.

Fife, K., Herd, R., Lalondrelle, S., Plummer, R., Strong, A., Jones, S., and Lear, J.T. (2017). Managing adverse events associated with vismodegib in the treatment of basal cell carcinoma. Future Oncol *13*, 175-184.

Fletcher, R.B., Prasol, M.S., Estrada, J., Baudhuin, A., Vranizan, K., Choi, Y.G., and Ngai, J. (2011). p63 regulates olfactory stem cell self-renewal and differentiation. Neuron *72*, 748-759.

Fuentealba, L.C., Obernier, K., and Alvarez-Buylla, A. (2012). Adult neural stem cells bridge their niche. Cell Stem Cell *10*, 698-708.

Gallet, A., and Therond, P.P. (2005). Temporal modulation of the Hedgehog morphogen gradient by a patched-dependent targeting to lysosomal compartment. Dev Biol *277*, 51-62.

Goodrich, L.V., Johnson, R.L., Milenkovic, L., McMahon, J.A., and Scott, M.P. (1996). Conservation of the hedgehog/patched signaling pathway from flies to mice: induction of a mouse patched gene by Hedgehog. Genes Dev *10*, 301-312.

Gordon, M.K., Mumm, J.S., Davis, R.A., Holcomb, J.D., and Calof, A.L. (1995). Dynamics of MASH1 expression in vitro and in vivo suggest a non-stem cell site of MASH1 action in the olfactory receptor neuron lineage. Mol Cell Neurosci *6*, 363-379.

Grachtchouk, M., Mo, R., Yu, S., Zhang, X., Sasaki, H., Hui, C.C., and Dlugosz, A.A. (2000). Basal cell carcinomas in mice overexpressing Gli2 in skin. Nat Genet *24*, 216-217.

Grachtchouk, M., Pero, J., Yang, S.H., Ermilov, A.N., Michael, L.E., Wang, A., Wilbert, D., Patel, R.M., Ferris, J., Diener, J., et al. (2011). Basal cell carcinomas in mice arise from hair follicle stem cells and multiple epithelial progenitor populations. J Clin Invest *121*, 1768-1781.

Graziadei, P.P. (1973). Cell dynamics in the olfactory mucosa. Tissue Cell *5*, 113-131.

Graziadei, P.P., and Graziadei, G.A. (1979). Neurogenesis and neuron regeneration in the olfactory system of mammals. I. Morphological aspects of differentiation and structural organization of the olfactory sensory neurons. J Neurocytol *8*, 1-18.

Guo, Z., Packard, A., Krolewski, R.C., Harris, M.T., Manglapus, G.L., and Schwob, J.E. (2010). Expression of pax6 and sox2 in adult olfactory epithelium. J Comp Neurol *518*, 4395-4418.

Hahn, H., Wicking, C., Zaphiropoulous, P.G., Gailani, M.R., Shanley, S., Chidambaram, A., Vorechovsky, I., Holmberg, E., Unden, A.B., Gillies, S., et al. (1996). Mutations of the human homolog of Drosophila patched in the nevoid basal cell carcinoma syndrome. Cell *85*, 841-851.

Hall, J.M., Bell, M.L., and Finger, T.E. (2003). Disruption of sonic hedgehog signaling alters growth and patterning of lingual taste papillae. Dev Biol *255*, 263-277.

Hamamichi, R., Asano-Miyoshi, M., and Emori, Y. (2006). Taste bud contains both short-lived and long-lived cell populations. Neuroscience *141*, 2129-2138.

Han, Y.G., Spassky, N., Romaguera-Ros, M., Garcia-Verdugo, J.M., Aguilar, A., Schneider-Maunoury, S., and Alvarez-Buylla, A. (2008). Hedgehog signaling and primary cilia are required for the formation of adult neural stem cells. Nat Neurosci *11*, 277-284.

Haycraft, C.J., Banizs, B., Aydin-Son, Y., Zhang, Q., Michaud, E.J., and Yoder, B.K. (2005). Gli2 and Gli3 localize to cilia and require the intraflagellar transport protein polaris for processing and function. PLoS Genet *1*, e53.

Herrick, D.B., Guo, Z., Jang, W., Schnittke, N., and Schwob, J.E. (2018). Canonical Notch Signaling Directs the Fate of Differentiating Neurocompetent Progenitors in the Mammalian Olfactory Epithelium. J Neurosci *38*, 5022-5037.

Herrick, D.B., Lin, B., Peterson, J., Schnittke, N., and Schwob, J.E. (2017). Notch1 maintains dormancy of olfactory horizontal basal cells, a reserve neural stem cell. Proc Natl Acad Sci U S A *114*, E5589-E5598.

Holbrook, E.H., Szumowski, K.E., and Schwob, J.E. (1995). An immunochemical, ultrastructural, and developmental characterization of the horizontal basal cells of rat olfactory epithelium. J Comp Neurol *363*, 129-146.

Holbrook, E.H., Wu, E., Curry, W.T., Lin, D.T., and Schwob, J.E. (2011). Immunohistochemical characterization of human olfactory tissue. Laryngoscope *121*, 1687-1701.

Hoover, K.C. (2010). Smell with inspiration: the evolutionary significance of olfaction. Am J Phys Anthropol *143 Suppl 51*, 63-74.

Hsu, Y.C., Li, L., and Fuchs, E. (2014). Transit-amplifying cells orchestrate stem cell activity and tissue regeneration. Cell *157*, 935-949.

Huangfu, D., and Anderson, K.V. (2005). Cilia and Hedgehog responsiveness in the mouse. Proc Natl Acad Sci U S A *102*, 11325-11330.

Huangfu, D., Liu, A., Rakeman, A.S., Murcia, N.S., Niswander, L., and Anderson, K.V. (2003). Hedgehog signalling in the mouse requires intraflagellar transport proteins. Nature *426*, 83-87.

Huard, J.M., and Schwob, J.E. (1995). Cell cycle of globose basal cells in rat olfactory epithelium. Dev Dyn *203*, 17-26.

Hui, C.C., and Angers, S. (2011). Gli proteins in development and disease. Annu Rev Cell Dev Biol *27*, 513-537.

Hui, C.C., Slusarski, D., Platt, K.A., Holmgren, R., and Joyner, A.L. (1994). Expression of three mouse homologs of the Drosophila segment polarity gene cubitus interruptus, Gli, Gli-2, and Gli-3, in ectoderm- and mesoderm-derived tissues suggests multiple roles during postimplantation development. Dev Biol *162*, 402-413.

Humke, E.W., Dorn, K.V., Milenkovic, L., Scott, M.P., and Rohatgi, R. (2010). The output of Hedgehog signaling is controlled by the dynamic association between Suppressor of Fused and the Gli proteins. Genes Dev *24*, 670-682.

Hurtt, M.E., Morgan, K.T., and Working, P.K. (1987). Histopathology of acute toxic responses in selected tissues from rats exposed by inhalation to methyl bromide. Fundam Appl Toxicol *9*, 352-365.

Hutchin, M.E., Kariapper, M.S., Grachtchouk, M., Wang, A., Wei, L., Cummings, D., Liu, J., Michael, L.E., Glick, A., and Dlugosz, A.A. (2005). Sustained Hedgehog signaling is required for basal cell carcinoma proliferation and survival: conditional skin tumorigenesis recapitulates the hair growth cycle. Genes Dev *19*, 214-223.

Ingham, P.W., Nakano, Y., and Seger, C. (2011). Mechanisms and functions of Hedgehog signalling across the metazoa. Nat Rev Genet *12*, 393-406.

Ingham, P.W., Nystedt, S., Nakano, Y., Brown, W., Stark, D., van den Heuvel, M., and Taylor, A.M. (2000). Patched represses the Hedgehog signalling pathway by promoting modification of the Smoothened protein. Curr Biol *10*, 1315-1318.

Ingham, P.W., Taylor, A.M., and Nakano, Y. (1991). Role of the Drosophila patched gene in positional signalling. Nature *353*, 184-187.

Iwai, N., Zhou, Z., Roop, D.R., and Behringer, R.R. (2008). Horizontal basal cells are multipotent progenitors in normal and injured adult olfactory epithelium. Stem Cells *26*, 1298-1306.

Jeffries, S., Robbins, D.J., and Capobianco, A.J. (2002). Characterization of a high-molecular-weight Notch complex in the nucleus of Notch(ic)-transformed RKE cells and in a human T-cell leukemia cell line. Mol Cell Biol *22*, 3927-3941.

Jia, C., Hayoz, S., Hutch, C.R., Iqbal, T.R., Pooley, A.E., and Hegg, C.C. (2013). An IP3R3- and NPY-expressing microvillous cell mediates tissue homeostasis and regeneration in the mouse olfactory epithelium. PLoS One *8*, e58668.

Johnson, R.L., Rothman, A.L., Xie, J., Goodrich, L.V., Bare, J.W., Bonifas, J.M., Quinn, A.G., Myers, R.M., Cox, D.R., Epstein, E.H., Jr., and Scott, M.P. (1996). Human homolog of patched, a candidate gene for the basal cell nevus syndrome. Science *272*, 1668-1671.

Joiner, A.M., Green, W.W., McIntyre, J.C., Allen, B.L., Schwob, J.E., and Martens, J.R. (2015). Primary Cilia on Horizontal Basal Cells Regulate Regeneration of the Olfactory Epithelium. J Neurosci *35*, 13761-13772.

Kato, H., Taniguchi, Y., Kurooka, H., Minoguchi, S., Sakai, T., Nomura-Okazaki, S., Tamura, K., and Honjo, T. (1997). Involvement of RBP-J in biological functions of mouse Notch1 and its derivatives. Development *124*, 4133-4141.

Kawagishi, K., Ando, M., Yokouchi, K., Sumitomo, N., Karasawa, M., Fukushima, N., and Moriizumi, T. (2014). Stereological quantification of olfactory receptor neurons in mice. Neuroscience *272*, 29-33.

Kinzler, K.W., Ruppert, J.M., Bigner, S.H., and Vogelstein, B. (1988). The GLI gene is a member of the Kruppel family of zinc finger proteins. Nature *332*, 371-374.

Kinzler, K.W., and Vogelstein, B. (1990). The GLI gene encodes a nuclear protein which binds specific sequences in the human genome. Mol Cell Biol *10*, 634-642.

Kopan, R., Schroeter, E.H., Weintraub, H., and Nye, J.S. (1996). Signal transduction by activated mNotch: importance of proteolytic processing and its regulation by the extracellular domain. Proc Natl Acad Sci U S A *93*, 1683-1688.

Krauss, S., Concordet, J.P., and Ingham, P.W. (1993). A functionally conserved homolog of the Drosophila segment polarity gene hh is expressed in tissues with polarizing activity in zebrafish embryos. Cell *75*, 1431-1444.

Kumari, A., Ermilov, A.N., Allen, B.L., Bradley, R.M., Dlugosz, A.A., and Mistretta, C.M. (2015). Hedgehog pathway blockade with the cancer drug LDE225 disrupts taste organs and taste sensation. J Neurophysiol *113*, 1034-1040.

Kumari, A., Ermilov, A.N., Grachtchouk, M., Dlugosz, A.A., Allen, B.L., Bradley, R.M., and Mistretta, C.M. (2017). Recovery of taste organs and sensory function after severe loss from Hedgehog/Smoothened inhibition with cancer drug sonidegib. Proc Natl Acad Sci U S A *114*, E10369-E10378.

Lai, E.C. (2004). Notch signaling: control of cell communication and cell fate. Development *131*, 965-973.

Lai, K., Kaspar, B.K., Gage, F.H., and Schaffer, D.V. (2003). Sonic hedgehog regulates adult neural progenitor proliferation in vitro and in vivo. Nat Neurosci *6*, 21-27.

Lee, C.S., Buttitta, L., and Fan, C.M. (2001). Evidence that the WNT-inducible growth arrest-specific gene 1 encodes an antagonist of sonic hedgehog signaling in the somite. Proc Natl Acad Sci U S A *98*, 11347-11352.

Lehmann, R., Jimenez, F., Dietrich, U., and Campos-Ortega, J.A. (1983). On the phenotype and development of mutants of early neurogenesis inDrosophila melanogaster. Wilehm Roux Arch Dev Biol *192*, 62-74.

Leung, C.T., Coulombe, P.A., and Reed, R.R. (2007). Contribution of olfactory neural stem cells to tissue maintenance and regeneration. Nat Neurosci *10*, 720-726.

Lex, R.K., Ji, Z., Falkenstein, K.N., Zhou, W., Henry, J.L., Ji, H., and Vokes, S.A. (2020). GLI transcriptional repression regulates tissue-specific enhancer activity in response to Hedgehog signaling. Elife *9*.

Li, Z., Wei, M., Shen, W., Kulaga, H., Chen, M., and Lane, A.P. (2022). Sox2 regulates globose basal cell regeneration in the olfactory epithelium. Int Forum Allergy Rhinol *12*, 286-292.

Liang, F. (2020). Sustentacular Cell Enwrapment of Olfactory Receptor Neuronal Dendrites: An Update. Genes (Basel) *11*.

Liem, K.F., Jr., He, M., Ocbina, P.J., and Anderson, K.V. (2009). Mouse Kif7/Costal2 is a cilia-associated protein that regulates Sonic hedgehog signaling. Proc Natl Acad Sci U S A *106*, 13377-13382.

Lin, B., Coleman, J.H., Peterson, J.N., Zunitch, M.J., Jang, W., Herrick, D.B., and Schwob, J.E. (2017). Injury Induces Endogenous Reprogramming and Dedifferentiation of Neuronal Progenitors to Multipotency. Cell Stem Cell *21*, 761-774 e765.

Liu, A., Wang, B., and Niswander, L.A. (2005). Mouse intraflagellar transport proteins regulate both the activator and repressor functions of Gli transcription factors. Development *132*, 3103-3111.

Liu, H.X., Ermilov, A., Grachtchouk, M., Li, L., Gumucio, D.L., Dlugosz, A.A., and Mistretta, C.M. (2013a). Multiple Shh signaling centers participate in fungiform papilla and taste bud formation and maintenance. Dev Biol *382*, 82-97.

Liu, H.X., Maccallum, D.K., Edwards, C., Gaffield, W., and Mistretta, C.M. (2004). Sonic hedgehog exerts distinct, stage-specific effects on tongue and taste papilla development. Dev Biol *276*, 280-300.

Liu, L., Kugler, M.C., Loomis, C.A., Samdani, R., Zhao, Z., Chen, G.J., Brandt, J.P., Brownell, I., Joyner, A.L., Rom, W.N., and Munger, J.S. (2013b). Hedgehog signaling in neonatal and adult lung. Am J Respir Cell Mol Biol *48*, 703-710.

Machold, R., Hayashi, S., Rutlin, M., Muzumdar, M.D., Nery, S., Corbin, J.G., Gritli-Linde, A., Dellovade, T., Porter, J.A., Rubin, L.L., et al. (2003). Sonic hedgehog is required for progenitor cell maintenance in telencephalic stem cell niches. Neuron *39*, 937-950.

Malnic, B., Hirono, J., Sato, T., and Buck, L.B. (1999). Combinatorial receptor codes for odors. Cell *96*, 713-723.

Manglapus, G.L., Youngentob, S.L., and Schwob, J.E. (2004). Expression patterns of basic helix-loop-helix transcription factors define subsets of olfactory progenitor cells. J Comp Neurol *479*, 216-233.

Marigo, V., Davey, R.A., Zuo, Y., Cunningham, J.M., and Tabin, C.J. (1996). Biochemical evidence that patched is the Hedgehog receptor. Nature *384*, 176-179.

Martinelli, D.C., and Fan, C.M. (2007). Gas1 extends the range of Hedgehog action by facilitating its signaling. Genes Dev *21*, 1231-1243.

Mason, R.J., and Williams, M.C. (1977). Type II alveolar cell. Defender of the alveolus. Am Rev Respir Dis *115*, 81-91.

Matise, M.P., Epstein, D.J., Park, H.L., Platt, K.A., and Joyner, A.L. (1998). Gli2 is required for induction of floor plate and adjacent cells, but not most ventral neurons in the mouse central nervous system. Development *125*, 2759-2770.

McClintock, T.S., Khan, N., Xie, C., and Martens, J.R. (2020). Maturation of the Olfactory Sensory Neuron and Its Cilia. Chem Senses *45*, 805-822.

McDonnell, A.M., and Dang, C.H. (2013). Basic review of the cytochrome p450 system. J Adv Pract Oncol *4*, 263-268.

Menco, B.P. (1984). Ciliated and microvillous structures of rat olfactory and nasal respiratory epithelia. A study using ultra-rapid cryo-fixation followed by freeze-substitution or freeze-etching. Cell Tissue Res *235*, 225-241.

Mistretta, C.M., Liu, H.X., Gaffield, W., and MacCallum, D.K. (2003). Cyclopamine and jervine in embryonic rat tongue cultures demonstrate a role for Shh signaling in taste papilla development and patterning: fungiform papillae double in number and form in novel locations in dorsal lingual epithelium. Dev Biol *254*, 1-18.

Miura, H., Scott, J.K., Harada, S., and Barlow, L.A. (2014). Sonic hedgehog-expressing basal cells are general post-mitotic precursors of functional taste receptor cells. Dev Dyn *243*, 1286-1297.

Mombaerts, P. (2004). Genes and ligands for odorant, vomeronasal and taste receptors. Nat Rev Neurosci *5*, 263-278.

Mombaerts, P., Wang, F., Dulac, C., Chao, S.K., Nemes, A., Mendelsohn, M., Edmondson, J., and Axel, R. (1996). Visualizing an olfactory sensory map. Cell *87*, 675-686.

Moran, D.T., Rowley, J.C., 3rd, and Jafek, B.W. (1982a). Electron microscopy of human olfactory epithelium reveals a new cell type: the microvillar cell. Brain Res *253*, 39-46.

Moran, D.T., Rowley, J.C., 3rd, Jafek, B.W., and Lovell, M.A. (1982b). The fine structure of the olfactory mucosa in man. J Neurocytol *11*, 721-746.

Morris, R.J., Fischer, S.M., and Slaga, T.J. (1986). Evidence that a slowly cycling subpopulation of adult murine epidermal cells retains carcinogen. Cancer Res *46*, 3061-3066.

Morrison, E.E., and Costanzo, R.M. (1989). Scanning electron microscopic study of degeneration and regeneration in the olfactory epithelium after axotomy. J Neurocytol *18*, 393-405.

Murphy, C., Schubert, C.R., Cruickshanks, K.J., Klein, B.E., Klein, R., and Nondahl, D.M. (2002). Prevalence of olfactory impairment in older adults. JAMA *288*, 2307-2312.

Nakano, Y., Guerrero, I., Hidalgo, A., Taylor, A., Whittle, J.R., and Ingham, P.W. (1989). A protein with several possible membrane-spanning domains encoded by the Drosophila segment polarity gene patched. Nature *341*, 508-513.

Nei, M., Niimura, Y., and Nozawa, M. (2008). The evolution of animal chemosensory receptor gene repertoires: roles of chance and necessity. Nat Rev Genet *9*, 951-963.

Niewiadomski, P., Kong, J.H., Ahrends, R., Ma, Y., Humke, E.W., Khan, S., Teruel, M.N., Novitch, B.G., and Rohatgi, R. (2014). Gli protein activity is controlled by multisite phosphorylation in vertebrate Hedgehog signaling. Cell Rep *6*, 168-181.

Nusslein-Volhard, C., and Wieschaus, E. (1980). Mutations affecting segment number and polarity in Drosophila. Nature *287*, 795-801.

Ohtsuka, T., Ishibashi, M., Gradwohl, G., Nakanishi, S., Guillemot, F., and Kageyama, R. (1999). Hes1 and Hes5 as notch effectors in mammalian neuronal differentiation. EMBO J *18*, 2196-2207.

Oro, A.E., and Higgins, K. (2003). Hair cycle regulation of Hedgehog signal reception. Dev Biol *255*, 238-248.

Packard, A., Schnittke, N., Romano, R.A., Sinha, S., and Schwob, J.E. (2011). DeltaNp63 regulates stem cell dynamics in the mammalian olfactory epithelium. J Neurosci *31*, 8748-8759.

Palma, V., Lim, D.A., Dahmane, N., Sanchez, P., Brionne, T.C., Herzberg, C.D., Gitton, Y., Carleton, A., Alvarez-Buylla, A., and Ruiz i Altaba, A. (2005). Sonic hedgehog controls stem cell behavior in the postnatal and adult brain. Development *132*, 335-344.

Pan, Y., Bai, C.B., Joyner, A.L., and Wang, B. (2006). Sonic hedgehog signaling regulates Gli2 transcriptional activity by suppressing its processing and degradation. Mol Cell Biol *26*, 3365-3377.

Park, H.L., Bai, C., Platt, K.A., Matise, M.P., Beeghly, A., Hui, C.C., Nakashima, M., and Joyner, A.L. (2000). Mouse Gli1 mutants are viable but have defects in SHH signaling in combination with a Gli2 mutation. Development *127*, 1593-1605.

Peng, T., Frank, D.B., Kadzik, R.S., Morley, M.P., Rathi, K.S., Wang, T., Zhou, S., Cheng, L., Lu, M.M., and Morrisey, E.E. (2015). Hedgehog actively maintains adult lung quiescence and regulates repair and regeneration. Nature *526*, 578-582.

Perea-Martinez, I., Nagai, T., and Chaudhari, N. (2013). Functional cell types in taste buds have distinct longevities. PLoS One *8*, e53399.

Petrova, R., Garcia, A.D., and Joyner, A.L. (2013). Titration of GLI3 repressor activity by sonic hedgehog signaling is critical for maintaining multiple adult neural stem cell and astrocyte functions. J Neurosci *33*, 17490-17505.

Petrova, R., and Joyner, A.L. (2014). Roles for Hedgehog signaling in adult organ homeostasis and repair. Development *141*, 3445-3457.

Porter, J.A., Young, K.E., and Beachy, P.A. (1996). Cholesterol modification of hedgehog signaling proteins in animal development. Science *274*, 255-259.

Potter, M.R., Chen, J.H., Lobban, N.S., and Doty, R.L. (2020). Olfactory dysfunction from acute upper respiratory infections: relationship to season of onset. Int Forum Allergy Rhinol *10*, 706-712.

Rebay, I., Fleming, R.J., Fehon, R.G., Cherbas, L., Cherbas, P., and Artavanis-Tsakonas, S. (1991). Specific EGF repeats of Notch mediate interactions with Delta and Serrate: implications for Notch as a multifunctional receptor. Cell *67*, 687-699.

Reed, C.J. (1993). Drug metabolism in the nasal cavity: relevance to toxicology. Drug Metab Rev *25*, 173-205.

Reifenberger, J., Wolter, M., Weber, R.G., Megahed, M., Ruzicka, T., Lichter, P., and Reifenberger, G. (1998). Missense mutations in SMOH in sporadic basal cell carcinomas of the skin and primitive neuroectodermal tumors of the central nervous system. Cancer Res *58*, 1798-1803.

Riddle, R.D., Johnson, R.L., Laufer, E., and Tabin, C. (1993). Sonic hedgehog mediates the polarizing activity of the ZPA. Cell *75*, 1401-1416.

Rodriguez, S., Sickles, H.M., Deleonardis, C., Alcaraz, A., Gridley, T., and Lin, D.M. (2008). Notch2 is required for maintaining sustentacular cell function in the adult mouse main olfactory epithelium. Dev Biol *314*, 40-58.

Rohatgi, R., Milenkovic, L., and Scott, M.P. (2007). Patched1 regulates hedgehog signaling at the primary cilium. Science *317*, 372-376.

Sarafoleanu, C., Mella, C., Georgescu, M., and Perederco, C. (2009). The importance of the olfactory sense in the human behavior and evolution. J Med Life *2*, 196-198.

Sasaki, H., Hui, C., Nakafuku, M., and Kondoh, H. (1997). A binding site for Gli proteins is essential for HNF-3beta floor plate enhancer activity in transgenics and can respond to Shh in vitro. Development *124*, 1313-1322.

Sasaki, H., Nishizaki, Y., Hui, C., Nakafuku, M., and Kondoh, H. (1999). Regulation of Gli2 and Gli3 activities by an amino-terminal repression domain: implication of Gli2 and Gli3 as primary mediators of Shh signaling. Development *126*, 3915-3924.

Schroeter, E.H., Kisslinger, J.A., and Kopan, R. (1998). Notch-1 signalling requires ligand-induced proteolytic release of intracellular domain. Nature *393*, 382-386.

Schwob, J.E., Huard, J.M., Luskin, M.B., and Youngentob, S.L. (1994). Retroviral lineage studies of the rat olfactory epithelium. Chem Senses *19*, 671-682.

Schwob, J.E., Jang, W., Holbrook, E.H., Lin, B., Herrick, D.B., Peterson, J.N., and Hewitt Coleman, J. (2017). Stem and progenitor cells of the mammalian olfactory epithelium: Taking poietic license. J Comp Neurol *525*, 1034-1054.

Schwob, J.E., Youngentob, S.L., and Mezza, R.C. (1995). Reconstitution of the rat olfactory epithelium after methyl bromide-induced lesion. J Comp Neurol *359*, 15-37.

Shepherd, G.M. (2004). The human sense of smell: are we better than we think? PLoS Biol *2*, E146.

St-Jacques, B., Dassule, H.R., Karavanova, I., Botchkarev, V.A., Li, J., Danielian, P.S., McMahon, J.A., Lewis, P.M., Paus, R., and McMahon, A.P. (1998). Sonic hedgehog signaling is essential for hair development. Curr Biol *8*, 1058-1068.

Stone, D.M., Hynes, M., Armanini, M., Swanson, T.A., Gu, Q., Johnson, R.L., Scott, M.P., Pennica, D., Goddard, A., Phillips, H., et al. (1996). The tumour-suppressor gene patched encodes a candidate receptor for Sonic hedgehog. Nature *384*, 129-134.

Struhl, G., and Adachi, A. (1998). Nuclear access and action of notch in vivo. Cell *93*, 649-660.

Sun, X., Are, A., Annusver, K., Sivan, U., Jacob, T., Dalessandri, T., Joost, S., Fullgrabe, A., Gerling, M., and Kasper, M. (2020). Coordinated hedgehog signaling induces new hair follicles in adult skin. Elife *9*.

Tamura, K., Taniguchi, Y., Minoguchi, S., Sakai, T., Tun, T., Furukawa, T., and Honjo, T. (1995). Physical interaction between a novel domain of the receptor Notch and the transcription factor RBP-J kappa/Su(H). Curr Biol *5*, 1416-1423.

Teglund, S., and Toftgard, R. (2010). Hedgehog beyond medulloblastoma and basal cell carcinoma. Biochim Biophys Acta *1805*, 181-208.

Tenzen, T., Allen, B.L., Cole, F., Kang, J.S., Krauss, R.S., and McMahon, A.P. (2006). The cell surface membrane proteins Cdo and Boc are components and targets of the Hedgehog signaling pathway and feedback network in mice. Dev Cell *10*, 647-656.

Wang, B., Fallon, J.F., and Beachy, P.A. (2000). Hedgehog-regulated processing of Gli3 produces an anterior/posterior repressor gradient in the developing vertebrate limb. Cell *100*, 423-434.

Wang, B., and Li, Y. (2006). Evidence for the direct involvement of {beta}TrCP in Gli3 protein processing. Proc Natl Acad Sci U S A *103*, 33-38.

Wang, C., de Mochel, N.S.R., Christenson, S.A., Cassandras, M., Moon, R., Brumwell, A.N., Byrnes, L.E., Li, A., Yokosaki, Y., Shan, P., et al. (2018). Expansion of hedgehog disrupts mesenchymal identity and induces emphysema phenotype. J Clin Invest *128*, 4343-4358.

Wang, Y.Z., Yamagami, T., Gan, Q., Wang, Y., Zhao, T., Hamad, S., Lott, P., Schnittke, N., Schwob, J.E., and Zhou, C.J. (2011). Canonical Wnt signaling promotes the proliferation and neurogenesis of peripheral olfactory stem cells during postnatal development and adult regeneration. J Cell Sci *124*, 1553-1563.

Watkins, D.N., Berman, D.M., Burkholder, S.G., Wang, B., Beachy, P.A., and Baylin, S.B. (2003). Hedgehog signalling within airway epithelial progenitors and in small-cell lung cancer. Nature *422*, 313-317.

Williams, C.L., McIntyre, J.C., Norris, S.R., Jenkins, P.M., Zhang, L., Pei, Q., Verhey, K., and Martens, J.R. (2014). Direct evidence for BBSome-associated intraflagellar transport reveals distinct properties of native mammalian cilia. Nat Commun *5*, 5813.

Wilson, C.W., and Chuang, P.T. (2010). Mechanism and evolution of cytosolic Hedgehog signal transduction. Development *137*, 2079-2094.

Wu, L., Sun, T., Kobayashi, K., Gao, P., and Griffin, J.D. (2002). Identification of a family of mastermind-like transcriptional coactivators for mammalian notch receptors. Mol Cell Biol *22*, 7688-7700.

Young, J.M., Friedman, C., Williams, E.M., Ross, J.A., Tonnes-Priddy, L., and Trask, B.J. (2002). Different evolutionary processes shaped the mouse and human olfactory receptor gene families. Hum Mol Genet *11*, 535-546.

Chapter 2 *Gli2* and *Gli3* Regulate Horizontal Basal Cell-Mediated Regeneration of the Olfactory Epithelium

2.1 Abstract

The olfactory epithelium (OE) is a specialized neuroepithelium that is replenished by two stem cell populations: globose basal cells (GBCs) and horizontal basal cells (HBCs). Previous work indicated that HBCs contain primary cilia, organelles that mediate Hedgehog (HH) pathway activity. However, a role for HH signaling in HBCs has not been investigated. We find that GLI2 and GLI3, transcriptional effectors of the HH pathway, are expressed in HBCs in the adult OE and that their expression expands following injury. Further, *Gli2*-expressing descendants contribute to all major OE cell types during OE regeneration. HBC-specific expression of constitutively active GLI2 drives inappropriate HBC proliferation, alters HBC identity, and culminates in a failure of HBCs to differentiate into olfactory sensory neurons (OSNs) following injury. HBC-specific deletion of endogenous *Gli2* and *Gli3* results in decreased HBCs and OSNs following OE injury. These data identify GLI2 and GLI3 as key regulators of HBC-mediated OE regeneration.

2.2 Introduction

Olfactory dysfunction affects approximately 13.3 million older Americans (Hoffman et al., 2016). This can be due to factors that affect regeneration of the olfactory epithelium (OE), including physical injuries or pathogenic infections. The recent COVID-19 pandemic has resulted in loss of smell (anosmia) in patients (Aziz et al., 2021). To more effectively treat

olfactory disorders, we need to better understand the signals that govern OE regeneration. The OE is a highly specialized neuroepithelium that contains olfactory sensory neurons (OSNs), which relay smell information (Graziadei and Graziadei, 1979). OSNs are vulnerable to the environmental toxins and pathogens present in the air, making the OE one of the few adult sites of neurogenesis (Graziadei and Graziadei, 1979; Morrison and Costanzo, 1989). Fortunately, two presumed stem cell populations can replenish OSNs: rapidly dividing globose basal cells (GBCs), and relatively quiescent horizontal basal cells (HBCs) (Schwob et al., 2017). HBCs lie in a monolayer along the OE basement membrane, with GBCs situated just above the HBCs. Both HBCs and GBCs can generate neuronal and non-neuronal progenitors, which give rise to immature OSNs (iOSNs), supporting glial-like Sustentacular cells (Sus), Bowman's gland, and Microvillar cells (MVCs; (Schwob *et al.*, 2017); Figure 1A). Although HBCs and GBCs mediate OE regeneration, the signals governing their function in homeostasis and injury-mediated repair are largely unexplored.

Hedgehog (HH) signaling is necessary for adult stem cell maintenance and function in many tissues, including multiple different epithelia (Petrova and Joyner, 2014). Notably, HH signaling is necessary for taste bud maintenance and renewal in the tongue, another chemosensory organ (Mistretta and Kumari, 2019). Targeted deletion of the HH transcription factor *Gli2* in the lingual epithelium results in taste bud loss and formation of atypical taste organs (Ermilov et al., 2016). Similar experiments with the HH pathway inhibitor LDE225 demonstrated a loss of taste buds and taste sensation in mice (Kumari et al., 2015; Kumari et al., 2017). Given the importance of HH signaling in lingual epithelial regeneration, it is possible that HH signaling is playing a similar role in another chemosensory epithelium – the olfactory epithelium.

HH signaling is mediated by the primary cilium, a microtubule-based signaling center (Huangfu et al., 2003; Haycraft et al., 2005; Liu et al., 2005). In the absence of HH ligand, the canonical HH receptor Patched 1 (PTCH1) inhibits the activity of the GPCR-like protein Smoothened (SMO) resulting in phosphorylation and processing/degradation of GLI proteins, the transcriptional effectors of the HH pathway (Humke *et al.*, 2010; Niewiadomski et al., 2014). In the presence of HH ligand, HH binding to PTCH1 results in de-repression of SMO, allowing SMO to accumulate in the cilium, resulting in GLIs accumulating at tips of primary cilia, and processing of GLIs into transcriptional activators that induce HH target gene expression (e.g. *Ptch1* and *Gli1*; (Briscoe and Therond, 2013)). GLI1 functions exclusively as a transcriptional activator and is also a target of HH signaling; GLI2 is typically the major transcriptional activator of the HH pathway; conversely GLI3 acts largely as a transcriptional repressor (Briscoe and Therond, 2013). GLI2 and GLI3 contain an N-terminal repressor domain and a C-terminal activator domain, and can be post-translationally processed into either their full length activator form or truncated repressor form (Sasaki et al., 1997; Sasaki et al., 1999). Though GLI2 and GLI3 are typically thought to have opposing roles, they can also play redundant roles depending on the context of the tissue (Chang et al., 2016; McDermott et al., 2005).

Previous work demonstrated that HBCs possess primary cilia and that HBC-specific ablation of primary cilia result in defective OE regeneration, indicating a functional role for primary cilia in HBCs (Joiner et al., 2015). Given that 1) HH signaling is a key regulator of tissue renewal across multiple epithelia, 2) HH signaling also is a key regulator of adult neurogenesis, and that 3) HH/GLI signaling rely on the primary cilium, a structure that is essential for HBC-mediated OE regeneration, we wondered whether HH signaling might play a role in stem cell-mediated adult OE regeneration.

Here, we show that the HH transcription factors *Gli2* and *Gli3* are expressed in HBCs and a subset of Sus cells in the OE. Additionally, we show that *Gli2*+ HBCs can give rise to GBCs, OSNs, and Sus cells following injury. Further, we show that expression of constitutively active *Gli2* (GLI2A) in HBCs results in abnormal HBC proliferation and altered cell identity. Further, GLI2A-expressing HBCs fail to differentiate into OSNs following injury. Conditional *Gli2* and *Gli3* deletion in HBCs results in loss of HBCs and OSNs following injury. Together, these data suggest novel roles for GLI2 and GLI3 transcription factors in adult OE regeneration.

2.3 Results

To investigate the expression of GLI transcription factors in the adult OE we utilized mice carrying *lacZ* reporter alleles for $Gli1^{lacZ/+}$ (Bai et al., 2002), $Gli2^{lacZ/+}$ (Bai and Joyner, 2001), and $Gli3^{lacZ/+}$ (Garcia et al., 2010). Specifically, we performed X-GAL staining on coronal sections, focusing on two different regions, the dorsal septum, and a ventral turbinate (Figure 2.1 A). Like *Gli1*, *Gli2* is also expressed in the stroma underlying the OE; however, *Gli2* is more broadly expressed in both the proximal and distal stroma of the OE compared to *Gli1* (Figure 2.1 F-F'). In contrast to *Gli1*, *Gli2* is also expressed in basal epithelial cells throughout the OE (Figure 2.1 F-F', H-H'). Further, *Gli2* is expressed in a subset of apical epithelial cells in the turbinates (Figure 2.1 H-H'; black arrowheads). *Gli3* is also expressed broadly in the underlying stroma, and in basal cells throughout the OE (Figure 2.1 G-G', I-I'). Distinct from *Gli2*, *Gli3* is expressed in apical epithelial cells both at the septum (Figure 2.1 G-G'; black arrowheads) and at turbinates (Figure 2.1 I-I';black arrowheads).

To define the cell types that expressed *Gli2* and *Gli3* in the OE, we used immunofluorescent antibody detection to mark *Gli*-expressing cells ($BGAL^+$) and horizontal basal cells (HBCs; $p63^+$) (Packard et al., 2011). While no BGAL signal was detected in WT

animals (Figure 2.1K inset), in *Gli2*$^{lacZ/+}$ mice, BGAL co-localizes with NP63 (Figure 2.1K-K’’’; yellow arrow). Likewise, in *Gli3*$^{lacZ/+}$ mice, BGAL also co-localizes with p63 (Figure 2.1L-L’’’; yellow arrow), demonstrating that both *Gli2* and *Gli3* are expressed in HBCs of the adult OE. Co-staining with BGAL and a sustentacular (Sus) cell marker, SOX2 (Guo et al., 2010), revealed that BGAL co-localizes with apical SOX2^{+} cells in the ventral turbinates in both *Gli2*$^{lacZ/+}$ (Figure 2.2 B-B’’’) and *Gli3*$^{lacZ/+}$ mice (Figure 2.2 C-C’’’), indicating that *Gli2* and *Gli3* are expressed in distinct subsets of Sus cells in the OE. Together, these data demonstrate that *Gli2* and *Gli3*, but not *Gli1*, are expressed in the adult OE, displaying similar, but not identical expression patterns.

To further explore *Gli2* and *Gli3* expression in HBCs, a cell type that is quiescent during homeostasis (Fletcher et al., 2011; Packard *et al.*, 2011), we sought to activate HBCs with an injury to the OE. Upon delivery of methimazole to the OE, Sus cells in the OE metabolize methimazole into a toxicant that results in the destruction of most of the OE (Genter et al., 1995). Notably, HBCs will be spared– they will proliferate and give rise to both neuronal and non-neuronal lineages, and at 8 weeks will fully regenerate the OE (Leung et al., 2007). We delivered 75mg/kg of methimazole to *Gli2*$^{lacZ/+}$ and *Gli3*$^{lacZ/+}$ via intraperitoneal (IP) injection, followed by analysis at 4 days of recovery post-injury a time point when HBCs are most active during regeneration (Packard *et al.*, 2011). We performed *in situ* hybridization detection of *lacZ* transcripts, followed by immunofluorescent antibody detection of NP63 to mark HBC nuclei. Importantly, no *lacZ* expression is detected in wild-type uninjured and injured OE, demonstrating specificity of the *lacZ* probe (Figure 2.3 A-C, D-F). Sparse *lacZ*+ puncta are detected in NP63+ HBCs and stromal cells in uninjured *Gli2*$^{lacZ/+}$ (Figure 2.3 G-I) and Gli3$^{lacZ/+}$ (Figure 2.3 M-O) animals. At four days post injury, however, *Gli2* expression is significantly

increased throughout the OE (Figure 2.3 J-L, S) as well as specifically in NP63+ HBCs (Figure 2.3 U). Similarly, *Gli3* expression is also significantly increased in the OE following injury (Figure 2.3 P-R, T) and in HBCs (Figure 2.3 V). We confirmed these findings by performing X-GAL staining on *Gli2*$^{lacZ/+}$ and *Gli3*$^{lacZ/+}$ mice at 4 days and 8 weeks post methimazole injury (Figure 2.3 A-L'). Notably, X-GAL staining was not detected in WT animals at either timepoint (Figure 2.3 A-B', G-H'). Similar to the *in situ* data, increased X-GAL staining was detected in *Gli2*$^{lacZ/+}$ mice at 4 days following injury, especially at ventral turbinates compared to the dorsal septum region (Figure 2.4 C-D'). Since *Gli1* is a transcriptional readout for active HH signaling, we also used an endogenous *Gli1 in situ* probe to visualize *Gli1* expression prior to and following injury (Figure 2.2 C-K). *Gli1* expression was not detected in the OE of uninjured mice, similar to X-GAL staining of *Gli1*$^{lacZ/+}$ animals (Figure 2.2 I). No *Gli1* expression was detected in the OE 4 days following injury (Figure 2.2 I), although stromal *Gli1* levels are significantly upregulated (Figure 2.2 J-K). Taken together, these data suggest *Gli2* and *Gli3,* but not *Gli1,* are upregulated in the OE during early injury recovery.

Since *Gli2* expression in HBCs expands following injury, we employed a genetic lineage tracing approach to investigate the ability of *Gli2*-expressing cells and their descendants to contribute to different OE cell types. To achieve this, we bred *Gli2Cre*^{ER} mice with a *ROSA26-lox-STOP-lox-tdtomato* reporter allele (Madisen et al., 2010; Wang et al., 2018). Coronal sections from the heads of mice treated with vehicle (corn oil) or tamoxifen (Figure 2.5 A) were immunolabelled with antibodies directed against NP63 (HBCs) and SEC8 (GBCs). After either vehicle or tamoxifen treatment mice were rested for 72 hours then injected with methimazole to injure the OE (Figure 2.5 A-G''''). We analyzed *Gli2*-expressing descendants at 8 weeks (full recovery) after injury by immunolabelling for different OE cell types- NP63/CD54 (HBCs),

SEC8 (GBCs), SOX2 (Sus cells), and CBX8 (OSNs). Notably, no tdTomato+ progeny were visible in vehicle treated *Gli2Cre^{ER}; tdTomato/+* mice (Figure 2.5 B-B'''', D-D'''', F-F''''). We detected tdTomato+ labelled HBCs (Figure 2.5 C'', C''''; white arrowhead) and GBCs (Figure 2.5 C''', C''''; yellow arrowhead) in fully recovered mice. Further, we detected tdTomato+ Sus cells (Figure 2.5 E-E''''; blue arrowheads) and OSNs (Figure 2.5 G-G''''; green arrowheads). These findings suggest that *Gli2+* HBCs can give rise to all major cell types of adult OE, namely GBCs, Sus cells, and OSNs.

Given that increased *Gli2* expression correlates with HBC activation and that *Gli2* descendants contribute to all major OE cell types, we wondered whether the primarily transcriptional activator function ascribed to GLI2 in other systems (Bai *et al.*, 2002) might drive HBC activation in the OE. To test this notion, we utilized a doxycycline inducible system to express a constitutively active form of GLI2 lacking the N-terminal repressor domain (GLI2ΔN) in HBCs. We crossed mice that contain a reverse tetracycline transactivator driven by a Keratin 5 promoter (Krt5rtTA) (Diamond et al., 2000) to mice containing a tet operon inducible MYC-tagged *GLI2ΔN* transgene (Grachtchouk et al., 2011) (Figure 2.6). Mice were fed a doxycycline diet to induce *GLI2ΔN* expression in HBCs and analyzed at 1 day, 3 days, 5 days, and 8 days following induction (Figure 2.6 B-G'''', Figure 2.7 A-D). Due to the aggressive nature of driving overactive HH signaling these mice do not survive past 7-8 days (Grachtchouk *et al.*, 2011). Coronal sections of heads from control and experimental mice were stained with antibodies directed against MYC (GLI2ΔN), CD54 (HBCs), and Ki67 (actively cycling cells). While no MYC expression was detected in vehicle-treated *Krt5rtTA;GLI2ΔN* mice (Figure 2.6 B'), MYC immunostaining was detected in HBCs of *Krt5rtTA;GLI2ΔN* mice treated with doxycycline for 1 day (Figure 2.6 C'). Immunostaining for Ki67 (Figure 2.6 B'', C''), a marker for actively cycling

cells, identifies GBCs lying apical to CD54+ HBCs (Figure 2.6 B’’’, C’’’; white arrowheads) but not HBCs themselves, indicating that at 1 day post doxycycline induction HBCs are not actively proliferating. In contrast, at 3 days post doxycycline induction MYC^+ HBCs (Figure 2.6 E’, E’’’; yellow arrowheads) express Ki67 (Figure 2.6 E’’; yellow arrowheads), while control HBCs do not (Figure 2.6 D-D’’’’). At 5 days post doxycycline induction MYC^+ HBCs (Figure 2.6 G’, G’’’; yellow arrowheads) continue expressing Ki67 (Figure 2.6 G’’; yellow arrowheads), while control HBCs do not (Figure 2.6 G-G’’’’). Notably, GLI2ΔN protein is detected in HBC-associated primary cilia, an important organelle for HH signal transduction, at 8 days following doxycycline administration (Figure 2.9 F-J; white arrowhead). HBCs reach peak proliferation at 3 days post doxycycline induction (Figure 2.7 C-D), resulting in significantly increased HBC number at 3, 5, and 8 days post doxycycline induction (Figure 2.7 A, D). These data suggest that GLI activator can induce HBC proliferation.

To further analyze the effect of GLI2A on HBCs we performed immunostaining for GBC markers. Strikingly, at 8 days post doxycycline induction HBCs begin to co-express SEC8, a pan GBC marker (Joiner *et al.*, 2015) (Figure 2.8 F-M), in contrast to control mice (Figure 2.8 A-E). The total number of HBCs (Figure 2.8 K) is significantly increased while the total number of GBCs remains unchanged (Figure 2.8 L). Further, we performed immunostaining for SOX2, which labels a subset of HBCs and GBCs basally and Sus cells apically in control mice (Figure 2.8 N-Q). HBCs expressing GLI2A significantly upregulate SOX2 (Figure 2.8 R-V). Immunolabelling for SOX9 (Bowmann’s glad cells) showed a significant increase of SOX9 in HBCs of *Krt5rtTA;GLI2ΔN* mice (Figure S4E-I), compared to control mice (Figure 2.8 K-R, S). Interestingly, *Krt5rtTA;GLI2ΔN* HBCs did not co-express neuronal marker CBX8 (Figure 2.9 T), and there was no significant change in neurons in *Krt5rtTA;GLI2ΔN* OE (Figure 2.9 U). In

contrast, there is a small but significant increase in Sus cell number in mice expressing GLI2A (Figure 2.8 W). Taken together, these data suggest continuous active HH signaling results in a hybrid HBC identity and increased Sus cells.

Next, we assessed the effect of GLI2A on HBC function. Since HBCs are primarily quiescent in homeostatic conditions, we sought to activate them by injuring the OE. After inducing control and *Krt5rtTA;GLI2ΔN* mice with doxycycline for 24 hours, we injured the OE with an IP injection of methimazole at 75mg/kg (Figure 2.10 A-T, Figure 2.11 A-N). Mice were maintained on a doxycycline diet following injury and allowed to recover for 7 days. We first analyzed the basal cells in control and GLIA mice following methimazole injury (Figure 2.11 A-N). Coronal sections of mice collected at 7 days following injury were stained with antibodies for different OE markers in addition to Ki67 to mark actively cycling cells. While HBCs in control OE were not very proliferative (Figure 2.11 A-E, K), GLI2A HBCs were significantly more proliferative (Figure 2.11 F-K). HBC number in GLI2A OE was also significantly upregulated (Figure 2.11 L). In contrast, GBC number was significantly downregulated in GLIA OE (Figure 2.11 M). We also observed an upregulation in SOX9 progenitors in GLI2A OE (Figure 2.11 N). We then wanted to investigate if the increase in proliferating HBCs in GLI2A tissue had any effect on more differentiated OE cell types, such as early neurons and Sus cells. To do this, we immunostained coronal sections of control and *Krt5rtTA;GLI2ΔN* mice with SOX2 to mark Sus cell progenitors. We discovered that HBCs expressing GLI2A gave rise to a significantly higher amount of total $SOX2^+$ progenitors, in comparison to control HBCs (Figure 2.10 J). The OE in control HBCs also appeared more organized with a clear layer of early apical Sus cells separate from basal cells (Figure 2.10 B-E), whereas GLI2A OE appeared much more disorganized with diffuse SOX2 staining (Figure 2.10 F-I). Additionally, we immunolabelled for

early neurons using TUJ1 (Figure 2.10 K-S). Surprisingly, there was a significant decrease in $TUJ1^+$ progenitors in GLI2A OE compared to control OE (Figure 2.10 S). HBCs expressing GLI2A gave rise to very few neurons (Figure 2.10 O-R) compared to control HBCs which had a well-defined $TUJ1^+$ layer of cells (Figure 2.10 K-N). In short, while wild-type HBCs can give rise to both neurons and Sus cells following injury, HBCs with overactive HH signaling primarily give rise to Sus cells and not neurons (Figure 2.10 T). This suggests that HH signaling plays a role in differentiation of HBCs into Sus cells, but must be eventually downregulated to prevent over proliferation of HBCs into Sus cells.

We sought to further understand the function of GLIs in HBCs by utilizing a conditional deletion mouse model to selectively delete *Gli2* and *Gli3* in HBCs. We crossed in an HBC-specific tamoxifen inducible *Krt5-Cre^{ER}* (Diamond *et al.*, 2000) to *Gli2$^{fl/fl}$* (Corrales et al., 2006) and *Gli3$^{fl/fl}$* (Blaess et al., 2008) alleles containing loxP sites. A *ROSA26-lox-STOP-LOX-tdTomato* (Madisen *et al.*, 2010) allele was also crossed in to track HBC lineages following methimazole injury. Mice were treated with 100mg/kg of tamoxifen for 5 consecutive days, thus generating *Gli2^{CKO}*, *Gli3^{CKO}*, and *GLI2/3^{CKO}* mice lacking either *Gli2*, *Gli3*, or both in their HBCs. Since HBCs are typically a quiescent cell type, we performed a methimazole injury at 75mg/kg to stimulate HBC proliferation and differentiation. We collected and analyzed HBC progeny in *Gli2^{CKO}* (Figure 2.12 A-J), *Gli3^{CKO}* (Figure 2.12 F-J), and *GLI2/3^{CKO}* (Figure 2.13 A-O) mice 8 weeks following methimazole injury (full recovery). We used the tdTomato reporter to track HBC-derived cells and performed immunolabeling for different OE markers to determine the effect on conditional deletion of *Glis* on OE recovery. *Gli2^{CKO}* OE appeared comparable to control OE across all cell types. We observed no significant difference in HBCs (Figure 2.12 B), GBCs (Figure 2.12 C), OSNs (Figure 2.12 D), and Sus cells (Figure 2.12 E). In contrast, *Gli3^{CKO}*

OE had subtle but significant increase in HBCs (Figure 2.12 G), GBCs (Figure 2.12 H), and Sus cells (Figure 2.12 J). The number of OSNs was slightly downregulated but not significantly (Figure 2.12 I). Notably, the increase in basal and Sus cells in *Gli3*^{CKO} OE is similar to our previous findings using the constitutively active GLI2 transgene (Figure 2.10).

Since *Gli2* and *Gli3* can have redundant functions (McDermott *et al.*, 2005), we sought to delete *Gli2* and *Gli3* simultaneously in HBCs (*GLI2/3*^{CKO}) (Figure 2.13). We first confirmed efficient deletion of *Gli2* and *Gli3* in our genetic mouse model using *in situ* hybridization prior to methimazole injury (Figure 2.14 A-F). *Gli2* was significantly downregulated in *GLI2/3*^{CKO} OE (Figure 2.14 C, E) compared to control mice (Figure 2.14 A, E). *Gli3* was also significantly downregulated in *GLI2/3*^{CKO} OE (Figure 2.14 D, F) compared to control mice (Figure 2.14 B, F). *GLI2/3*^{CKO} OE displayed a range of severity following injury- while some regions looked disturbed and thin (Figure 2.14 G, I) others looked normal (Figure 2.14 H, J). We looked more closely at basal cells in *GLI2/3*^{CKO} OE and discovered HBCs were significantly decreased (Figure 2.13 E-G, H), compared to control OE (Figure 2.13 B-D, H). GBCs were also decreased, but not significantly (Figure 2.13 E-G, Figure 2.13 R). Next, we co-immunolabelled for TUJ1 and CBX8 to mark OSNs (Figure 2.13 I-O). We discovered OSNs were significantly decreased in *GLI2/3*^{CKO} OE (Figure 2.13 L-N, O), compared to control OE (Figure 2.13 I-K, O). These findings suggest that HBCs are unable to properly regenerate the OE following injury in the absence of *Gli2* and *Gli3*. We observed no significant decrease in Sus cells (Figure 2.14 K-Q), even in more significantly perturbed areas (Figure 2.14 N inset). To summarize, *Gli2*^{CKO} results in no significant change in OE cell composition, *Gli3*^{CKO} results in a similar, but subtler, change in OE cell composition, while *GLI2/3*^{CKO} results in the most severe change in OE cell composition (Figure 2.14 S). Taken together, these data illustrate that *Gli2* and *Gli3* have crucial

and synergistic roles in OE regeneration by regulating the proliferation and differentiation of HBCs following injury.

2.4 Discussion

2.4.1 Summary of results

Here, we explored the contribution of the HH pathway to OE regeneration. Specifically, we found that *Gli2* and *Gli3*, encoding two key transcriptional effectors of the HH pathway, are expressed in HBCs and distinct subset of Sus cells in the OE. Further, we discovered that *Gli2* and *Gli3* expression expands following OE injury. Constitutive GLI2A expression in HBCs results in HBC hyperproliferation and defective differentiation following OE injury. These data suggest that transient GLI activation following OE injury allows for HBC activation and proliferation, but that abrogation of GLI activator function is necessary for subsequent HBC differentiation (Figure 2.15). HBC-specific conditional *Gli2* deletion does not result in any detectable phenotype, while HBC-specific conditional *Gli3* deletion results in increased HBC, GBC and Sus cell numbers. Simultaneous conditional *Gli2* and *Gli3* deletion in HBCs results in improper OE regeneration and significantly decreased HBC, GBC, and OSN numbers. Together, these data illustrate novel roles for GLI signaling in HBC function and demonstrate that GLI2 and GLI3 are necessary for OE regeneration post-injury.

2.4.2 Diversity of HH response across different types of epithelia.

HH signaling plays important but diverse roles in many adult regenerative epithelia. Two such examples are the lingual and respiratory epithelium. HH signaling is essential for proper maintenance and function of taste organs in the lingual epithelium (Mistretta and Kumari, 2019). SHH ligand is present in the stem cells and nerves that innervate the taste bud (Ermilov *et al.*,

2016; Liu et al., 2013). As in the OE, *Gli2* is also expressed in basal cells of the lingual epithelium as well as in the underlying stroma (Liu *et al.*, 2013). *Gli1* is also present in the lingual stroma and epithelium, which differs from the OE where it is expressed exclusively in the stroma (Ermilov *et al.*, 2016). GLI2A expression in Keratin5+, *Gli2*+ cells in the tongue results in aberrant proliferation of lingual epithelial cells (Liu *et al.*, 2013). These findings are remarkably like the OE, where GLI2A-expressing HBCs become hyperproliferative. Further, the lingual epithelium is dependent on active HH signaling for maintenance. Chemical HH pathway inhibition using a SMO antagonist LDE225 results in disrupted taste organs and taste sensation (Kumari *et al.*, 2015). Further studies in the OE with chemical HH pathway blockade can elucidate if canonical HH signaling is necessary for OE maintenance and regeneration.

HH signaling is also a key component of adult lung regeneration and maintenance (Wang et al., 2019). During lung homeostasis, SHH ligand in the epithelium signals to surrounding GLI1+ mesenchymal cells (Peng et al., 2015). Genetic ablation of *Shh* results in mesenchymal cell proliferation and an increase in epithelial cells in the airway (Peng *et al.*, 2015). Additionally, genetic activation of HH signaling in the lung mesenchyme (through expression of oncogenic *Smo*) results in an emphysema-like phenotype (Wang *et al.*, 2018). Thus, HH signaling appears to have a restrictive role and maintains quiescence in the lung. Conversely, HH signaling is necessary for HBC proliferation and can drive proliferation in the olfactory epithelium. The adult lingual, respiratory, and olfactory epithelia are all regenerative, diverse, and unique structures. The differential deployment of HH/GLI signaling in each of these epithelial appears to be one mechanism by which a single pathway can contribute to the maintenance and regeneration of related, but distinct tissues.

2.4.3 Regulation of GLI expression and function in the olfactory epithelium.

Our data indicate an increase in *Gli2* and *Gli3* expression following injury in the OE. In contrast, there is no detectable expression of the HH target gene *Gli1* in the OE with *Gli1* expression remains solely stromal even following OE injury. These data suggest potentially non-canonical roles for GLI2 and GLI3 in the OE. While a definitive source of HH-producing cells in the OE remains to be elucidated, one potential source includes SHH in nerves that innervate the OE (Gong et al., 2009). SHH ligand is also present in the olfactory bulb (OB), particularly in the glomeruli (Gong et al., 2009). Further, OSNs are able to respond to SHH ligand *in vitro* (Gong *et al.*, 2009). Since OSNs directly connect the OE with the OB, it is possible that SHH is delivered to HBCs and the underlying stroma through OSN axonal projections. Another promising source of ligand is IHH, which is expressed in bone and regulates proliferation and differentiation of chondrocytes (Vortkamp et al., 1996). The OE and underlying stroma are directly in contact with the bone in the turbinates, making the turbinates a potential source of IHH. Further careful investigation into *Shh* and *Ihh* expression in the OE and surrounding tissues is necessary to elucidate if canonical HH signaling is regulates *Gli2* and *Gli3* in the OE.

Since HH target gene expression is not detected in the OE, it is possible that GLI2 and GLI3 function independently of HH ligands. A possible avenue of GLI regulation in the OE is through the NP63 transcription factor. NP63 is an important regulator of stemness in HBCs as illustrated in (Packard *et al.*, 2011). NP63 maintains HBC quiescence and transiently turns off following MeBr gas injury to the OE (Packard *et al.*, 2011). Our data illustrate an upregulation of *Gli2* and *Gli3* immediately following injury to the OE. It is possible that NP63 could negatively regulate *Gli2* and *Gli3* during OE homeostasis, resulting in upregulation of *Gli2* and *Gli3* when NP63 levels decrease following injury. Previous studies in mammary cancer stem cells illustrated that NP63 can directly regulate HH pathway genes such as SHH and GLI2 by binding

to upstream regulatory regions (Memmi et al., 2015). Additionally, our data indicates that driving GLI2A results in significant upregulation of NP63. This suggests a possible feedback loop between GLIs and NP63 expression. Careful investigation of whether NP63 can bind at *Gli2* and *Gli3* loci in HBCs can further our understanding of GLI regulation in HBCs.

2.4.4 Crosstalk between Hedgehog and Notch signaling.

While the primary focus of this study is on HH signaling and GLI transcription factors, other signaling pathways have been described in the adult OE. Specifically, Notch signaling has been implicated in OE regeneration (Schwob *et al.*, 2017). Importantly, Notch signaling pathway components are present in HBCs, along with Sus cells and underlying stroma (Herrick et al., 2018; Herrick et al., 2017). Previously work demonstrated that modulation of various Notch signaling pathway components altered HBC cell fate following OE injury (Herrick *et al.*, 2018). These findings echo our observations in the OE following GLI2A overexpression in HBCs. Similarly, in our HH overactivation model HBC cell fate is altered to Sus/non-neuronal following injury. It is possible that HH and Notch signaling coordinate to dictate HBC cell fates in response to injury. Along these lines, previous studies have demonstrated that Notch and HH signaling can work in conjunction in the context of development. For example, Notch signaling directs HH morphogen activity in the developing ventral spinal cord (Kong et al., 2015). Additionally, the HH co-receptor GAS1 directly binds to NOTCH1 in the developing forebrain, and coordinates HH and Notch signaling in the neuroepithelium (Marczenke et al., 2021). Notch has also been demonstrated to regulate HH pathway component SMO localization in the primary cilium (Stasiulewicz et al., 2015). This is important to note since HBCs have primary cilia that are functional and necessary for regeneration (Joiner *et al.*, 2015). Future studies examining

Notch signaling pathway components in our genetic models can elucidate cooperation between HH and Notch signaling in HBCs.

While our data demonstrates that *GLI2/3^{CKO}* mice have defective OE regeneration, our data slightly differs from the IFT88 HBC-specific deletion described in (Joiner *et al.*, 2015). Importantly, HBC number is unaffected in IFT88 HBC-specific deletion mice following injury (Joiner *et al.*, 2015), while we demonstrated a significant decrease of HBCs in *GLI2/3^{CKO}* mice. Similar to our genetic model, GBC and OSN numbers were significantly downregulated in IFT88 HBC-specific deletion mice following injury (Joiner *et al.*, 2015). Importantly, there was a decrease of tyrosine hydroxylase staining in the OB of IFT88 mice, indicating a decline in the synaptic input of OSNs to the OB (Joiner *et al.*, 2015). This implicated a loss of OSN function, which can be explained by their lack of primary cilia which are necessary for odorant signal transmission, due to their descendance from HBCs lacking primary cilia (Joiner *et al.*, 2015). Overall, the data described in (Joiner *et al.*, 2015) indicated a more severe phenotype in OSNs compared to our studies. Our data in *GLI2/3^{CKO}* mice indicate a presence of a ciliary layer by TUJ1 staining, implicating that OSNs derived from HBCs that lack GLI2 and GLI3 may still have functional cilia.

2.4.5 Limitations of Study

This study used multiple gain-of-function and loss-of-function mouse genetic approaches to investigate the roles of GLI2 and GLI3 in HBCs during OE regeneration. Nevertheless, we could broaden our study by including human tissue in our analysis. Previous studies have successfully isolated single cell transcripts from mOSNs of human patients (Durante et al., 2020). A similar approach could be utilized by sorting HBCs and examining HH pathway

transcripts in human patients. Understanding the role of HH signaling in human OE can also open therapeutic avenues for patients with loss of smell.

Though our work focused primarily on HBCs and regeneration, we also discovered that *Gli2* and *Gli3* are expressed in other cell types in the OE as well. For example, GLI2 and GLI3 are regionally expressed in Sus cells in the OE, opening a potential avenue of study of HH signaling in Sus cells. There is a precedent for key developmental pathways playing a role in Sus cell maintenance – for example genetic ablation of Notch2 results in Sus cell death in post-natal OE (Rodriguez et al., 2008). It is possible that genetic ablation of *Gli2* and *Gli3* specifically in Sus cells could affect Sus cell function. Additionally, it is possible that Sus cells and HBCs directly communicate through HH signaling. Similar studies have shown expression of both Notch ligand and receptors in HBCs and Sus cells, suggesting possible cell-cell communication (Herrick *et al.*, 2017). Using a similar approach, we could study the expression of additional HH pathway components in Sus cells to assess the potential for juxtracrine signaling between HBCs and Sus cells. Overall, a closer study of HH signaling in Sus cells would broaden our understanding of Sus cell function in the adult OE.

The functional role of the underlying stroma, also known as the lamina propria, during OE injury remains largely unexplored. The stroma is a highly vascularized tissue where fibroblasts, dendritic bundles from OSNs, and blood vessels are all present. During infection, the stroma is an important source of inflammatory cytokines and defense against invading parasites (Imamura and Hasegawa-Ishii, 2016). Studies have examined the stroma in chronic inflammatory rhinosinusitis models of mice and demonstrated that the immune system can directly affect HBCs and the OE (Chen et al., 2019). Thus, the immune response could be playing a role in OE regeneration following methimazole-induced injury. Notably, recent work

from our lab indicate that GLIs regulate the immune response in the context of pancreatic cancer (Scales et al., 2022). In this study we determined that all three *Glis* are expressed in the stroma underlying the OE. These data raise the question of GLI-dependent stromal contributions to maintenance and regeneration of the OE.

2.5 Materials and Methods

Animals and breeding

All mice were maintained on a mixed BL/6, 129, and CD1 genetic background. *Gli1*$^{lacZ/+}$ (Bai *et al.*, 2002), *Gli2*$^{lacZ/+}$ (Bai and Joyner, 2001), and *Gli3*$^{lacZ/+}$ (Garcia *et al.*, 2010) mice have all been described previously. *Keratin5rtTA;tetOGli2ΔN* (Grachtchouk *et al.*, 2011) mice were provided by Dr. Andrzej Dlugosz (University of Michigan, Ann Arbor MI). *Gli2Cre*^{ERT2} mice were provided by Dr. Tien Peng (University of California, San Francisco). HBC-specific *Gli2* and *Gli3* deletion was accomplished by breeding animals carrying a *Keratin5Cre*^{ERT2} allele with mice carrying *Gli2* and *Gli3* alleles flanked by loxP sites. To lineage trace progeny from HBCs that underwent *Cre*-mediated recombination, we crossed in a *ROSA26fl-STOP-fl-tdTomato* allele (JAX: 007908) into all conditional deletion mouse lines (*Gli2*^{fl} and *Gli3*^{fl}). For all experiments male and female adult mice (6-8 weeks of age) were used. All animal procedures were reviewed and approved by the Institutional Animal Care and Use Committee (IACUC) at the University of Michigan.

Tamoxifen preparation and administration

Tamoxifen was dissolved in sterile corn oil at 55°C for approximately 2-3 h at 40mg/mL with occasional agitation until in solution. For all experiments with conditional deletion mice (*ROSA26fl-STOP-fl-tdTomato*, *Gli2*^{fl}, and *Gli3*^{fl}) mice were injected 100mg/kg of tamoxifen

intraperitoneally (I.P.) for 5 consecutive days. Mice were allowed to rest for 72 h prior to methimazole lesion (described below).

Doxycycline preparation and administration

Doxycycline powder was dissolved at 200µg/ml in 5% sucrose in autoclaved water and administered to mice through drinking water. *Keratin5rtTA;tetOGli2ΔN* mice were given doxycycline water during first three days of doxycycline chow treatment. Doxycycline chow (1g/kg, Bio-Serv #F3949) was administered to *Keratin5rtTA;tetOGli2ΔN* mice at 6-8 weeks until date of euthanasia.

Methimazole lesion

Methimazole (2-mercapto-1-methylimdazole) was dissolved in sterile 1X PBS and administered to control and experimental mice through an intraperitoneal (IP) injection at 75mg/kg following either tamoxifen or doxycycline treatment.

X-gal staining

Mice were anesthetized with 30% isoflurane, transcardially perfused with 2% PLP solution (2% paraformaldehyde, 0.01M sodium periodate, 0.01M monobasic and dibasic phosphates, and 90mM L-lysine as described in (Packard *et al.*, 2011), and decapitated. Heads were post-fixed in 2% PLP for 1hr at 4 °C. Tissue was then decalcified in 0.5 M EDTA overnight at 4°C; cryoprotected in 10% (1h), 20% (1h), and 30% sucrose overnight at 4°C; and frozen in OCT compound. Coronal sections of the olfactory epithelium and olfactory bulb (OB) were cut at 12µm thickness on a Epredia™ Microm HM525 NX Cryostat. Sections were stored at -80 °C

until the day of staining. Beta-galactosidase activity was detected with X-gal staining solution (5mM $K_3Fe(CN)_6$, 5mM $K_4Fe(CN)_6$, 2mM $MgCl_2$, 0.01% Na deoxycholate, 0.02% NP-40, 1mg/mL X-gal). Sections were incubated with X-gal staining solution overnight in 37 °C. After staining, sections were washed 3 x 5 min with 1x PBS, pH 7.4, counterstained with nuclear fast red for 5 min and dehydrated in an ethanol series (70% ethanol, 95% ethanol, 100% ethanol and 100% Xylenes) followed by application of coverslips with permount mounting media. Sections were visualized on a Nikon E-800 Upright Widefield Microscope.

Immunohistochemistry

Mice were anesthetized with 30% Fluriso (isoflurane, VetOne), transcardially perfused with 4% paraformaldehyde (PFA), and decapitated. Heads were post-fixed in 4% PFA for 20–24 h at 4°C. Tissue was then decalcified in 0.5 M EDTA overnight at 4°C; cryoprotected in 10% (1h), 20% (1h), and 30% sucrose overnight at 4°C; and frozen in OCT compound. 12μm thick coronal sections of the olfactory epithelium and olfactory bulb (OB) were collected on a Epredia™ Microm HM525 NX Cryostat. Sections were stored at -80°C until day of staining. On the day of staining, sections were baked at 70°C for 10 min, washed 3 x 5 min with 1X PBST (0.01% Triton X), pH 7.4, then immediately placed in TRIS antigen retrieval solution for 15 minutes in a 92°C water bath. Sections were then blocked with 10% donkey serum for 1h at RT then incubated with primary antibody overnight at 4°C. The next day sections were washed with 3 x 5 min with 1X PBST (0.01% Triton X), pH 7.4, then incubated with secondary antibody for 1h at RT, For some antibodies (SEC8, CBX8) TSA amplification was used to detect signal. Nuclei were labeled with DAPI for 10 min at room temperature (RT) and slides were mounted with

coverslips using Immu-mount aqueous mounting medium. Sections were visualized on a Leica upright SP5X confocal microscope.

In situ hybridization

Mice were anesthetized with 30% Fluriso (isoflurane, VetOne), transcardially perfused with 10% neutral buffered formalin (10% NBF), and decapitated. Heads were post-fixed in 10% NBF for 24 h at RT. Tissue was then decalcified in 0.5 M EDTA overnight at 4°C; cryoprotected in 10% (1h), 20% (1h), and 30% sucrose overnight at 4°C; and frozen in OCT compound. Coronal sections of the olfactory epithelium and olfactory bulb (OB) were cut at 12µm thickness on a Epredia™ Microm HM525 NX Cryostat. Sections were stored at -80 °C until the day of staining when sections were baked at 70°C for 10 min then washed 5 min in 1X PBST (0.01% Triton X), pH 7.4. Fluorescent *in situ* hybridization was performed using ACD RNAscope Multiplex Fluorescent Reagent Kit v2, according to manufacturer's instructions (ACD 323100-USM). Pretreatment conditions were optimized for the olfactory epithelium: antigen retrieval was performed for 15 min, and protease treatment was performed for 1 min. Following the RNAscope assay, slides were incubated in primary antibody and followed the immunohistochemistry staining protocol described above. Sections were visualized on a Leica upright SP5X confocal microscope.

Quantitation and Statistical analysis

All the data are represented as mean ± standard deviation. All statistical analyses were performed using GraphPad statistic calculator (GraphPad Software, La Jolla California USA, www.graphpad.com). Statistical significance was determined using two-tailed Student's t-test.

Significance was defined according GraphPad Prism style: non-significant ($p>0.05$) and significant ($p\leq0.05$). For all the experimental analyses a minimum of 3 mice of each genotype were examined; each n represents a mouse. To quantify cell counts all images were blinded and four separate areas of the OE (dorsal septum, dorsal turbinate, ventral septum, and ventral turbinate) were averaged per n. All the statistical details (statistical tests used, statistical significance and exact value of each n) for each experiment are specified in the figure legends.

2.6 Tables

Table 2.1 Antibodies

REAGENT or RESOURCE	SOURCE	IDENTIFIER
Antibodies		
Rabbit anti-p63-alpha (D2K8X) (1:500)	Cell Signaling	13109T
Goat anti-CD54 (ICAM1) (1:100)	R&D Systems	AF796
Mouse anti-SEC8 (1:100)	BD Biosciences	610659
Mouse anti-Tuj1 (1:2500)	Promega	G7121
Mouse anti-MYC Epitope (1:500)	DSHB	9E 10
Rabbit anti-Ki67 (1:500)	Abcam	ab15580
Rabbit anti-CBX8 (1:500)	Cell Signaling	14696
Chicken anti-Beta-Galactosidase (1:2500)	Abcam	ab134435
Rabbit anti-SOX2 (1:2000)	Seven Hills Bio	WRAB-1236
Rabbit anti-SOX9 (1:500)	Millipore	AB5535
Rabbit anti-ARL13B (1:2000)	Proteintech	17711-1-AP
Biotin-Donkey anti-Rabbit (1:500)	Jackson Immuno	711-065-152
Biotin-Donkey anti-Mouse (1:500)	Jackson Immuno	715-065-150
Alexa488-Donkey anti-Chicken (1:500)	Jackson Immuno	703-545-155
Alexa488-Donkeyanti-Goat (1:500)	Invitrogen	A11055
Alexa488-Donkeyanti-Mouse (1:500)	Invitrogen	A21202
Alexa555-Donkey anti-Goat (1:500)	Invitrogen	A21432
Alexa555-Donkey anti-Mouse (1:500)	Invitrogen	A31570
Alexa647-Donkey anti-Rabbit (1:500)	Invitrogen	A31573
Alexa647-Donkey anti-Goat (1:500)	Invitrogen	A11055

Table 2.2 Chemicals, peptides, and recombinant proteins

Chemicals, peptides, and recombinant proteins	SOURCE	IDENTIFIER
Tamoxifen	Sigma	T5648
2-mercapto-1-methylimdazole (Methimazole)	Sigma	301507
Normal Donkey Serum	Jackson Immuno	NC9624464
Doxycycline	Thermo Fisher	BP26535
Doxycycline Chow (1g/kg)	Bio-Serv	F3949
EDTA	EMD/VWR	4005
Sucrose	EMD/VWR	8550
Paraformaldehyde	Thermo Fisher	50980489
DAPI	Thermo Fisher	D1306
BSA	Sigma	A7906
L-lysine	Sigma	W384720

Sodium Periodate	Sigma	311448
Sodium Monobasic phosphate (Na_2HPO_4)	Sigma	SX0709
Sodium Dibasic phosphate (Na_2HPO_4)	Sigma	8210-OP
Igepal (NP-40)	Sigma	I8896
$K_3Fe(CN)_6$	Sigma	PX1455
$K_4Fe(CN)_6$	Sigma	P9387
$MgCl_2$	VWR	0288
NaCl	Sigma	SX0420-3
Na deoxycholate	VWR	SX0480-2
Permount	Thermo Fisher	SP15100
Triton X-100	VWR	9410
Tween-20	VWR	9480
X-gal	Goldbio	X4281C
Xylenes	VWR	XX00555
EtOH	Thermo Fisher	04355222
OCT	Thermo Fisher	23730571
Antigen Unmasking Solution, Tris-Based	Vector	H-3301-250

Table 2.3 Critical commercial assays

Critical commercial assays	SOURCE	IDENTIFIER
Alexa-488 Tyramide SuperBoost Kit, streptavidin	Thermo Fisher	NC1439037
RNAscope Multiplex Fluorescent Reagent Kit v2	ACD	323100

Table 2.4 Experimental models: Organisms/strains

Experimental models: Organisms/strains	SOURCE	IDENTIFIER
Mouse: *Keratin5^{CreERT2}*	(Indra et al., 1999)	JAX: 018394
Mouse: *Gli2Cre^{CreERT2}*	(Wang *et al.*, 2018)	
Mouse: *Gli1$^{lacZ/+}$*	(Bai *et al.*, 2002)	JAX: 008211
Mouse: *Gli2$^{lacZ/+}$*	(Bai and Joyner, 2001)	JAX: 007922
Mouse: *Gli3$^{lacZ/+}$*	(Garcia *et al.*, 2010)	MGI: 4838603
Mouse: *Gli2^{fl}*	(Corrales *et al.*, 2006)	JAX: 007926
Mouse: *Gli3^{fl}*	(Blaess *et al.*, 2008)	JAX: 008873
Mouse: *Smo^{fl}*	(Long et al., 2001)	JAX: 004526
Mouse: *ROSA26fl-STOP-fl-tdTomato*	(Madisen *et al.*, 2010)	JAX: 007908
Mouse: *Keratin5rtTA*	(Diamond *et al.*, 2000)	MGI: 4867436
Mouse: *tetOGli2ΔN*	(Grachtchouk *et al.*, 2011)	

Table 2.5 Software and algorithms

Software and algorithms	SOURCE	IDENTIFIER
Prism 9	Graph Pad	https://www.graphpad.com/scientific-software/prism/
FIJI	FIJI	https://imagej.net/software/fiji/

Table 2.6 In Situ Hybridization Probes

In Situ Hybridization Probes	SOURCE	IDENTIFIER
RNAscope Ecoli-lacZ probe	ACD	313451
RNAscope Probe Ms-Gli1	ACD	311001
RNAscope Probe Ms-Gli2E7E8	ACD	412101
RNAscope Probe Ms-Gli3	ACD	445511

2.7 Figures

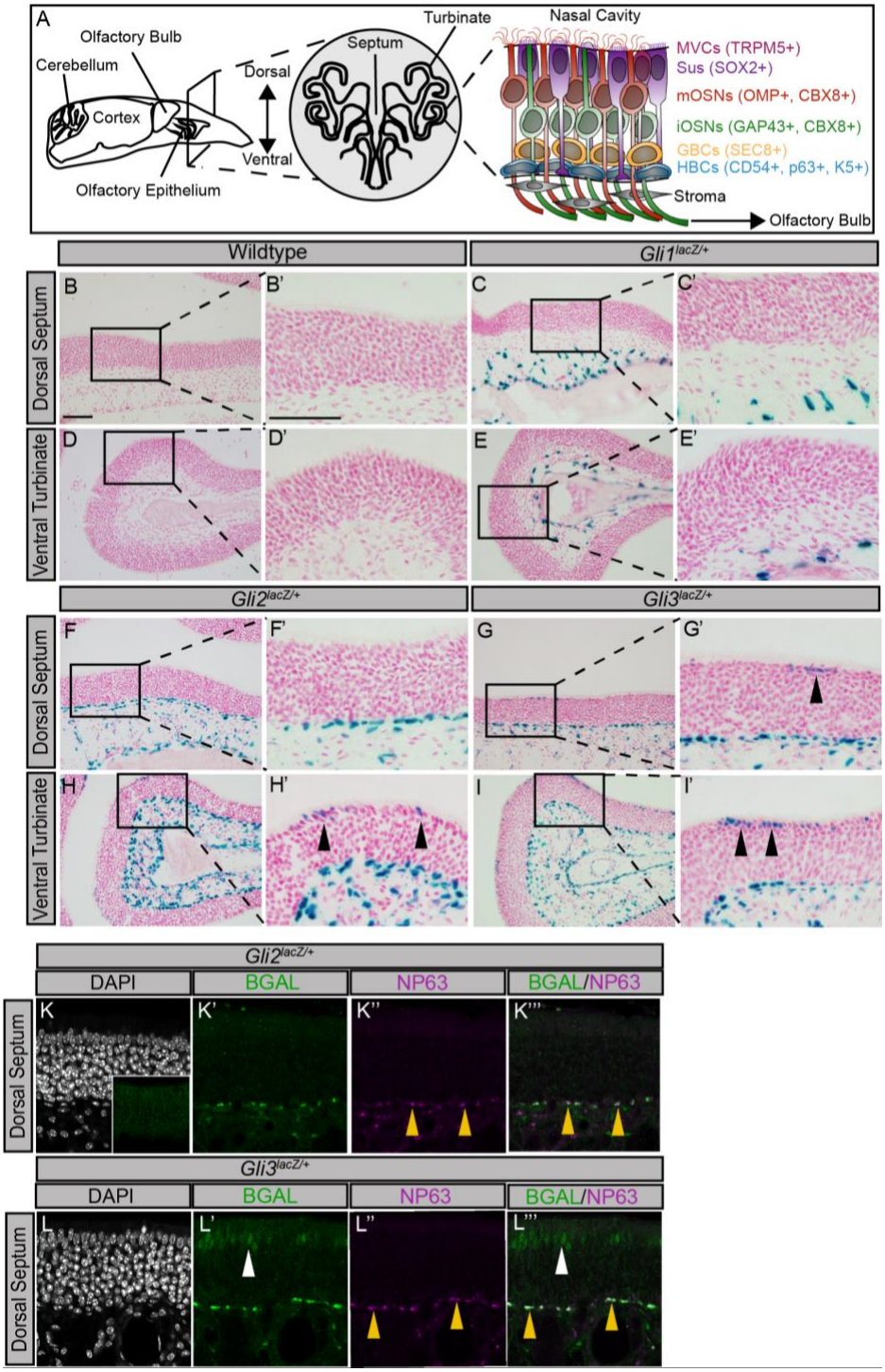

Figure 2.1 *Gli2* and *Gli3* are expressed in horizontal basal cells of the adult olfactory epithelium.

(A) Cartoon of a sagittal view of the adult mouse head (left). Coronal view of a section through the adult mouse olfactory epithelium (middle). Schematic of OE cell types (right), including horizontal basal cells (HBCs; blue), globose basal cells (GBCs; orange), immature olfactory sensory neurons (iOSNs; green), mature olfactory sensory neurons (mOSNs; red), sustentacular cells (Sus; purple), and microvillar cells (MVCs; magenta). (B-I) X-gal staining of coronal sections from adult wildtype (B, B', D, D'), *Gli1*$^{lacZ/+}$ (C, C', E, E'), *Gli2*$^{lacZ/+}$ (F, F', H, H'), and *Gli3*$^{lacZ/+}$ (G, G', I, I') reporter mice. Images are taken from both the dorsal septum (B-C', F-G') and a ventral turbinate (D-E', H-I'). Black arrowheads indicate BGAL^{+} apical cells in *Gli2*$^{lacZ/+}$ (H') and *Gli3*$^{lacZ/+}$ (G'. I') mice. (J-M) Antibody detection of β-galactosidase (BGAL, green; J', K', L', M'), the HBC nuclear marker NP63 (magenta; J", K", L). DAPI denotes nuclei (gray; J, K, L, M). NP63 (magenta) and BGAL co-localization (green) in *Gli2*$^{lacZ/+}$ animals (K'''; yellow arrowhead) and *Gli3*$^{lacZ/+}$ (L'''; yellow arrowhead). Note that *Gli3*, but not *Gli2*, is expressed in apical cells at the septum of the adult OE (L'; L"''; white arrowhead). Scale bars, B, B', J = 50μm.

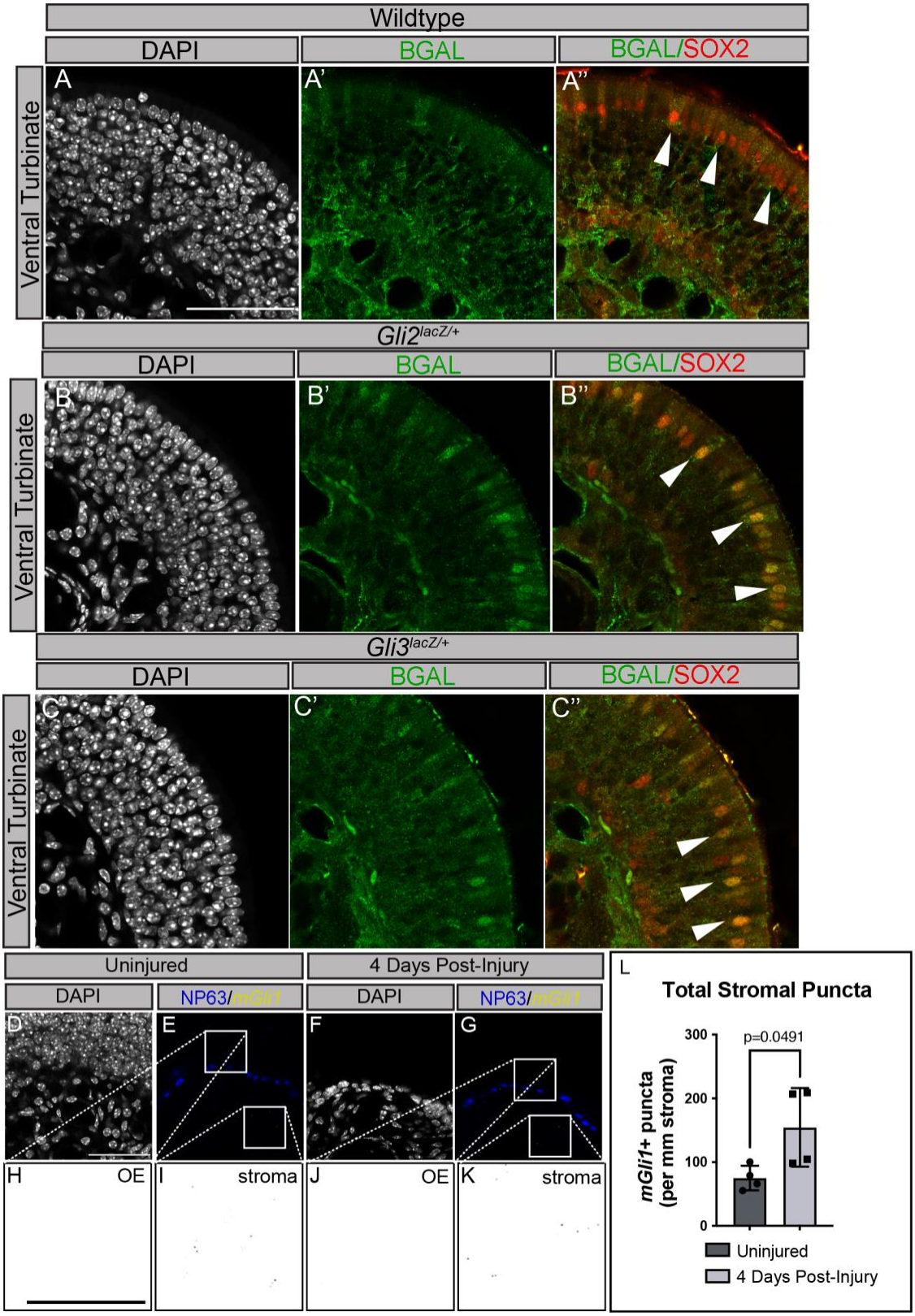

Figure 2.2 *Gli2* and *Gli3* are expressed in turbinate-associated sustentacular cells, while *Gli1* expression is stromally restricted, even following OE injury.

(A-B) Coronal sections of adult WT, *Gli2*$^{lacZ/+}$, and *Gli3*$^{lacZ/+}$ mice were stained with antibodies against β-galactosidase (green; A'-C') and a marker for Sus cells, SOX2 (red; A''-C''). DAPI denotes nuclei (gray; A-C). Scale bar= 50μm. (D-K) Adult mice were either collected at 6-8 weeks of age or injured with a 75mg/kg IP injection of methimazole. Coronal sections of either uninjured OE or OE 4 days following injury were processed for *in situ* hybridization with a probe to detect endogenous mouse *Gli1* (yellow; E, G). Antibodies directed against NP63 demarcate HBCs (blue; E, G). Inverted images of the *mGli1* probe in OE (black; H, J) and stroma (black; I, J). DAPI denotes nuclei (D, F), scale bars, 50μm (A, D), 25μm (H). Quantitation of *mGli1* puncta in the stroma underlying the OE, n=4 uninjured, n=4 injured (K). Data are mean ± standard deviation. P-values were determined by a two-tailed unpaired t-test; n.s.= not significant ($p>0.05$).

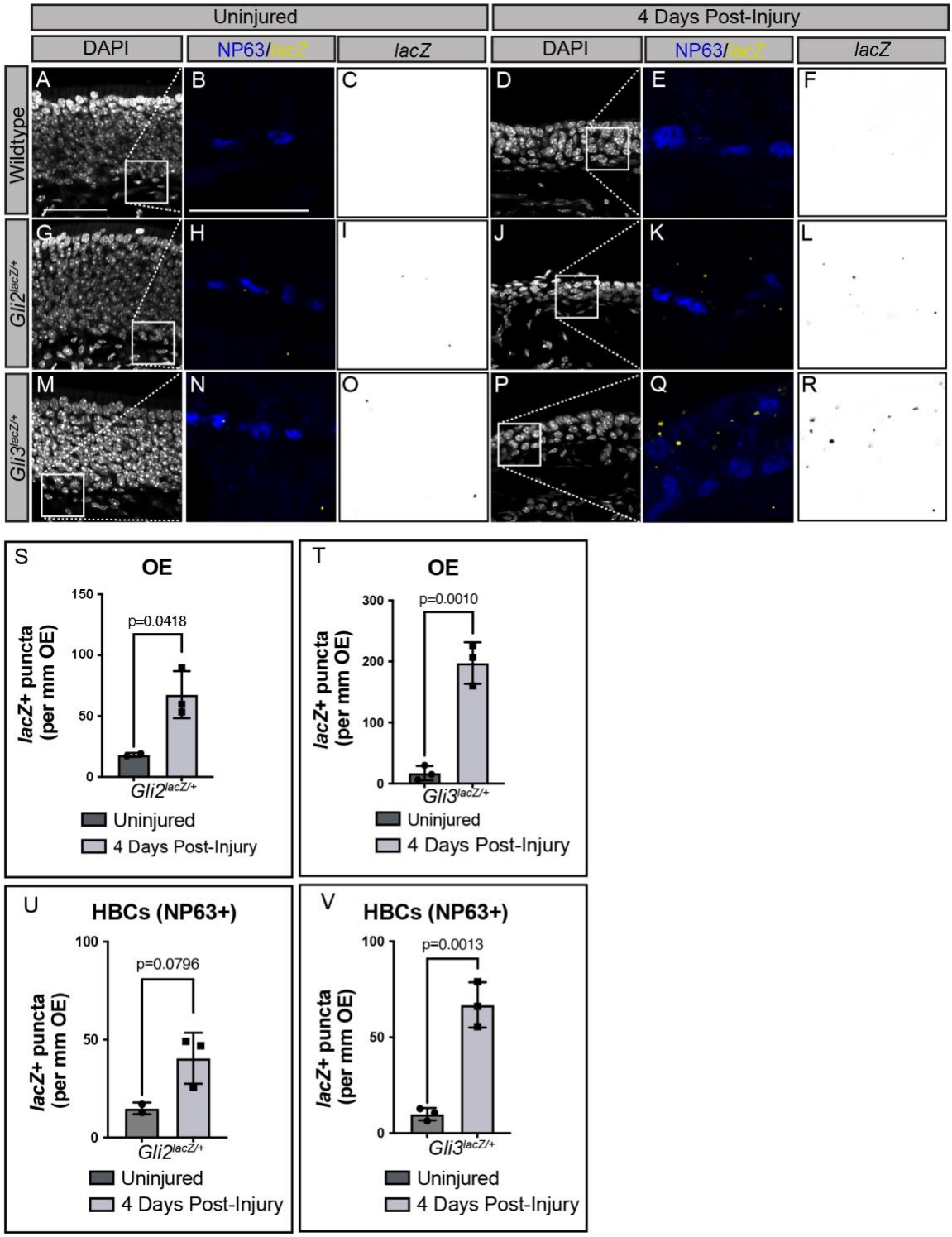

Figure 2.3 Selective upregulation of *Gli2* and *Gli3* expression in mice following methimazole-induced OE injury.

(A-V) Adult WT, *Gli2*$^{lacZ/+}$ and *Gli3*$^{lacZ/+}$ reporter mice were either collected at 6-8 weeks of age or injured with a 75mg/kg IP injection of methimazole. Coronal sections were collected from the heads of either uninjured (A-C, G-I, M-O) or 4 days post methimazole injury mice (D-F, J-L, P-

R). *In situ* hybridization detection of *lacZ* transcripts in sections from WT, *Gli2*$^{lacZ/+}$ and *Gli3*$^{lacZ/+}$ reporter mice prior to and following injury (yellow; B, H, N, E, K, Q). Inverted images of *lacZ* transcripts (black; C, I, O, F, L, R). Co-immunostaining with NP63 (blue; B, H, E, K, Q) demarcates HBCs. DAPI denotes nuclei (A, D, G, J, M, P), scale bar 50μm (A) and 25μm (B). Quantitation of *lacZ* puncta in the OE in *Gli2*$^{lacZ/+}$ (S) and *Gli3*$^{lacZ/+}$ (T) reporter mice prior and following methimazole injury. Quantitation of *lacZ*+ puncta in HBCs from *Gli2*$^{lacZ/+}$ (U) and *Gli3*$^{lacZ/+}$ (V) reporter mice prior and following methimazole injury. N=2 uninjured *Gli2*$^{lacZ/+}$, n=3 injured *Gli2*$^{lacZ/+}$, n=3 uninjured *Gli3*$^{lacZ/+}$, n=3 injured *Gli3*$^{lacZ/+}$. Data are mean ± standard deviation. P-values were determined by a two-tailed unpaired t-test; n.s.= not significant ($p>0.05$). Scale Bar=50μm (A), 25μm (B).

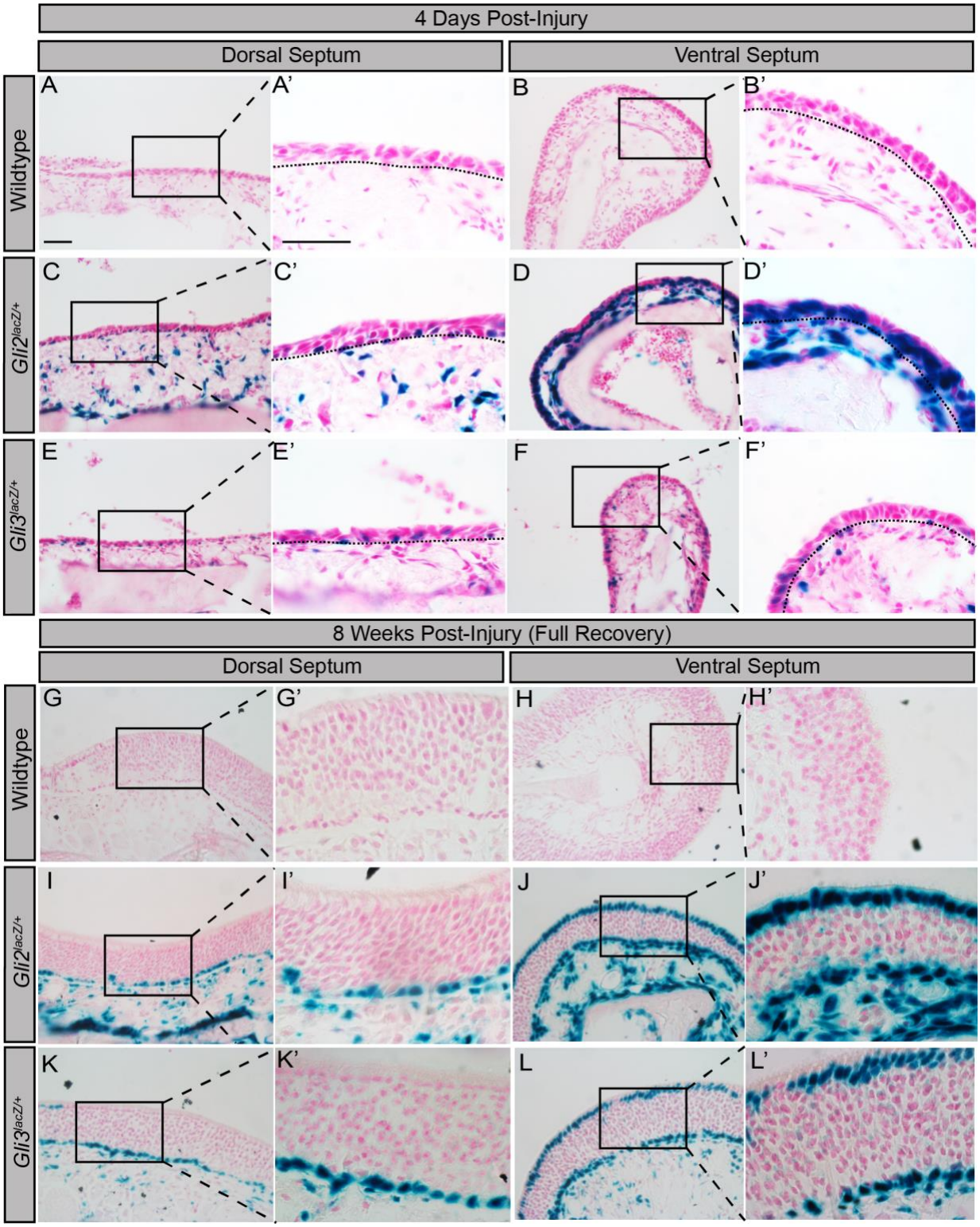

Figure 2.4 *Gli2* expression is up-regulated in ventral turbinate-associated OE at 4 days following methimazole injury.

Adult wild type, *Gli2*$^{lacZ/+}$, and *Gli3*$^{lacZ/+}$mice were injured with 75mg/kg methimazole and allowed to recover for either 4 days (A-F') or 8 weeks for full recovery (G-L'). X-GAL staining

of coronal sections from adult wildtype (A-B', G-H'), *Gli2*$^{lacZ/+}$ (C-D', I-J'), and *Gli3*$^{lacZ/+}$ (E-F', K-L') reporter mice. Images are taken from both the dorsal septum (A, A', C, C', E, E', G, G', I, I', K, K') and a ventral turbinate (B, B', D, D', F, F', H, H', J, J', L, L').

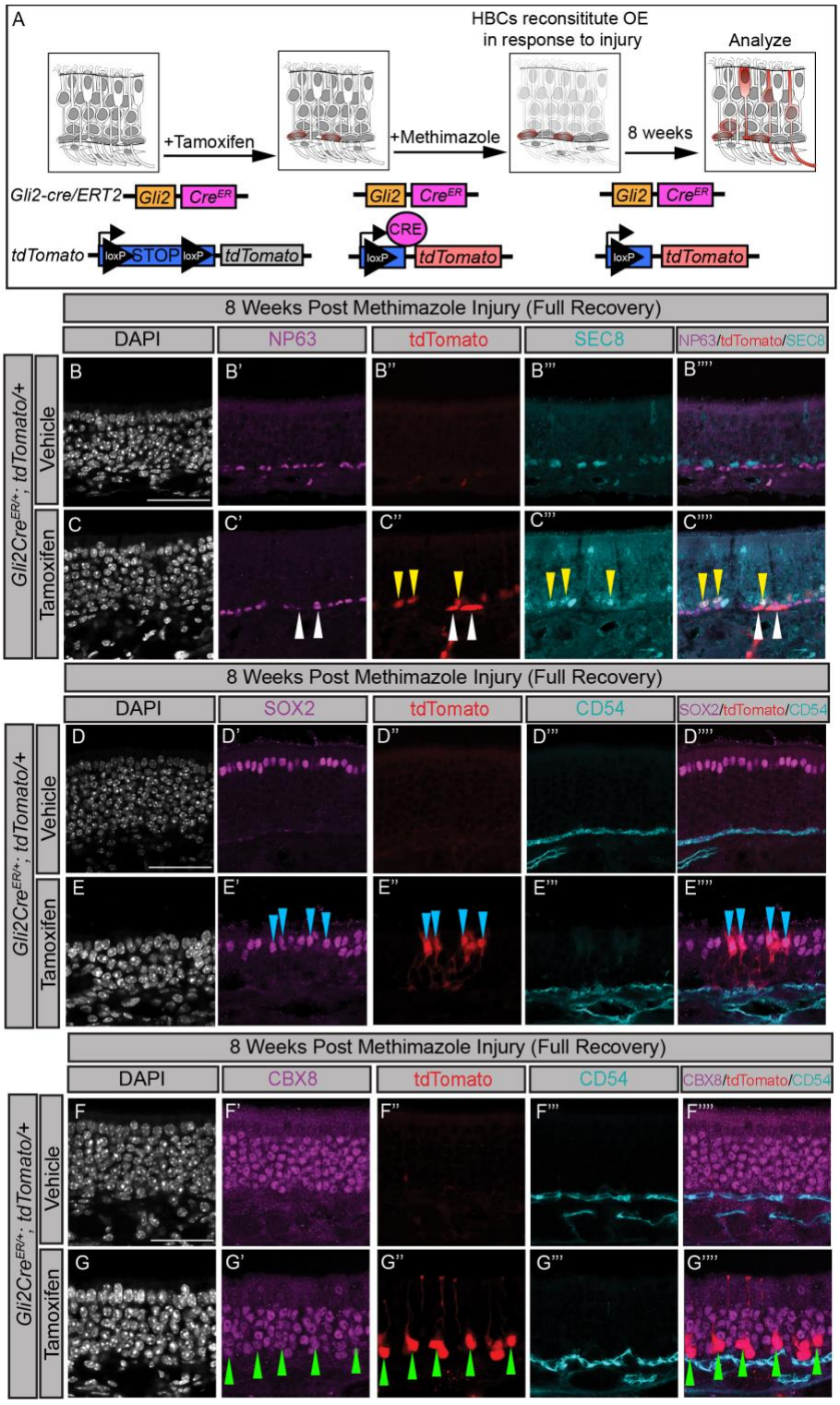

Figure 2.5 *Gli2*-descendants give rise to GBCs, Sus cells, and neurons following injury.

(A) Cartoon of *Gli2* lineage tracing model using a tamoxifen inducible *Gli2Cre^{ER}* mouse to mark *Gli2*-expressing cells. Mice carrying *Gli2Cre^{ER}; tdTomato* alleles were given an IP injection with either vehicle (corn oil) or tamoxifen for 5 consecutive days at 100mg/kg. Upon tamoxifen administration, Cre recombinase excised the stop codon preceding the tdTomato gene, labelling

Gli2-expressing cells and their descendants red. Mice were then injured with 75mg/kg methimazole and collected 8 weeks following injury (B-G’’’’). Coronal sections of vehicle- and tamoxifen-treated mice were stained with antibodies directed against NP63 label HBCs (magenta; B’, C’; white arrowheads) and SEC8 mark GBCs (cyan; B’’’, C’’’; yellow arrowheads). Antibodies directed against SOX2 label Sus cells apically (magenta; D’, E’; blue arrowheads) while antibodies directed against CD54 label HBCs (cyan; D’’’, E’’’, F’’’, G’’’). Antibodies directed against CBX8 denote neurons (magenta; F’, G’; green arrowheads). Cells originating from a *Gli2* lineage are labelled with tdTomato (red; B’’, C’’. D’’, E’’, F’’, G’’). Merged images of NP63, tdTomato and SEC8 (B’’’’, C’’’’), SOX2, tdTomato, CD54 (D’’’’, E’’’’), and CBX8, tdTomato, and CD54 (F’’’’, G’’’’). DAPI denotes nuclei (gray; B, C, D, E, F, G), scale bar (B, D, F) = 50μm.

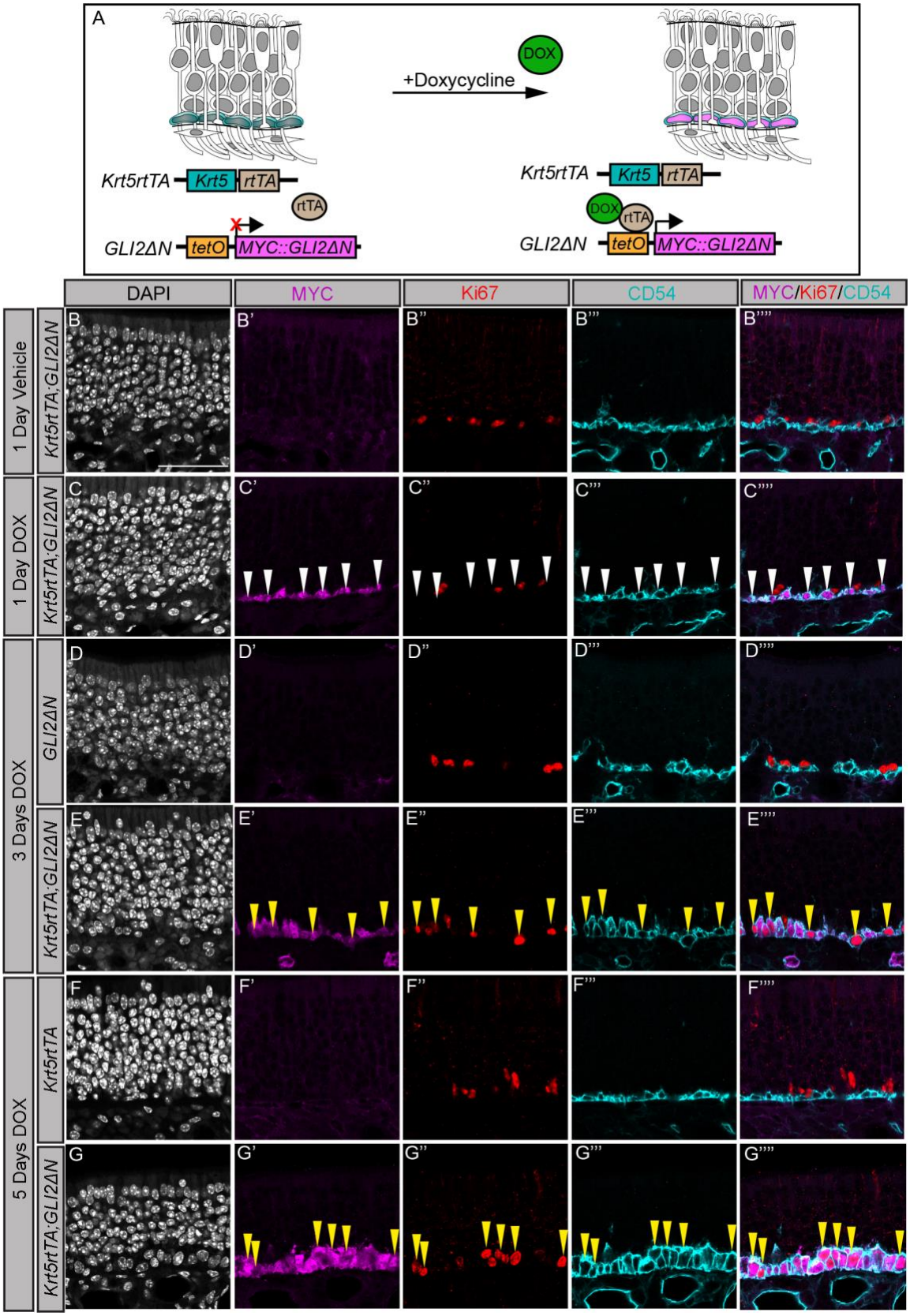

Figure 2.6 Constitutively active GLI2 drives HBC proliferation.

(A) Cartoon of *GLI2ΔN* transgene activation using a doxycycline-inducible mouse model. Upon doxycycline (DOX, green) administration, mice carrying a Keratin 5 reverse tetracycline transactivator (*Krt5rtTA*, blue) transgene and a tet-regulated MYC-tagged *GLI2ΔN* transgene (pink) express constitutively active *GLI2ΔN* specifically in HBCs of the OE by the rtTA (brown) protein binding at the tet operon (oragnge). (B-G’’’’) Antibody detection of MYC (magenta, B’-G’), Ki67 (red, B’’-G’’), and CD54 (cyan, B’’’-G’’’) at 1 Day Vehicle treatment (B-B’’’’), 1 Day DOX treatment (C-C’’’’), 3 days DOX treatment (D-D’’’’, E-E’’’’), and 5 days DOX treatment (F-F’’’’, G-G’’’’). DAPI denotes nuclei (gray; B-G). Merged MYC, Ki67, and CD54 images (B’’’’-G’’’’). MYC::GLI2ΔN protein is detectable at 1 day following DOX treatment (magenta, C’, C’’’’; white arrowheads). Following 3 days of DOX administration HBCs express Ki67 (red, E’’, E’’’’; yellow arrowheads). Ki67 expression in HBCs persists following 5 days of DOX administration (red, G’’, G’’’’; yellow arrowheads). Scale bar (B), 50μm.

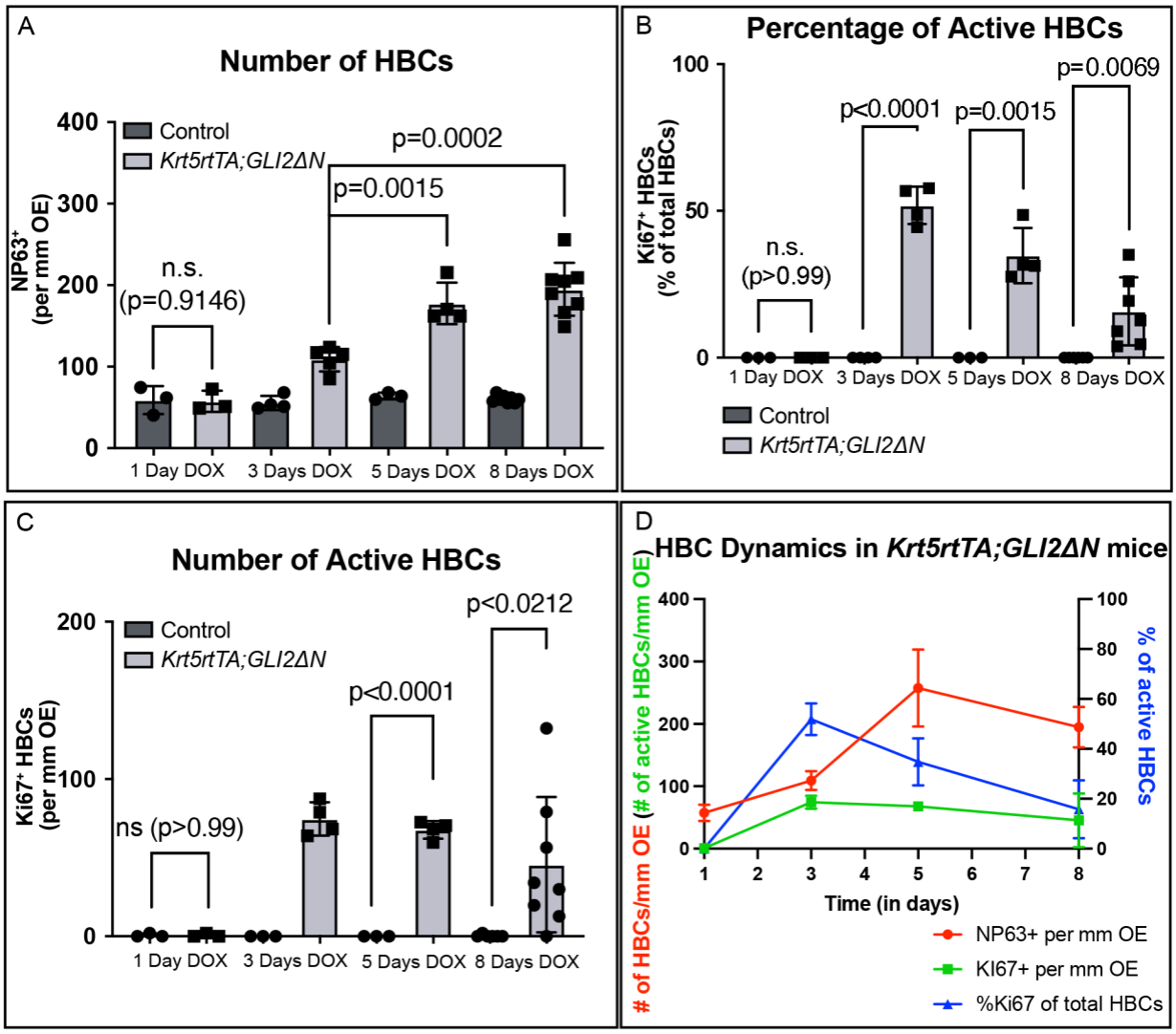

Figure 2.7 Quantitation of GLI2A-mediated HBC proliferation.

(A) Quantitation of HBC number per millimeter (mm) of olfactory epithelium at 1 Day, 3 Days, 5 Days, and 8 Days following doxycycline induction. (B) Quantitation of the percentage of Ki67$^+$ HBCs of total HBCs in the olfactory epithelium at 1 Day, 3 Days, 5 Days, and 8 Days following doxycycline induction. n=3 control, 3 *Krt5rtTA*; *GLI2ΔN* animals analyzed for 1 Day DOX. (C) Quantitation of Ki67$^+$ HBCs per mm of olfactory epithelium at 1 Day, 3 Days, 5 Days, and 8 Days following doxycycline induction. n=4 control, n=5 *Krt5rtTA*; *GLI2ΔN* animals analyzed for 3 Days DOX. n=3 control, 4 *Krt5rtTA*; *GLI2ΔN* animals analyzed for 5 Days DOX. n=6 control, 7 *Krt5rtTA*; *GLI2ΔN* animals analyzed for 8 Days DOX. Control refers to mice containing either the *Krt5rtTA* transgene or *GLI2ΔN* transgene. Data are represented as the mean ± standard deviation. P-values were determined by a two-tailed unpaired t-test; n.s.= not significant. (D) Summary graph of HBC dynamics in *Krt5rtTA*; *GLI2ΔN* animals, red indicates the number of HBCs per mm OE, green indicates the number of Ki67$^+$ HBCs per mm OE, and blue indicates the percentage of Ki67$^+$ HBCs from total HBCs in the OE.

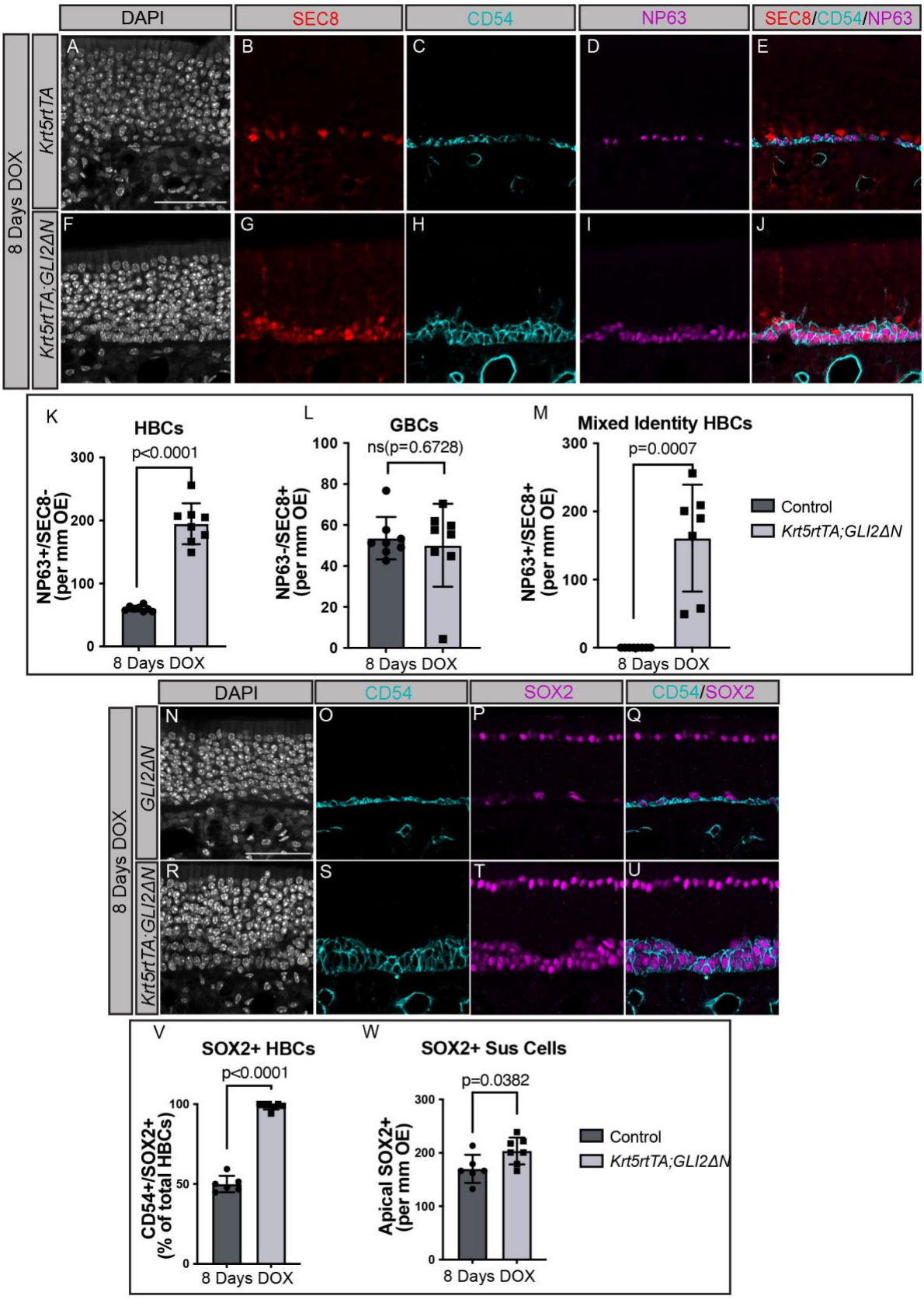
DAPI
SEC8
CD54
NP63
SEC8/CD54/NP63
8 Days DOX
Krt5rtTA
Krt5rtTA;GLI2ΔN
A
B
C
D
E
F
G
H
I
J
K
HBCs
p<0.0001
NP63+/SEC8-
(per mm OE)
8 Days DOX
L
GBCs
ns(p=0.6728)
NP63-/SEC8+
(per mm OE)
8 Days DOX
M
Mixed Identity HBCs
p=0.0007
NP63+/SEC8+
(per mm OE)
8 Days DOX
Control
Krt5rtTA;GLI2ΔN
DAPI
CD54
SOX2
CD54/SOX2
8 Days DOX
GLI2ΔN
Krt5rtTA;GLI2ΔN
N
O
P
Q
R
S
T
U
V
SOX2+ HBCs
p<0.0001
CD54+/SOX2+
(% of total HBCs)
8 Days DOX
W
SOX2+ Sus Cells
p=0.0382
Apical SOX2+
(per mm OE)
8 Days DOX
Control
Krt5rtTA;GLI2ΔN

Figure 2.8 Constitutively active GLI2 alters HBC identity.

(A-J) Coronal sections from adult mice treated with DOX for 8 days were analyzed with immunostaining using different OE markers. Antibodies directed against SEC8 (red; B, G) identify GBCs, while antibody detection of CD54 (cyan; C,H) and NP63 (magenta; D,I) denotes HBCs. DAPI indicates nuclei (gray; A, F). Merged SEC8, CD54, and NP63 images (E, J). Quantitation of HBCs ($NP63^+$, $SEC8^-$; K), GBCs ($NP63^-$,$SEC8^+$; L), and mixed identity HBCs ($NP63^+$, $SEC8^+$; M). n=8 control and n=8 *Krt5rtTA*;*GLI2ΔN* animals analyzed (K-M). (N-U) Coronal sections from adult mice treated with DOX for 8 days were analyzed with immunostaining using different OE markers. Antibody detection of CD54 (cyan; O,S) and apical SOX2 (Sus cell marker, magenta; P,T). DAPI indicates nuclei (N, R). Merged CD54 and SOX2 images (Q,U). Quantitation of $SOX2^+$ HBCs ($SOX2^+$, $CD54^+$; V) and $SOX2^+$ Sus cells (Apical $SOX2^+$ cells; W). n=6 control and n=7 *Krt5rtTA*; *GLI2ΔN* animals analyzed (V-W). Scale bars (A, N) = 50μm. Control refers to mice containing either the *Krt5rtTA* or *GLI2ΔN* transgene. Data are mean ± standard deviation. P-values were determined by a two-tailed unpaired t-test; n.s.= not significant ($p>0.05$).

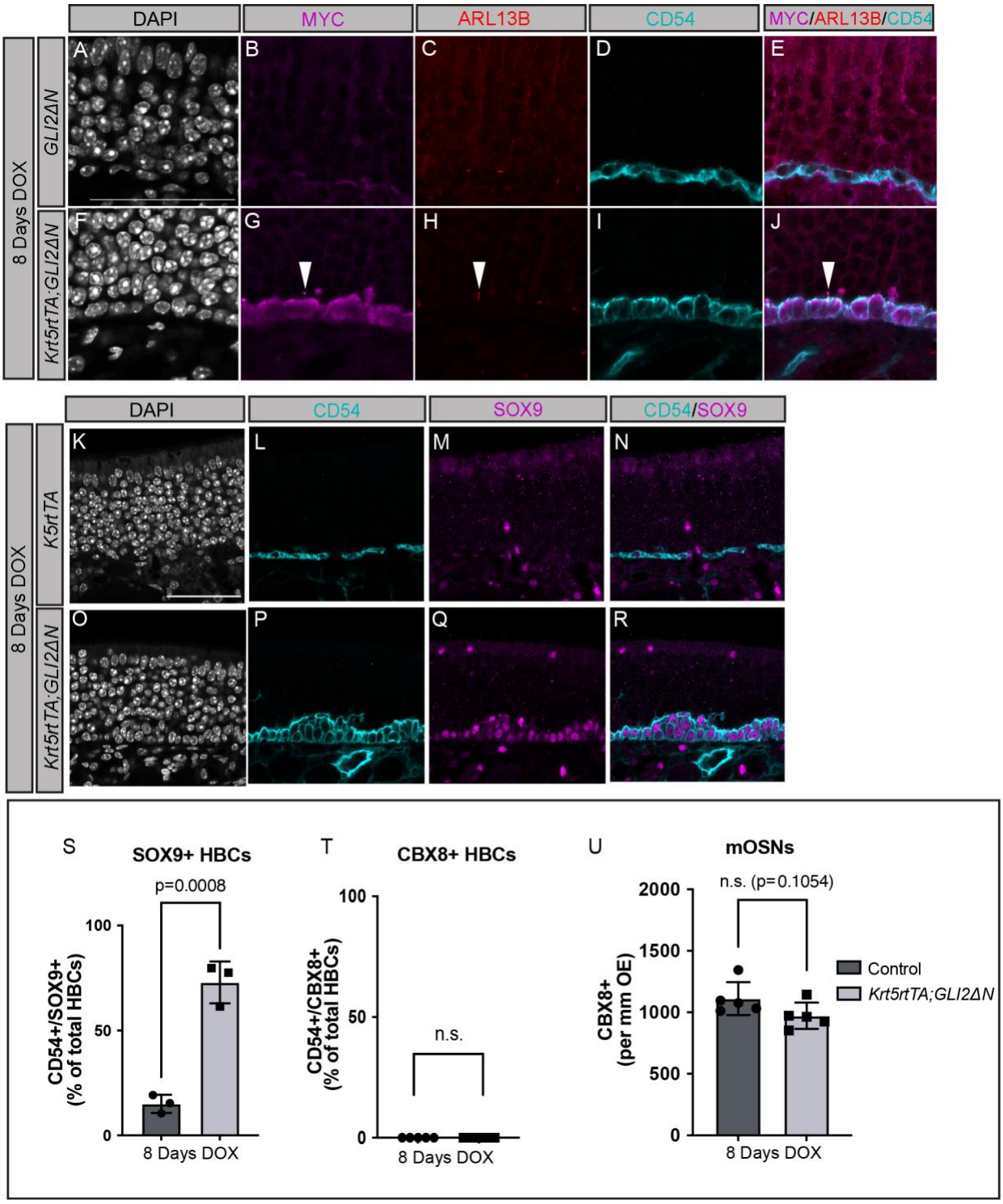

Figure 2.9 Constitutively Active GLI2 localizes to primary cilia in HBCs and increases SOX9 expression.

(A-U) Mice containing the *Krt5rtTA* and *GLI2ΔN* transgenes were treated with doxycycline for 8 days. Coronal sections from adult mice were treated with antibodies directed against MYC (magenta; B, G; white arrowhead) which detects GLI2ΔN, Arl13b (red; C, H; white arrowhead)

which labels primary cilia, and CD54 (cyan; D, I) which denotes HBCs. Merged MYC, Arl13b, CD54 images (E, J). DAPI denotes nuclei (A, F), scale bar (A) 50μm. (K-R) Coronal sections from adult mice treated with DOX for 8 days were analyzed with immunostaining using different OE markers. Antibodies directed against CD54 (cyan; L, P) denote HBCs, while antibody detection of SOX9 (magenta; M, Q) identifies Bowman's gland cells. DAPI indicates nuclei (gray; K, O). Scale bar (A), 50μm. Merged CD54 and SOX9 images (N, R). Quantitation of the percentage $SOX9^+$ HBCs, n=3 control and n=3 *Krt5rtTA*; *GLI2ΔN* animals analyzed (S). Quantitation of the percentage of $CBX8^+$ HBCs, n=5 control and n=5 *Krt5rtTA*; *GLI2ΔN* animals analyzed (T). Quantitation of mOSNs, n=5 control and n=5 *Krt5rtTA*; *GLI2ΔN* animals analyzed (U). Control refers to mice containing either the *Krt5rtTA* or *GLI2ΔN* transgene. Data are mean ± standard deviation. P-values were determined by a two-tailed unpaired t-test; n.s.= not significant ($p>0.05$).

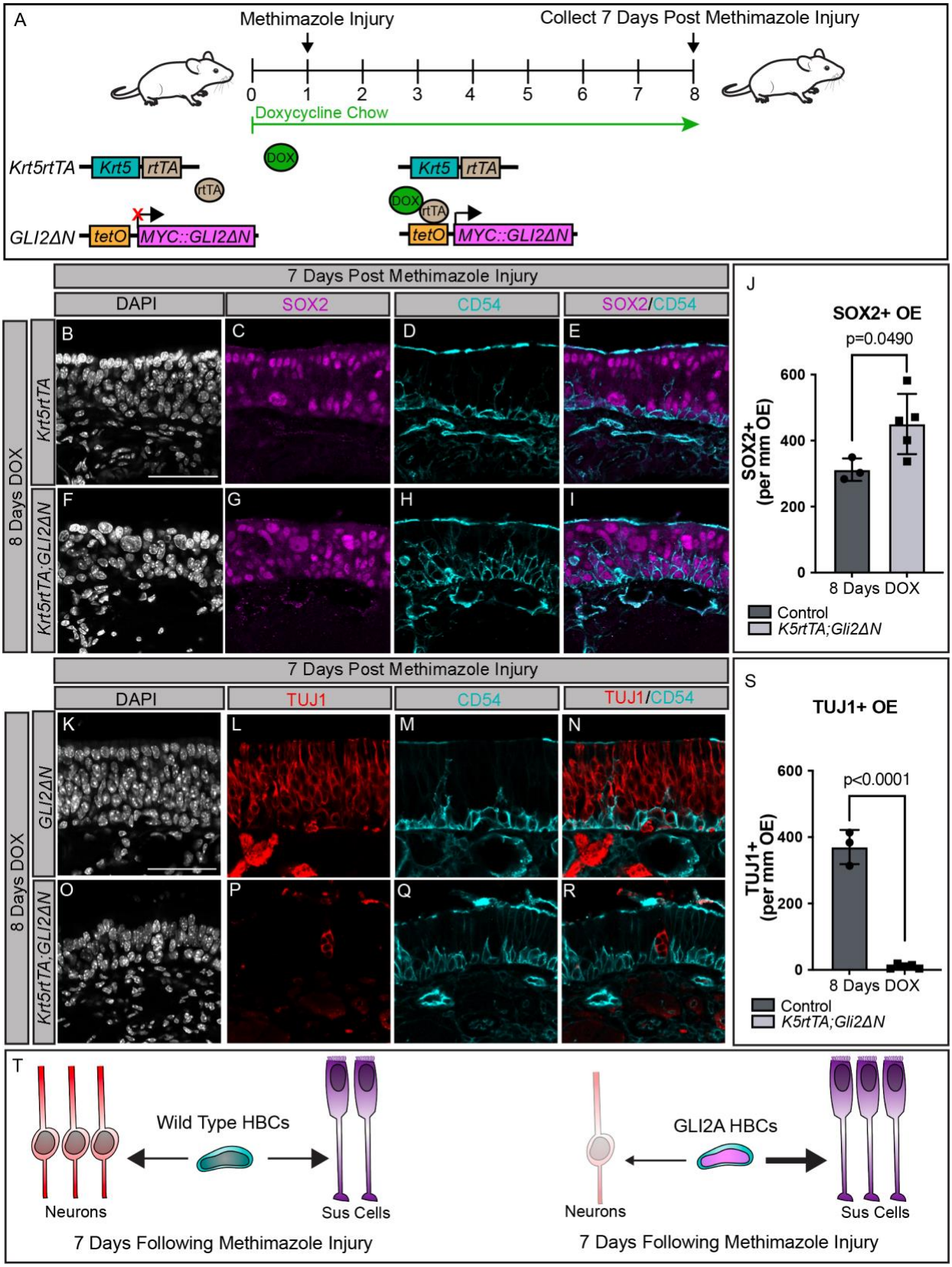
A
Methimazole Injury
Collect 7 Days Post Methimazole Injury
0 1 2 3 4 5 6 7 8
Doxycycline Chow
Krt5rtTA
Krt5
rtTA
DOX
GLI2ΔN
tetO
MYC::GLI2ΔN
7 Days Post Methimazole Injury
DAPI
SOX2
CD54
SOX2/CD54
8 Days DOX
Krt5rtTA
Krt5rtTA;GLI2ΔN
B
C
D
E
F
G
H
I
J
SOX2+ OE
p=0.0490
SOX2+ (per mm OE)
600
400
200
0
8 Days DOX
Control
K5rtTA;Gli2ΔN
7 Days Post Methimazole Injury
DAPI
TUJ1
CD54
TUJ1/CD54
8 Days DOX
GLI2ΔN
Krt5rtTA;GLI2ΔN
K
L
M
N
O
P
Q
R
S
TUJ1+ OE
p<0.0001
TUJ1+ (per mm OE)
600
400
200
0
8 Days DOX
Control
K5rtTA;Gli2ΔN
T
Wild Type HBCs
Neurons
Sus Cells
7 Days Following Methimazole Injury
GLI2A HBCs
Neurons
Sus Cells
7 Days Following Methimazole Injury

Figure 2.10 GLI2A-expressing HBCs fail to contribute to neuronal lineages following injury.

(A) Cartoon of *GLI2ΔN* transgene activation using a doxycycline-inducible mouse model. Upon doxycycline (DOX, green) administration, mice carrying a Keratin 5 reverse tetracycline transactivator (*Krt5-rtTA*, blue) transgene and a tet-regulated MYC-tagged *GLI2ΔN* transgene (pink) express constitutively active *GLI2ΔN* specifically in HBCs of the OE. 1 day following doxycycline induction, mice are injured with a 75mg/kg intraperitoneal (IP) injection of methimazole. Following methimazole injury, mice are kept on doxycycline and collected 7 days following injury. (B-S) Coronal sections from adult mice treated with DOX for 8 days, 7 days following methimazole injury, were analyzed with immunostaining using different OE markers. Antibodies directed against SOX2 (magenta; C, G) denote apical lying Sus cells and a subset of basal HBCs and GBCs, while antibody detection of CD54 (cyan; D, H, M, Q) exclusively identifies HBCs. Merged SOX2 and CD54 images (E, I). DAPI indicates nuclei (gray; B, F, K, O). Quantitation of the percentage of $SOX2^+$ cells in the OE (J). Antibodies directed against TUJ1 (red; L, P) denote neurons. Merged TUJ1 and CD54 images (N, R). Quantitation of the percentage of $TUJ1^+$ cells in the OE (S). Scale bar (B, K), 50μm. n=3 control and n=5 *Krt5rtTA*; *GLI2ΔN* animals analyzed. Control refers to mice containing either the *Krt5rtTA* or *GLI2ΔN* transgene. Data are mean ± standard deviation. P-values were determined by a two-tailed unpaired t-test; n.s.= not significant ($p>0.05$). (T) Summary of HBC-mediated OE reconstitution at 7 days following injury in wild type (left) and *Krt5rtTA*;*GLI2ΔN* mice (right).

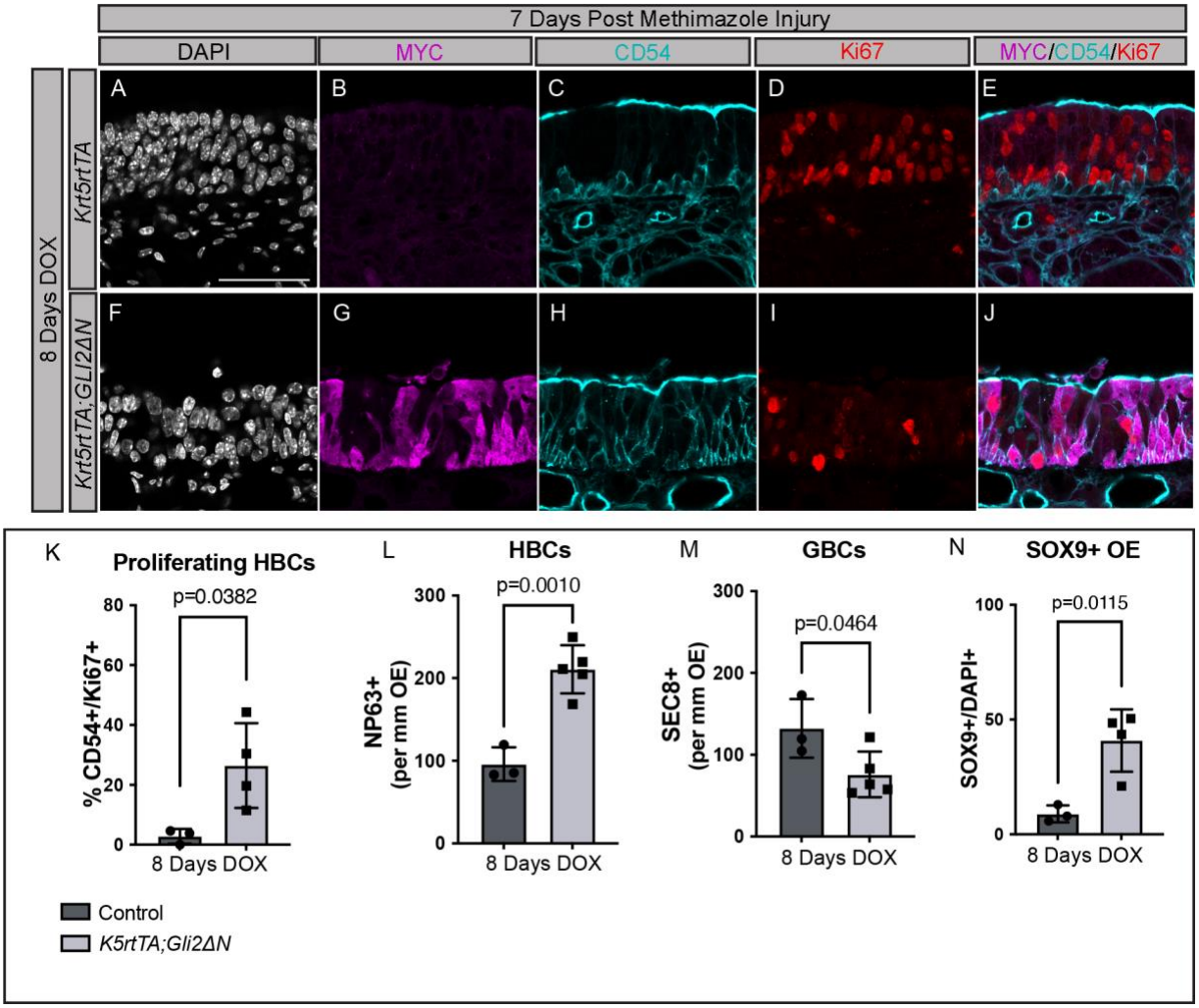

Figure 2.11 Constitutively Active GLI2 drives HBC proliferation following injury.

(A-J) Coronal sections from adult mice treated with DOX for 8 days, 7 days following methimazole injury, were analyzed with immunostaining using different OE markers. Antibodies directed against MYC (magenta; B, G) denote MYC tagged GLI2ΔN, while antibodies directed against CD54 (cyan; C, H) stain HBCs. Actively cycling cells are stained with Ki67 (red; D, I), DAPI denotes nuclei (gray; A, F), MYC, CD54, Ki67 merged images (E, J). Scale bar (A), 50μm. Quantitation of the percentage of $Ki67^{+}$ HBCs (K). Quantitation of the number of NP63+ HBCs (L), SEC8+ GBCs (M), and SOX9+ Sus cells (N) per mm of OE. n=3 control and n=5 *Krt5rtTA*; *GLI2ΔN* animals analyzed. Control refers to mice containing either the *Krt5rtTA* or *GLI2ΔN* transgene. Data are mean ± standard deviation. P-values were determined by a two-tailed unpaired t-test; n.s.= not significant (p>0.05).

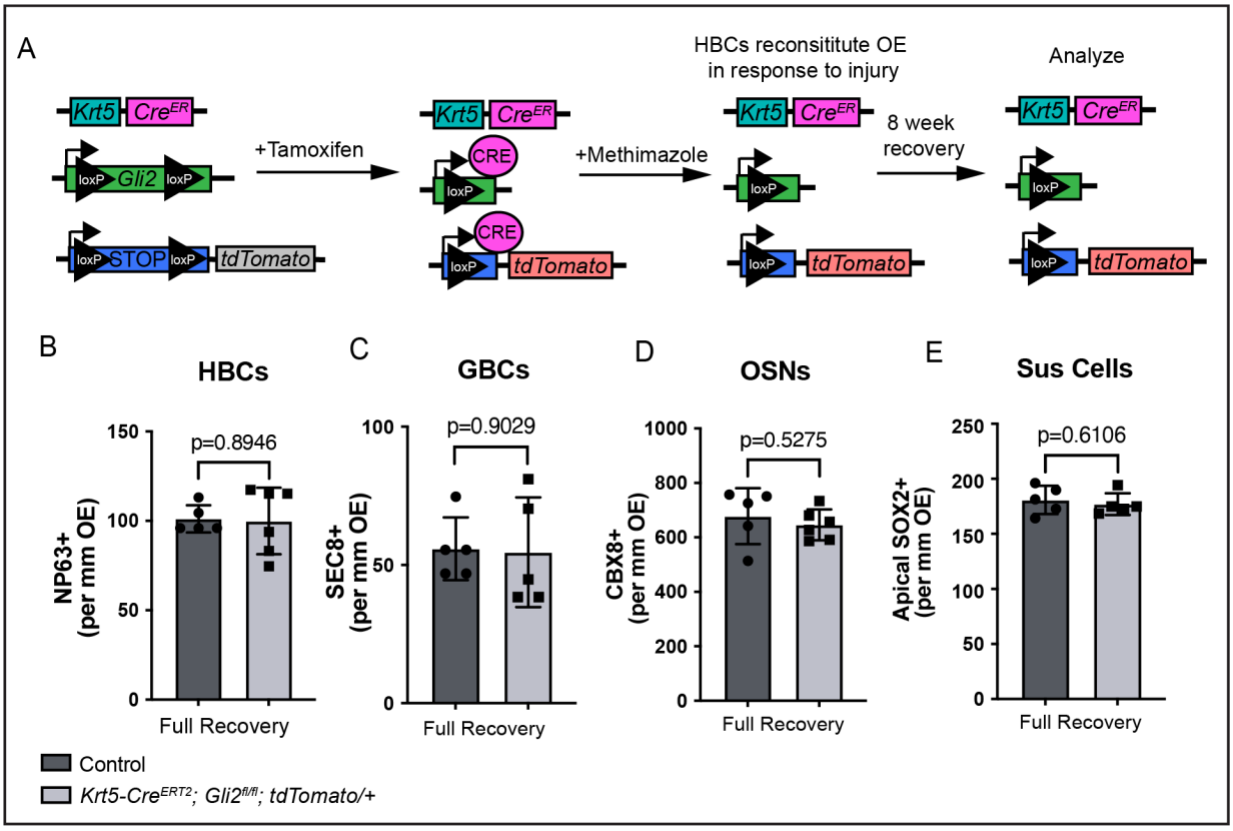
A
HBCs reconsititute OE in response to injury
Analyze
Krt5 CreER
loxP Gli2 loxP
loxP STOP loxP tdTomato
+Tamoxifen
CRE
+Methimazole
8 week recovery
B
HBCs
NP63+ (per mm OE)
p=0.8946
C
GBCs
SEC8+ (per mm OE)
p=0.9029
D
OSNs
CBX8+ (per mm OE)
p=0.5275
E
Sus Cells
Apical SOX2+ (per mm OE)
p=0.6106
Full Recovery
Control
Krt5-CreER2; Gli2fl/fl; tdTomato/+

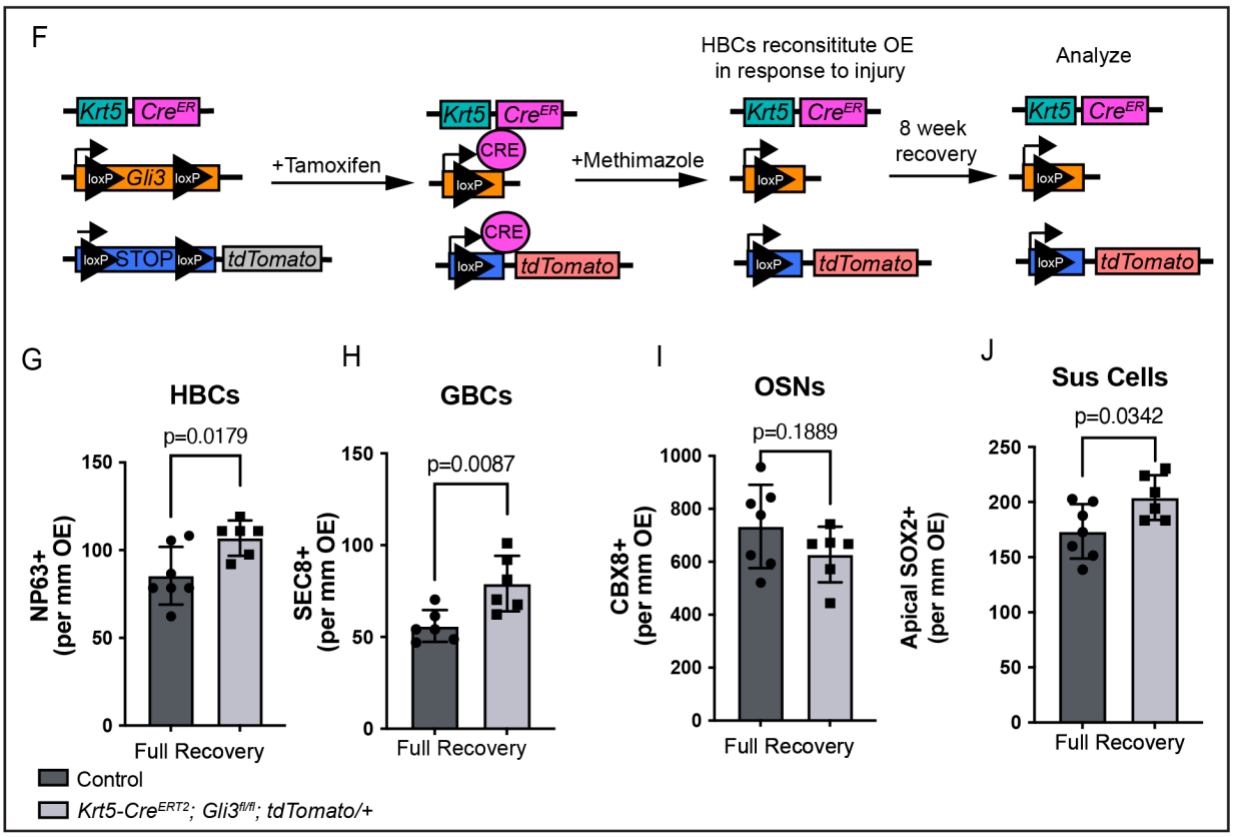
F
HBCs reconsititute OE in response to injury
Analyze
Krt5 CreER
loxP Gli3 loxP
loxP STOP loxP tdTomato
+Tamoxifen
CRE
+Methimazole
8 week recovery
G
HBCs
NP63+ (per mm OE)
p=0.0179
H
GBCs
SEC8+ (per mm OE)
p=0.0087
I
OSNs
CBX8+ (per mm OE)
p=0.1889
J
Sus Cells
Apical SOX2+ (per mm OE)
p=0.0342
Full Recovery
Control
Krt5-CreER2; Gli3fl/fl; tdTomato/+

Figure 2.12 HBC-specific individual *Gli3*, but not *Gli2* deletion results in improper OE regeneration.

(A, F) Cartoon of HBC-specific individual deletion of either *Gli2* or *Gli3*. Mice containing a *Krt5-Cre^{ER}* Cre allele were crossed with mice carrying either *Gli2$^{fl/fl}$* (A) or *Gli3$^{fl/fl}$* (F), alleles in addition to a *tdTomato* reporter allele. Upon tamoxifen administration (I.P., 100mg/kg for 5 consecutive days), mice were rested for 72 hours, then injured with methimazole (I.P., 75mg/kg) and allowed to recover for 8 weeks. Quantitation of HBCs (B), GBCs (C), OSNs (D), and Sus Cells (E) per mm of OE. n=5 control and n=6 *Krt5-Cre^{ER}*; *tdTomato/+*; *Gli2$^{fl/fl}$* animals analyzed. Control refers to *Krt5-Cre^{ER}*; *tdTomato/+*; *Gli2$^{fl/+}$* mice or mice lacking the *Krt5-Cre^{ER}* allele. Quantitation of HBCs (G), GBCs (H), OSNs (I), and Sus Cells (J) per mm of OE. n=7 control and n=6 *Krt5-Cre^{ER}*; *tdTomato/+*; *Gli3$^{fl/fl}$* animals analyzed. Control refers to *Krt5-Cre^{ER}*; *tdTomato/+*; *Gli3$^{fl/+}$* mice or mice lacking the *Krt5-Cre^{ER}* allele. Data are mean ± standard deviation. P-values were determined by a two-tailed unpaired t-test; n.s.= not significant ($p>0.05$).

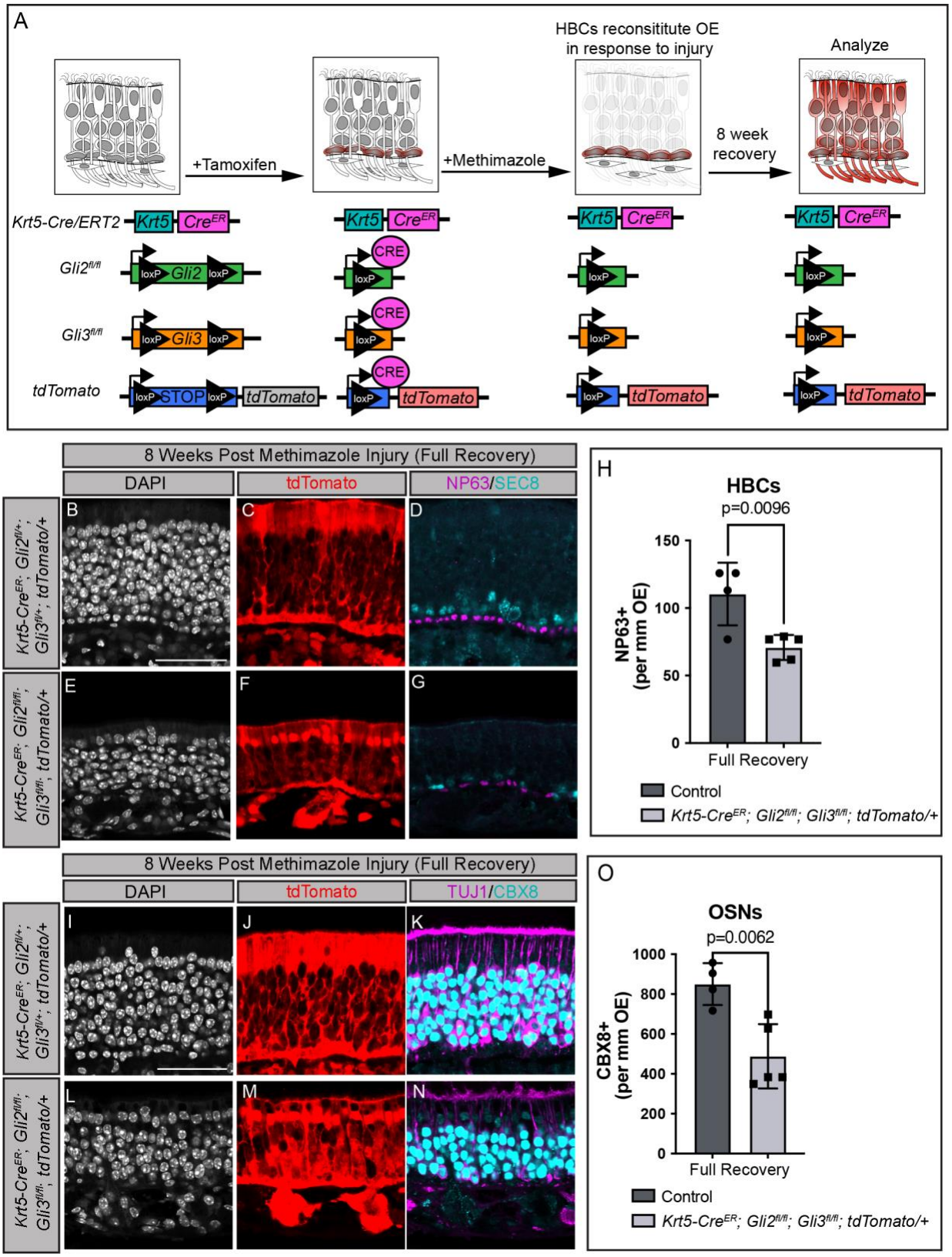
A
HBCs reconsititute OE in response to injury
Analyze
+Tamoxifen
+Methimazole
8 week recovery
Krt5-Cre/ERT2
Gli2fl/fl
Gli3fl/fl
tdTomato
Krt5
CreER
loxP
Gli2
Gli3
STOP
tdTomato
CRE
8 Weeks Post Methimazole Injury (Full Recovery)
DAPI
tdTomato
NP63/SEC8
TUJ1/CBX8
Krt5-CreER; Gli2fl/+; Gli3fl/+; tdTomato/+
Krt5-CreER; Gli2fl/fl; Gli3fl/fl; tdTomato/+
B
C
D
E
F
G
H
HBCs
p=0.0096
NP63+ (per mm OE)
150
100
50
0
Full Recovery
Control
Krt5-CreER; Gli2fl/fl; Gli3fl/fl; tdTomato/+
I
J
K
L
M
N
O
OSNs
p=0.0062
CBX8+ (per mm OE)
1000
800
600
400
200
0
Full Recovery
Control
Krt5-CreER; Gli2fl/fl; Gli3fl/fl; tdTomato/+

Figure 2.13 Simultaneous HBC-specific *Gli2* and *Gli3* deletion results in defective OE regeneration.

(A) Cartoon of tamoxifen-inducible HBC-specific *Gli2* and *Gli3* deletion. Mice carrying a *Krt5-Cre^{ER}* allele were crossed with mice containing *Gli2$^{fl/fl}$* and *Gli3$^{fl/fl}$* alleles as well as a *tdTomato* reporter allele. Tamoxifen administration induces Keratin 5 (*Krt5*)-expressing cells to drive *Gli2* and *Gli3* deletion and *tdTomato* expression. After tamoxifen administration (I.P., 100mg/kg for 5 consecutive days), mice were rested for 72 hours, then injured with methimazole (I.P., 75mg/kg) and allowed to recover for 8 weeks. (B-O) Coronal sections from adult mice collected 8 weeks following injury were analyzed with immunostaining for various OE markers. Antibodies directed against NP63 (magenta; D, G) mark HBCs, while antibodies directed against SEC8 (cyan; D, G) denote GBCs. Antibodies directed against Tuj1 (magenta; K, N) and CBX8 (cyan; K, N) mark OSNs. DAPI denotes nuclei (gray; B, E, I, L), scale bar (B, I), 50μm. Quantitation of HBC (H) and OSN (O) number per mm of OE. n=4 control and n=5 *Krt5-Cre^{ER}*; *tdTomato/+*; *Gli2$^{fl/fl}$*; *Gli3$^{fl/fl}$* animals analyzed. Endogenous tdTomato reporter immunofluorescence (red; C, F, J, M) demarcates HBCs and their lineages. Control animals refers to *Krt5-Cre^{ER}*;*tdTomato/+*;*Gli2$^{fl/+}$*;*Gli3$^{fl/+}$* mice or mice lacking the *Krt5-Cre^{ER}* allele. Data are mean ± standard deviation. P-values were determined by a two-tailed unpaired t-test; n.s.= not significant ($p>0.05$).

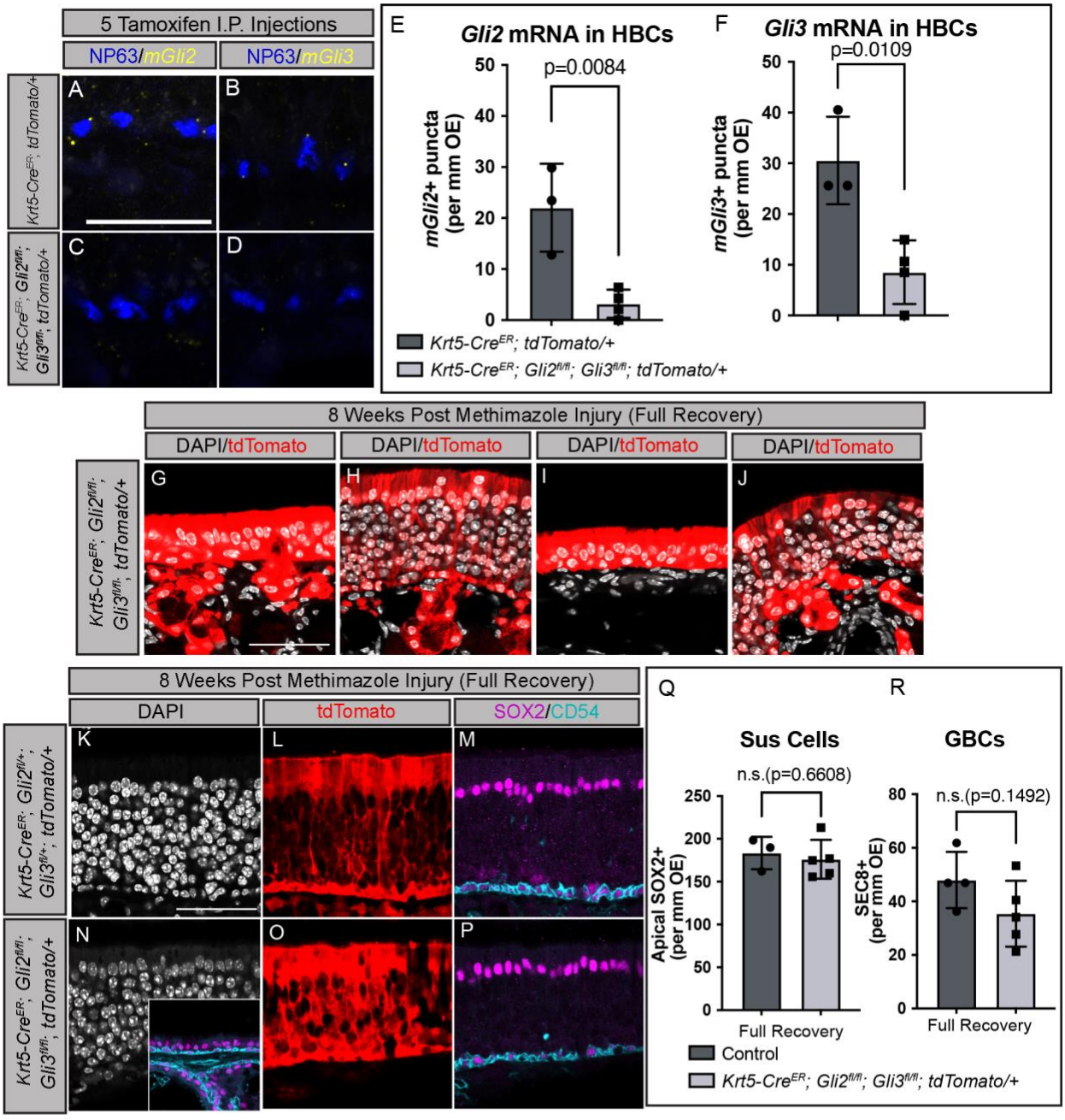

S	OE Cell Composition (Compared to Control)			
Genotype	HBCs	GBCs	OSNs	Sus
Gli2^{CKO}	No Change	No Change	No Change	No Change
Gli3^{CKO}	↑	↑	No Change	↑
Gli2/3^{CKO}	↓	↓	↓	No Change

Figure 2.14 Simultaneous HBC-specific Gli2 and Gli3 deletion results in defective OE regeneration.

(A-E) Coronal sections from adult *Krt5-Cre^{ER}*; *tdTomato/+*; *Gli2$^{fl/fl}$*; *Gli3$^{fl/fl}$* mice collected after 5 days of consecutive tamoxifen injections (I.P., 100mg/kg). Sections were treated with mRNA probes directed against endogenous *Gli2* (yellow; A, C) and *Gli3* (yellow; B, D). Antibodies directed against NP63 demarcate HBCs (blue; A-D). Quantitation of *Gli2* (E) puncta and *Gli3* (F) puncta adjacent to NP63+ nuclei. Scale bar (A), 25μm. Data are mean ± standard deviation. P-values were determined by a two-tailed unpaired t-test; n.s.= not significant (p>0.05). (G-P) Coronal sections from adult *Krt5-Cre^{ER}*; *tdTomato/+*; *Gli2$^{fl/fl}$*; *Gli3$^{fl/fl}$* mice collected 8 weeks following injury were analyzed with immunostaining for various OE markers. Mice lacking both *Gli2* and *Gli3* display a range of morphological phenotypes (G-J). Antibodies directed against SOX2 (magenta; M, P, inset in N) denote Sus cells apically, whereas antibodies directed against CD54 (cyan, M, P, inset in N) demarcate HBCs. DAPI denotes nuclei (gray; G-J, K, N), tdTomato marks HBCs and their progeny following injury (red; G-J, L, O), scale bar (G, K), 50μm. Quantitation of Sus cells (Q) and GBCs (R) per mm of OE. n=4 control and n=5 *Krt5-Cre^{ER}*; *tdTomato/+*; *Gli2$^{fl/fl}$*; *Gli3$^{fl/fl}$* animals analyzed. Control refers to *Krt5-Cre^{ER}*; *tdTomato/+*; *Gli2$^{fl/+}$*; *Gli3$^{fl/+}$* mice or mice lacking the *Krt5-Cre^{ER}* allele. Data are mean ± standard deviation. P-values were determined by a two-tailed unpaired t-test; n.s.= not significant (p>0.05). (S) Table summarizing OE cell composition in *Gli2^{CKO}*, *Gli3^{CKO}*, and *Gli2/3^{CKO}* mice compared to control mice. Green indicates increase in cell number, red indicates decrease, light gray indicates no change.

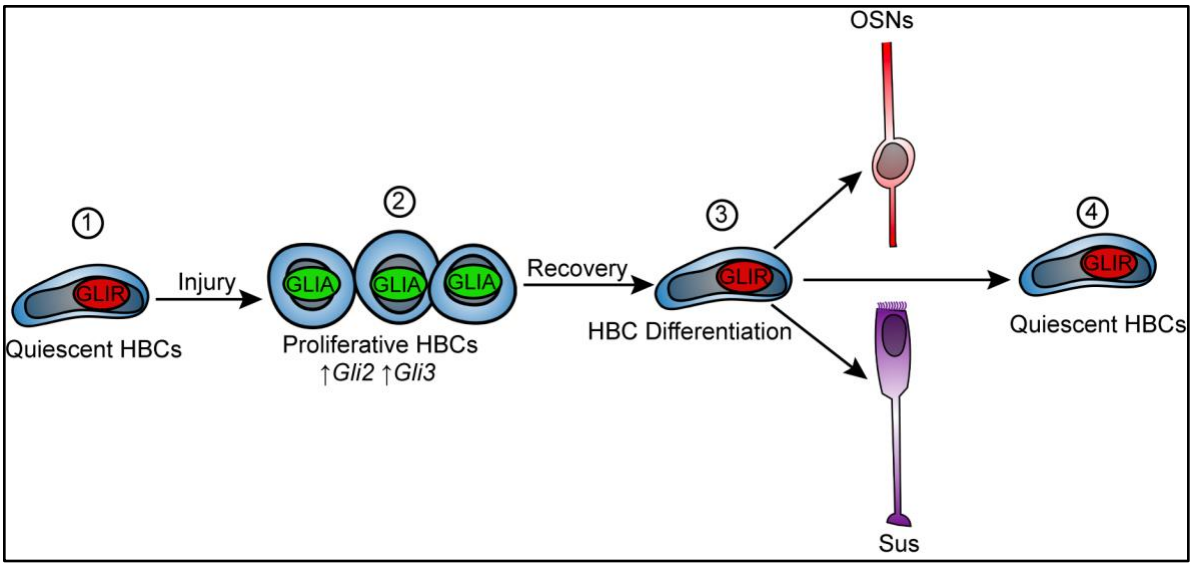

Figure 2.15 *Gli2* and *Gli3* play key roles in olfactory epithelium regeneration following injury.

Cartoon demonstrating the proposed role of *Glis* at homeostasis and following injury. (1) GLI2 and GLI3 are processed into transcriptional repressors (GLIR) in quiescent HBCs at homeostasis. (2) Following injury, *Gli2* and *Gli3* transcript is upregulated and GLI2 and GLI3 are processed into transcriptional activators (GLIA) as HBCs proliferate. (3) In order for HBCs to properly differentiate into mature OE cell types (OSNs and Sus cells) GLI2 and GLI3 are processed back to GLIR, which is maintained as the OE returns back to its normal state at full recovery (4).

2.8 References

Aziz, M., Goyal, H., Haghbin, H., Lee-Smith, W.M., Gajendran, M., and Perisetti, A. (2021). The Association of "Loss of Smell" to COVID-19: A Systematic Review and Meta-Analysis. Am J Med Sci *361*, 216-225.

Bai, C.B., Auerbach, W., Lee, J.S., Stephen, D., and Joyner, A.L. (2002). Gli2, but not Gli1, is required for initial Shh signaling and ectopic activation of the Shh pathway. Development *129*, 4753-4761.

Bai, C.B., and Joyner, A.L. (2001). Gli1 can rescue the in vivo function of Gli2. Development *128*, 5161-5172.

Blaess, S., Stephen, D., and Joyner, A.L. (2008). Gli3 coordinates three-dimensional patterning and growth of the tectum and cerebellum by integrating Shh and Fgf8 signaling. Development *135*, 2093-2103.

Briscoe, J., and Therond, P.P. (2013). The mechanisms of Hedgehog signalling and its roles in development and disease. Nat Rev Mol Cell Biol *14*, 416-429.

Chang, C.F., Chang, Y.T., Millington, G., and Brugmann, S.A. (2016). Craniofacial Ciliopathies Reveal Specific Requirements for GLI Proteins during Development of the Facial Midline. PLoS Genet *12*, e1006351.

Chen, M., Reed, R.R., and Lane, A.P. (2019). Chronic Inflammation Directs an Olfactory Stem Cell Functional Switch from Neuroregeneration to Immune Defense. Cell Stem Cell *25*, 501-513 e505.

Corrales, J.D., Blaess, S., Mahoney, E.M., and Joyner, A.L. (2006). The level of sonic hedgehog signaling regulates the complexity of cerebellar foliation. Development *133*, 1811-1821.

Diamond, I., Owolabi, T., Marco, M., Lam, C., and Glick, A. (2000). Conditional gene expression in the epidermis of transgenic mice using the tetracycline-regulated transactivators tTA and rTA linked to the keratin 5 promoter. J Invest Dermatol *115*, 788-794.

Durante, M.A., Kurtenbach, S., Sargi, Z.B., Harbour, J.W., Choi, R., Kurtenbach, S., Goss, G.M., Matsunami, H., and Goldstein, B.J. (2020). Single-cell analysis of olfactory neurogenesis and differentiation in adult humans. Nat Neurosci *23*, 323-326.

Ermilov, A.N., Kumari, A., Li, L., Joiner, A.M., Grachtchouk, M.A., Allen, B.L., Dlugosz, A.A., and Mistretta, C.M. (2016). Maintenance of Taste Organs Is Strictly Dependent on Epithelial Hedgehog/GLI Signaling. PLoS Genet *12*, e1006442.

Fletcher, R.B., Prasol, M.S., Estrada, J., Baudhuin, A., Vranizan, K., Choi, Y.G., and Ngai, J. (2011). p63 regulates olfactory stem cell self-renewal and differentiation. Neuron *72*, 748-759.

Garcia, A.D., Petrova, R., Eng, L., and Joyner, A.L. (2010). Sonic hedgehog regulates discrete populations of astrocytes in the adult mouse forebrain. J Neurosci *30*, 13597-13608.

Genter, M.B., Deamer, N.J., Blake, B.L., Wesley, D.S., and Levi, P.E. (1995). Olfactory toxicity of methimazole: dose-response and structure-activity studies and characterization of flavin-containing monooxygenase activity in the Long-Evans rat olfactory mucosa. Toxicol Pathol *23*, 477-486.

Gong, Q., Chen, H., and Farbman, A.I. (2009). Olfactory sensory axon growth and branching is influenced by sonic hedgehog. Dev Dyn *238*, 1768-1776.

Grachtchouk, M., Pero, J., Yang, S.H., Ermilov, A.N., Michael, L.E., Wang, A., Wilbert, D., Patel, R.M., Ferris, J., Diener, J., et al. (2011). Basal cell carcinomas in mice arise from hair follicle stem cells and multiple epithelial progenitor populations. J Clin Invest *121*, 1768-1781.

Graziadei, P.P., and Graziadei, G.A. (1979). Neurogenesis and neuron regeneration in the olfactory system of mammals. I. Morphological aspects of differentiation and structural organization of the olfactory sensory neurons. J Neurocytol *8*, 1-18.

Guo, Z., Packard, A., Krolewski, R.C., Harris, M.T., Manglapus, G.L., and Schwob, J.E. (2010). Expression of pax6 and sox2 in adult olfactory epithelium. J Comp Neurol *518*, 4395-4418.

Herrick, D.B., Guo, Z., Jang, W., Schnittke, N., and Schwob, J.E. (2018). Canonical Notch Signaling Directs the Fate of Differentiating Neurocompetent Progenitors in the Mammalian Olfactory Epithelium. J Neurosci *38*, 5022-5037.

Herrick, D.B., Lin, B., Peterson, J., Schnittke, N., and Schwob, J.E. (2017). Notch1 maintains dormancy of olfactory horizontal basal cells, a reserve neural stem cell. Proc Natl Acad Sci U S A *114*, E5589-E5598.

Hoffman, H.J., Rawal, S., Li, C.M., and Duffy, V.B. (2016). New chemosensory component in the U.S. National Health and Nutrition Examination Survey (NHANES): first-year results for measured olfactory dysfunction. Rev Endocr Metab Disord *17*, 221-240.

Huangfu, D., Liu, A., Rakeman, A.S., Murcia, N.S., Niswander, L., and Anderson, K.V. (2003). Hedgehog signalling in the mouse requires intraflagellar transport proteins. Nature *426*, 83-87.

Imamura, F., and Hasegawa-Ishii, S. (2016). Environmental Toxicants-Induced Immune Responses in the Olfactory Mucosa. Front Immunol *7*, 475.

Indra, A.K., Warot, X., Brocard, J., Bornert, J.M., Xiao, J.H., Chambon, P., and Metzger, D. (1999). Temporally-controlled site-specific mutagenesis in the basal layer of the epidermis: comparison of the recombinase activity of the tamoxifen-inducible Cre-ER(T) and Cre-ER(T2) recombinases. Nucleic Acids Res *27*, 4324-4327.

Joiner, A.M., Green, W.W., McIntyre, J.C., Allen, B.L., Schwob, J.E., and Martens, J.R. (2015). Primary Cilia on Horizontal Basal Cells Regulate Regeneration of the Olfactory Epithelium. J Neurosci *35*, 13761-13772.

Kong, J.H., Yang, L., Dessaud, E., Chuang, K., Moore, D.M., Rohatgi, R., Briscoe, J., and Novitch, B.G. (2015). Notch activity modulates the responsiveness of neural progenitors to sonic hedgehog signaling. Dev Cell *33*, 373-387.

Kumari, A., Ermilov, A.N., Allen, B.L., Bradley, R.M., Dlugosz, A.A., and Mistretta, C.M. (2015). Hedgehog pathway blockade with the cancer drug LDE225 disrupts taste organs and taste sensation. J Neurophysiol *113*, 1034-1040.

Kumari, A., Ermilov, A.N., Grachtchouk, M., Dlugosz, A.A., Allen, B.L., Bradley, R.M., and Mistretta, C.M. (2017). Recovery of taste organs and sensory function after severe loss from Hedgehog/Smoothened inhibition with cancer drug sonidegib. Proc Natl Acad Sci U S A *114*, E10369-E10378.

Leung, C.T., Coulombe, P.A., and Reed, R.R. (2007). Contribution of olfactory neural stem cells to tissue maintenance and regeneration. Nat Neurosci *10*, 720-726.

Liu, H.X., Ermilov, A., Grachtchouk, M., Li, L., Gumucio, D.L., Dlugosz, A.A., and Mistretta, C.M. (2013). Multiple Shh signaling centers participate in fungiform papilla and taste bud formation and maintenance. Dev Biol *382*, 82-97.

Long, F., Zhang, X.M., Karp, S., Yang, Y., and McMahon, A.P. (2001). Genetic manipulation of hedgehog signaling in the endochondral skeleton reveals a direct role in the regulation of chondrocyte proliferation. Development *128*, 5099-5108.

Madisen, L., Zwingman, T.A., Sunkin, S.M., Oh, S.W., Zariwala, H.A., Gu, H., Ng, L.L., Palmiter, R.D., Hawrylycz, M.J., Jones, A.R., et al. (2010). A robust and high-throughput Cre reporting and characterization system for the whole mouse brain. Nat Neurosci *13*, 133-140.

Marczenke, M., Sunaga-Franze, D.Y., Popp, O., Althaus, I.W., Sauer, S., Mertins, P., Christ, A., Allen, B.L., and Willnow, T.E. (2021). GAS1 is required for NOTCH-dependent facilitation of SHH signaling in the ventral forebrain neuroepithelium. Development *148*.

McDermott, A., Gustafsson, M., Elsam, T., Hui, C.C., Emerson, C.P., Jr., and Borycki, A.G. (2005). Gli2 and Gli3 have redundant and context-dependent function in skeletal muscle formation. Development *132*, 345-357.

Memmi, E.M., Sanarico, A.G., Giacobbe, A., Peschiaroli, A., Frezza, V., Cicalese, A., Pisati, F., Tosoni, D., Zhou, H., Tonon, G., et al. (2015). p63 Sustains self-renewal of mammary cancer stem cells through regulation of Sonic Hedgehog signaling. Proc Natl Acad Sci U S A *112*, 3499-3504.

Mistretta, C.M., and Kumari, A. (2019). Hedgehog Signaling Regulates Taste Organs and Oral Sensation: Distinctive Roles in the Epithelium, Stroma, and Innervation. Int J Mol Sci *20*.

Morrison, E.E., and Costanzo, R.M. (1989). Scanning electron microscopic study of degeneration and regeneration in the olfactory epithelium after axotomy. J Neurocytol *18*, 393-405.

Packard, A., Schnittke, N., Romano, R.A., Sinha, S., and Schwob, J.E. (2011). DeltaNp63 regulates stem cell dynamics in the mammalian olfactory epithelium. J Neurosci *31*, 8748-8759.

Peng, T., Frank, D.B., Kadzik, R.S., Morley, M.P., Rathi, K.S., Wang, T., Zhou, S., Cheng, L., Lu, M.M., and Morrisey, E.E. (2015). Hedgehog actively maintains adult lung quiescence and regulates repair and regeneration. Nature *526*, 578-582.

Petrova, R., and Joyner, A.L. (2014). Roles for Hedgehog signaling in adult organ homeostasis and repair. Development *141*, 3445-3457.

Rodriguez, S., Sickles, H.M., Deleonardis, C., Alcaraz, A., Gridley, T., and Lin, D.M. (2008). Notch2 is required for maintaining sustentacular cell function in the adult mouse main olfactory epithelium. Dev Biol *314*, 40-58.

Sasaki, H., Hui, C., Nakafuku, M., and Kondoh, H. (1997). A binding site for Gli proteins is essential for HNF-3beta floor plate enhancer activity in transgenics and can respond to Shh in vitro. Development *124*, 1313-1322.

Sasaki, H., Nishizaki, Y., Hui, C., Nakafuku, M., and Kondoh, H. (1999). Regulation of Gli2 and Gli3 activities by an amino-terminal repression domain: implication of Gli2 and Gli3 as primary mediators of Shh signaling. Development *126*, 3915-3924.

Schwob, J.E., Jang, W., Holbrook, E.H., Lin, B., Herrick, D.B., Peterson, J.N., and Hewitt Coleman, J. (2017). Stem and progenitor cells of the mammalian olfactory epithelium: Taking poietic license. J Comp Neurol *525*, 1034-1054.

Stasiulewicz, M., Gray, S.D., Mastromina, I., Silva, J.C., Bjorklund, M., Seymour, P.A., Booth, D., Thompson, C., Green, R.J., Hall, E.A., et al. (2015). A conserved role for Notch signaling in priming the cellular response to Shh through ciliary localisation of the key Shh transducer Smo. Development *142*, 2291-2303.

Vortkamp, A., Lee, K., Lanske, B., Segre, G.V., Kronenberg, H.M., and Tabin, C.J. (1996). Regulation of rate of cartilage differentiation by Indian hedgehog and PTH-related protein. Science *273*, 613-622.

Wang, C., Cassandras, M., and Peng, T. (2019). The Role of Hedgehog Signaling in Adult Lung Regeneration and Maintenance. J Dev Biol *7*.

Wang, C., de Mochel, N.S.R., Christenson, S.A., Cassandras, M., Moon, R., Brumwell, A.N., Byrnes, L.E., Li, A., Yokosaki, Y., Shan, P., et al. (2018). Expansion of hedgehog disrupts mesenchymal identity and induces emphysema phenotype. J Clin Invest *128*, 4343-4358.

Chapter 3 Summary and Future Directions

3.1 Summary of Key Findings

The data presented in Chapter 2 demonstrate a novel role for the HH transcription factors GLI2 and GLI3 in OE regeneration. Using gain-of-function and loss-of-function genetic approaches, I demonstrated that GLI2 and GLI3 regulate HBC proliferation and differentiation following OE injury.

I employed *lacZ* reporter mice and in situ hybridization to demonstrate that GLI transcription factors are expressed in the adult OE, specifically within HBCs and distinct subsets of Sus cells. Further, *Gli2* and *Gli3* expression is upregulated following methimazole injury to the OE. To extend these expression studies, I used a constitutively active form of GLI2 lacking the N-terminal repressor domain (GLI2ΔN) to activate HH signaling in HBCs. GLI2ΔN drives proliferation and alters cell identity in HBCs; *GLI2ΔN*-expressing HBCs are also defective in OSN differentiation following OE injury. These data suggest that GLI activator drives HBC proliferation and HBC differentiation to supporting cell types, but not OSNs. HBC-specific *Gli2* deletion does not result in any detectable phenotypes, although HBC-specific *Gli3* deletion only in HBCs results in increased numbers of HBCs, GBCs and Sus cells. Strikingly, combined *Gli2* and *Gli3* deletion in HBCs results in perturbed OE regeneration, including decreased HBCs, GBCs, and OSN numbers. These data suggest that GLI2 and GLI3 are necessary for HBC-mediated regeneration of the OE.

While my work primarily focused on GLI2 and GLI3 - the downstream effectors of the HH signaling pathway – in adult OE regeneration, a number of important questions remain

unexplored. Below I discuss a series of key outstanding questions, present preliminary data that informs the answers to these questions, and outline approaches to rigorously address these questions in the future.

3.2 Future Directions

3.2.1 Potential Roles for HH Ligands and Receptors in the Adult OE

While the data in Chapter 2 indicate that HH transcription factors are present and functional in HBCs, the roles for HH signaling pathway components upstream of GLIs in the OE remain unexplored. HH ligands have three mammalian paralogues – *Sonic hedgehog* (SHH), *Indian hedgehog* (IHH), and *Desert hedgehog* (DHH) (Echelard et al., 1993). Importantly, SHH expression has been defined in the olfactory bulb glomeruli, where axons from OSNs project to (Gong et al., 2009). To investigate if these ligands are present in the OE I used an *in situ* hybridization approach in adult uninjured OE, due to lack of reliable HH ligand antibodies (Figure 3.1). Since my data in Chapter 2 indicated that GLI2 and GLI3 are expanded 4 days following methimazole injury, I also examined *Shh* expression in injured mice (Figure 3.1). I was unable to detect *Shh* transcript in either uninjured or 4 day post-injury OE or stroma (Figure 3.1 A-H). I confirmed the specificity of the *Shh* probe by detection of *Shh* transcript in the glomeruli of the olfactory bulb (Figure 3.1 I-K). To corroborate these findings, I also examined $Shh^{lacZ/+}$ reporter mice both in uninjured and 4 days-post methimazole injury (Figure 3.1 L-O). Notably, most of the OE is BGAL negative except for a very rare $BGAL^{+}$ cell of unknown type (Figure 3.1 L-O). My preliminary data indicate there is no obvious source of *Shh*-producing cells in the OE or the stroma, though further studies are necessary to confirm these findings.

IHH is another potential HH ligand in the OE. The OE lies on top of bony turbinates, and bones express *Ihh* (St-Jacques et al., 1999). I used the same in situ hybridization approach to

examine *Ihh* transcript in uninjured OE and 4 days post-injury (Figure 3.1 P-S). Similar to the *Shh in situ* data, I did not detect *Ihh* in the OE in either uninjured or injured mice (Figure 3.1 P-S). I confirmed the specificity of the *Ihh* probe by positive detection of *Ihh* in the septum bone (Figure 3.1 T). In short, my data indicates that *Ihh* transcript is not expressed in the OE at homeostasis and at 4 days post-injury.

Another HH paralog is *Desert Hedgehog* (DHH), which has not been explored in the OE. *Dhh* is expressed in Schwann cells and is important for nerve sheath formation (Mirsky et al., 1999; Parmantier et al., 1999). Importantly, the OE contains olfactory ensheathing cells (OECs) that wrap OSNs and are necessary for proper regeneration of OSNs (Barber and Lindsay, 1982; Field et al., 2003; Schwob et al., 1992). Using the same *in situ* hybridization approach as described above, I can examine *Dhh* expression in the OE, paying close attention to the OECs. Given *Dhh*'s previously described function in sheathing cells, it is possible that *Dhh* could be playing a similar role in the OE.

The lack of either *Shh* or *Ihh* transcript in the OE could have several explanations. It is possible that they are never expressed in the adult OE and that GLI2 and GLI3 function independently of canonical HH signaling. One way to confirm this would be to examine the function of *Smo* in GLI-expressing cells, since HH ligand is necessary for the de-repression of *Smo*. To do this, I can breed *Keratin5CreER* and $Smo^{fl/fl}$ mice together to generate mice lacking *Smo* in their HBCs (Smo^{CKO}). Following tamoxifen treatment, I can injure Smo^{CKO} mice with methimazole and investigate the impact of *Smo* conditional deletion on HBC-mediated regeneration of the OE. Given that I have yet to find a source of HH ligand in the OE, I predict that GLIs are most likely working independently of canonical HH signaling. If there are no significant phenotypes, then it would stand to reason that GLI2 and GLI3 in HBCs may work

independently of canonical HH ligands. Then, it is possible that other upstream signaling pathways modulate GLI2 and GLI3 in HBCs. In this case, investigating other signaling pathways in GLI2ΔN and *Gli2/3*^{CKO} animals could be helpful. Notch signaling would be a good candidate of study since Notch signaling pathway components are expressed in HBCs and play important roles in OE regeneration (Herrick et al., 2018; Herrick et al., 2017). Additionally, Notch signaling has been demonstrated to direct HH morphogen activity in the developing ventral spinal cord (Kong et al., 2015), indicating that crosstalk between these two pathways is possible. Investigating Notch pathway components in GLI2ΔN and *Gli2/3*^{CKO} mice can elucidate this possible interaction further.

While *Shh* and *Ihh* transcripts are not expressed by cells in the adult OE, it is possible that HH ligands are being delivered to the OE from another source. One way I attempted to address this was analyzing *Shh*^{EGFP}*Cre; tdTomato/+* mice (Harfe et al., 2004)(Figure 3.2). This allele labels all *Shh* expressing cells and their progeny starting at embryonic development at E10 (Harfe *et al.*, 2004). I discovered that *Shh* lineages are present in the OE, and colocalize with HBC and Sus cell markers (Figure 3.2). Additionally, there are CD54 and SOX2 negative lineages present in the OE as well, which could be GBCs or OSNs (Figure 3.2). There are also *Shh* lineages present in the underlying stroma (Figure 3.2). While this data is certainly interesting, it is hard to conclude when exactly *Shh* was expressed in these cells, or if these cells are distant progeny of other *Shh* expressing cells. To better address this question, I can use a tamoxifen inducible *ShhCre*^{ER} crossed into a *tdTomato* reporter and induce expression in adult mice (Harfe *et al.*, 2004). This would also allow for temporal control of labeling *Shh*-expressing cells and follow up with methimazole injury to examine if there is expansion of *Shh*+ cells afterwards.

Another HH signaling pathway component of interest is *Ptch1* – a HH signaling pathway receptor. PTCH1 is a negative regulator of the HH signaling pathway, and a downstream target (Briscoe and Therond, 2013). To investigate if *Ptch1* is expressed in adult OE, I utilized *Ptch1*$^{lacZ/+}$ reporter mice and examined expression with XGAL. Unlike *Gli2* and *Gli3* expression, *Ptch1* expression in adult uninjured OE is quite broad (Figure 3.3 A-B). Particularly, there is heavy XGAL expression in the middle regions of the OE, where the OSNs reside (Figure 3.3 A-B). Also of note, expression of *Ptch1* appears heavier dorsally, and is also present in the underlying stroma like *Gli1* (Figure 3.3 A-B). Even more interesting is that *Gli1*, also a HH target gene, is exclusively stromal (see Chapter 2), while *Ptch1* has a much broader expression in the OE (Figure 3.3 A-B). One potential interpretation of this data is that *Ptch1* is acting as a repressor of the HH signaling pathway in homeostatic conditions. To examine this, I injured *Ptch1*$^{lacZ/+}$ reporter mice with methimazole and examined *Ptch1* expression by XGAL staining 4 days post-injury (Figure 3.3 C-D). Interestingly, no *Ptch1* expression was detected in the OE following methimazole injury (Figure 3.3 C-D). This is the opposite of *Gli2* and *Gli3* expression following methimazole injury, which is expanded (see Chapter 2). This result would fit with the notion that GLI2 and GLI3 function independently of HH signaling, since typically high HH signaling results in higher expression of HH targets *Gli1* and *Ptch1* (Briscoe and Therond, 2013), but both are notably absent from the OE following injury (see Chapter 2 and Figure 3.3C-D). To follow up on these studies, looking at later injury recovery time points, such as 8 weeks, would be informative to see if *Ptch1* levels return to baseline as HBCs become more quiescent. I predict that as the OE recovers from methimazole injury, *Ptch1* expression will return to normal as OSNs mature. Overall, my preliminary data suggests that *Ptch1* could have interesting and important roles in OE regeneration.

One way to examine *Ptch1* function in the OE would be to use a *Ptch* conditional deletion allele, *Ptch1*$^{fl/fl}$ (Uhmann et al., 2007). Since *Ptch1* is most strongly expressed in OSNs, I can achieve OSN-specific *Ptch1* deletion using an *OMPCre*^{ER} allele which is tamoxifen inducible and can target mature OSNs in adult mice (Holl, 2018). Then, I can examine the consequences of OSN-specific *Ptch1* deletion on OSNs both in homeostatic and in injury conditions (Figure 3.3 E). Prior to injury, I can examine if *Ptch1* deletion has any effect on OSN function by utilizing electroolfactograms (EOGs) (Scott and Scott-Johnson, 2002) (Figure 3.3 F). EOGs measure the electrical output from mOSNs in response to smell stimuli (Scott and Scott-Johnson, 2002) (Figure 3.3 F). If *Ptch1* plays a functional role in mOSN smell signal transduction, then I can expect aberrant EOG results. I can also examine the effect of *Ptch1* deletion on OE regeneration of OSNs following methimazole injury. Since *Ptch1* is expressed in discrete regions of the OE, I predict that dorsal areas of the OE will be adversely affected by this conditional deletion, where there is the strongest XGAL staining (Figure 3.3 A-B). It would be interesting to compare these results with my *Gli2/3*^{CKO} data, which indicated that GLI2 and GLI3 are necessary for proper OE regeneration.

To summarize, the role of HH ligands and receptors remains to be explored in the OE. My work in Chapter 2 details the function of GLI2 and GLI3 in HBCs but if these GLIs are working in a ligand dependent or independent manner remains to be answered. Fortunately, we have many genetic tools at our disposal to ask interesting and directed questions about upstream HH signaling in the OE, as detailed above.

3.2.2 Roles for HH Signaling in the Stroma Underlying the Adult OE

A relatively unexplored part of the OE is the stroma underneath the basement membrane, also known as the lamina propria. The stroma is highly vascularized, allowing for quick drug

delivery to the nasal epithelium (Stott et al., 1983). Additionally, the stroma is an important source of inflammatory cytokines and defense against invading parasites (Imamura and Hasegawa-Ishii, 2016). Inflammation from severe infections, and other factors, can result in conditions like chronic sinusitis, which can lead to anosmia (loss of smell) (Kern, 2000). Studies have examined the stroma in chronic inflammatory rhinosinusitis models of mice and demonstrated that the immune system can directly affect HBCs and the OE (Chen et al., 2017; 2019). This leads to a plethora of questions about the stroma, the immune system, and how they function together to maintain and support the OE.

The nature of the fibroblasts in the stroma is a matter of debate. Some studies have described them as "ectomesenchymal" and having stem cell like properties (Delorme et al., 2010; Rui et al., 2016). Whether or not the fibroblasts in the stroma are stem cells, it is certainly possible that they could play important roles in OE maintenance. Particularly, it is possible that stromal fibroblasts function in immune infiltration as well. Recent work from our lab showed that *Gli*-expressing fibroblasts promote immune infiltration and macrophage migration in the context of pancreatic cancer (Scales et al., 2022). It is important to note that my data in Chapter 2 indicated that *Gli1*, *Gli2*, and *Gli3* are expressed in the stroma underlying the OE, suggesting that fibroblasts in the stroma underlying the OE could function in a similar way.

To test this, I can utilize a *PdgfraCre*^{ER} mouse line to target the fibroblasts in the stroma (Chung et al., 2018). I have done some preliminary characterization of this allele and demonstrated its expression with a *tdTomato* reporter allele (Figure 3.4). In vehicle treated mice, there was very little leakiness of the *Cre* (Figure 3.4 A-E), whereas in tamoxifen treated mice, there was robust *tdTomato* expression in the stroma (Figure 3.4 F-J). I can then cross in this allele to *Gli2*$^{fl/fl}$ and *Gli3*$^{fl/fl}$ mice to conditionally delete *Gli2* and *Gli3* from stromal fibroblasts

and examine their effect on the OE both prior and following injury (Figure 3.4 K). Similarly, I can target *Smo* using $Smo^{fl/fl}$ mice and examine the effect of loss of *Smo* in the context of homeostasis and regeneration (Figure 3.4 L). To examine potential roles for stromal fibroblasts in inflammation and immune infiltration, I can cross these *Gli*- or *Smo*-deficient mice to the chronic rhinosinusitis mouse model described in (Chen *et al.*, 2019). I can then examine the impact on immune populations using a combination of immunofluorescence and FLOW cytometry. Based on work published from our lab showing that *Gli2* and *Gli3* deletion results in increased T cell infiltration in the pancreas (Scales *et al.*, 2022), I predict a similar phenotype in the proposed experiments above.

3.2.3 HH Signaling in Regenerative Epithelia – Not a Straightforward Tale

The olfactory epithelium is a regenerative epithelium, and one of only a few sites of adult neurogenesis (Graziadei, 1973; Graziadei and Graziadei, 1979). The specialized stem cells in the OE make this possible and are the reason why we retain our sense of smell throughout our lifetime (Schwob et al., 2017). These characteristics make the OE truly a unique system to study not only olfaction but also stem cell biology and regeneration. Similarly, the lingual epithelium also contains basal cells that are necessary for taste bud regeneration (Miura and Barlow, 2010). Like the OE, the tongue is a sensory epithelium that is responsible our sense of taste. Taste and smell together, combined with higher processing in the brain, join to create our perception of flavor (Spence, 2015).

The lingual epithelium also heavily relies on HH signaling for proper taste bud regeneration and maintenance (see Chapter 1). What remains interesting about the taste and smell epithelia is how differently HH signaling appears to function in both. In the taste epithelium, expressing a dominant-negative GLI2ΔC4 transgene, a truncated form of GLI2

lacking the activator domain, in basal cells results in loss of taste buds and loss of proliferation (Ermilov et al., 2016). Since activating the HH signaling pathway with GLI2ΔN caused increased proliferation in the OE (see Chapter 2), I was curious if using the opposite transgenic model (GLI2ΔC4) would result in loss of proliferation, like in the taste epithelium. Using the same transgenic mouse line, I expressed GLI2ΔC4 in HBCs and challenged the HBCs with a methimazole injury 24 hours after doxycycline induction (Figure 3.5 A). I collected the OE from control and experimental GLI2ΔC4 mice 7 days following methimazole injury (Figure 3.5 A). Interestingly, there were no significant phenotypes at 7 days post-injury (Figure 3.5 B-E). HBC, GBC, Sus cell, and OSN numbers were all slightly down but not significantly (Figure 3.5 B-E). This suggests that HBCs expressing GLI2ΔC4 are still able to properly proliferate and differentiate into different OE cell types following methimazole injury. The observed phenotypes in GLI2ΔC4 mice were very minor, if not nonexistent, compared to what was observed in the taste epithelium. This suggests that repressing HH signaling using GLI2ΔC4 is not sufficient to abrogate HBC function at early regeneration.

Several follow-up studies can be conducted to validate the findings in Figure 3.5. Perhaps most important is the validation of *GLI2ΔC4* transgene induction in the OE. Fortunately, I was able to confirm that the *GLI2ΔC4* transgene in my mouse colony was induced in the tongue through a collaboration with Dr. Archana Kumari in the Mistretta lab (Figure 3.5 F). She was able to detect atypical taste buds in *K5rtTA; GLI2ΔC4* mice following 3 weeks of DOX induction in tongues of mice that I collected (Figure 3.5 F), echoing already published studies (Ermilov *et al.*, 2016). What remains to be resolved is if this transgene is working just as robustly in the OE. One way to confirm this would be to detect the *GLI2ΔC4* transgene with FLAG

antibody staining or FLAG qPCR primers, since this transgene has a FLAG epitope tag (Figure 3.5 A).

Another approach would be to express GLI2ΔC4 for 8 weeks following injury and examine the effect of dominant-negative GLI2 on full OE recovery. Since combinatorial loss of GLI2 and GLI3 in HBCs shows significant phenotypes at 8 weeks – it is possible that this is the time point at which GLI2ΔC4 mice will display defects in OE regeneration. If no phenotypes are observed, then it is possible that GLIs in the OE function primarily in the repressor state. This would fit with the data I collected in Chapter 2 which suggest GLIs are only transiently in their activator form, since overexpression of GLI2A (GLI2ΔN) results in hyperproliferation and abrogated cell identities. To follow up, I can use several different approaches to test whether GLIs are endogenously in their repressor or activator form in the OE.

To examine the post-translational processing of GLIs in the OE, I can collect OE lysates from uninjured, acutely injured (4 days-post methimazole injury), and fully recovered (8 weeks post-methimazole injury) mice. Then I can run the lysates out on a Western gel and blot for endogenous GLI2 and GLI3 levels. If my prediction is correct, then both GLI2 and GLI3 will be primarily in their smaller, truncated repressor form when the OE is uninjured and when fully recovered. Opposingly, during acute regeneration (4 days-post methimazole injury) they will be primarily in their full-length activator forms. Some technical hurdles apply with this experiment 1) it is difficult to find reliable endogenous antibodies for GLI2 and GLI3 and 2) possible contamination from the stroma underlying the OE which also contains GLI2 and GLI3. To address point 1, I can utilize epitope tagged *Gli2*$^{HA/HA}$ and *Gli3*$^{FLAG/FLAG}$ mice that we have generated in the lab, allowing me to use HA and FLAG antibodies to detect GLI2 and GLI3

respectively. To address point 2, I can purify out stromal cells that also express GLI2 and GLI3 by using anti-PDGFRα-conjugated magnetic beads, which can bind to stromal cells.

The *Gli2*$^{HA/HA}$ and *Gli3*$^{FLAG/FLAG}$ epitope tagged experimental system can be taken even further in the context of OE regeneration. For example, in my GLI2ΔN experiments I observed an increase of NP63^{+} cells and conversely in *Gli2/3*^{CKO} experiments I observed a decrease in NP63^{+} cells (Chapter 2). This suggested to me that GLI2, and possibly GLI3, could potentially modulate NP63 gene transcription. My hypothesis is that GLI2 and GLI3 can modulate NP63 gene transcription by binding to regions upstream of the NP63 gene during OE regeneration in order to stimulate HBC proliferation. To test this, I can purify OE from *Gli2*$^{HA/HA}$ and *Gli3*$^{FLAG/FLAG}$ uninjured and methimazole lesioned mice and proceed with ChIP sequencing. Using ChIP-seq, I can examine where GLI2 and GLI3 are binding both in the context of regeneration and during homeostasis. Even if my prediction is incorrect, data from these experiments can elucidate where GLI2 and GLI3 are binding in HBCs, furthering our understanding of what GLI transcription factors are doing on a molecular level in HBCs.

To summarize, my preliminary data using GLI2ΔC4 to drive GLI2R is drastically different to what has been described in the tongue using the same mouse model. Additional studies in the tongue utilized a pharmacological inhibitor of the HH signaling pathway, LDE225 and also saw loss of taste buds, in addition to loss of taste sensation (Kumari et al., 2015; Kumari et al., 2017). LDE225 inhibits the HH signaling pathway by antagonizing SMO (Pan et al., 2010). Using LDE225 in the OE can help elucidate if canonical SMO-mediated HH signaling is necessary in the OE. The benefit of using pharmacological inhibition of SMO, rather than the genetic experiments using *Smo*$^{fl/fl}$ mice that were outlined above, is that LDE225 would target the entire OE. I can then examine the impact of SMO inhibition during maintenance and

regeneration. Since LDE225 will target the whole OE, I can use both methimazole to examine HBC-mediated regeneration and bulbectomy to target GBC-mediated regenerated. Given that this is a global inhibition of HH signaling, I expect to see defects in regeneration using either lesion model in the OE.

The OE is not the only regenerative epithelium that relies on basal stem cells. For example, the respiratory epithelium also contains basal NP63^{+} cells that have stem cell capabilities, like the HBCs in the OE (Wang et al., 2002). Despite this similarity, HH signaling plays an entirely different role in the respiratory epithelium and maintains quiescence in the lung (see Chapter 1), whereas HH signaling promotes proliferation in the OE (see Chapter 2). Perhaps these differences can be attributed to the fact that the OE is a sensory epithelium designed to optimally suss out odors in the air, while the respiratory epithelium is designed for maximum oxygen absorption by the blood. Regardless of the mechanism, HH signaling is important for both of these regenerative epithelia.

In summary, the data presented in this thesis describe functional roles for GLI proteins in OE regeneration and highlight the diverse employment of HH/GLI signaling across multiple epithelia. This work also has implications for therapeutic approaches to treat patients suffering from olfactory disorders.

3.3 Figures

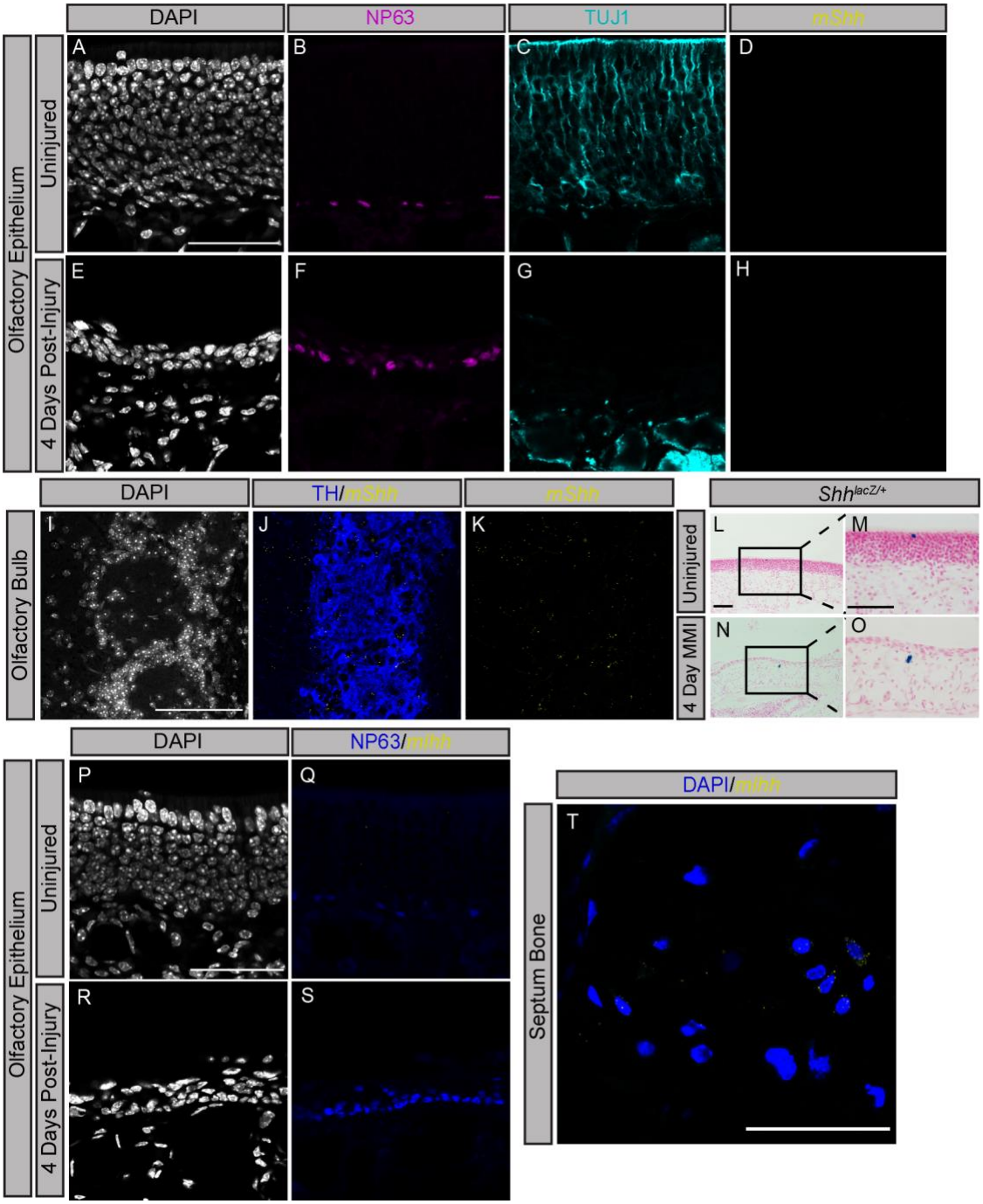

Figure 3.1 *Shh* and *Ihh* RNA are not Expressed in the Olfactory Epithelium

(A-T) Adult wildtype or *Shh*$^{lacZ/+}$ mice were either collected at 6-8 weeks of age or injured with a 75mg/kg IP injection of methimazole. Coronal sections were collected from the heads of either

uninjured (A-D, I-M, P-Q, T) or 4 days post methimazole injury mice (E-H, N-O, R-S). Antibodies directed against NP63 demarcate HBCs (B, F; magenta, Q, S, blue), TUJ1 mark OSNs (C, G; cyan), and tyrosine hydroxylase marks glomeruli (J; blue). *In situ* hybridization detection of HH ligand transcripts using a mouse *Shh* probe (D, H, K; yellow) and a mouse *Ihh* probe (Q, S, T; yellow). X-GAL staining of $Shh^{lacZ/+}$ mice (L-O). DAPI denotes nuclei (A, E, I, P, R; gray, T; blue). Scale bars=50μm (A, I, L, M, P, T).

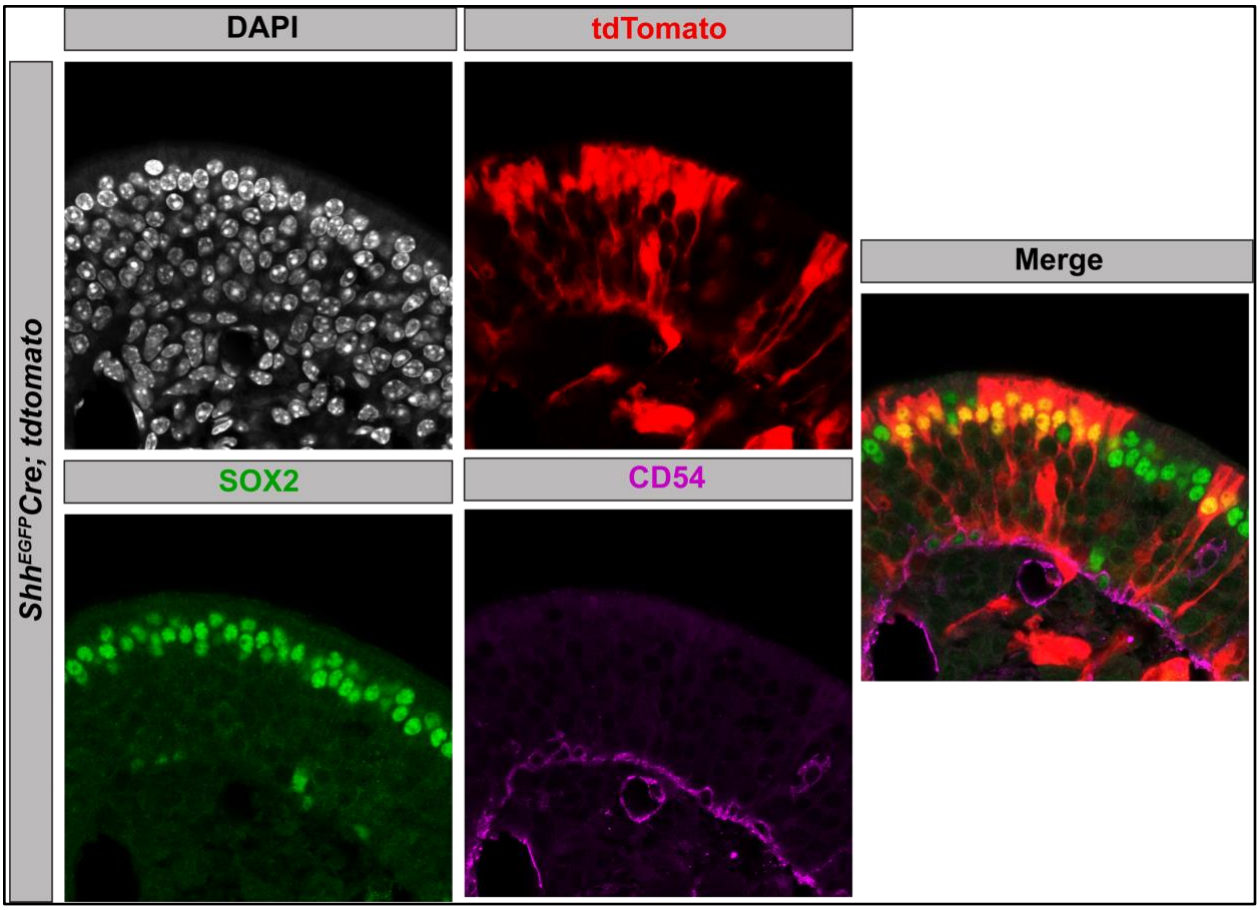

Figure 3.2 *Shh*+ Lineages are Present in the Adult Olfactory Epithelium

Adult *Shh*^{EGFP}*Cre; tdTomato/+* mice were collected at 6-8 weeks of age. Coronal sections were treated with antibodies directed against SOX2 (green) demarcating Sus cells apically or CD54 (magenta) marking HBCs. Merged image of tdTomato, SOX2, and CD54 staining on the far right. DAPI (gray) denotes nuclei.

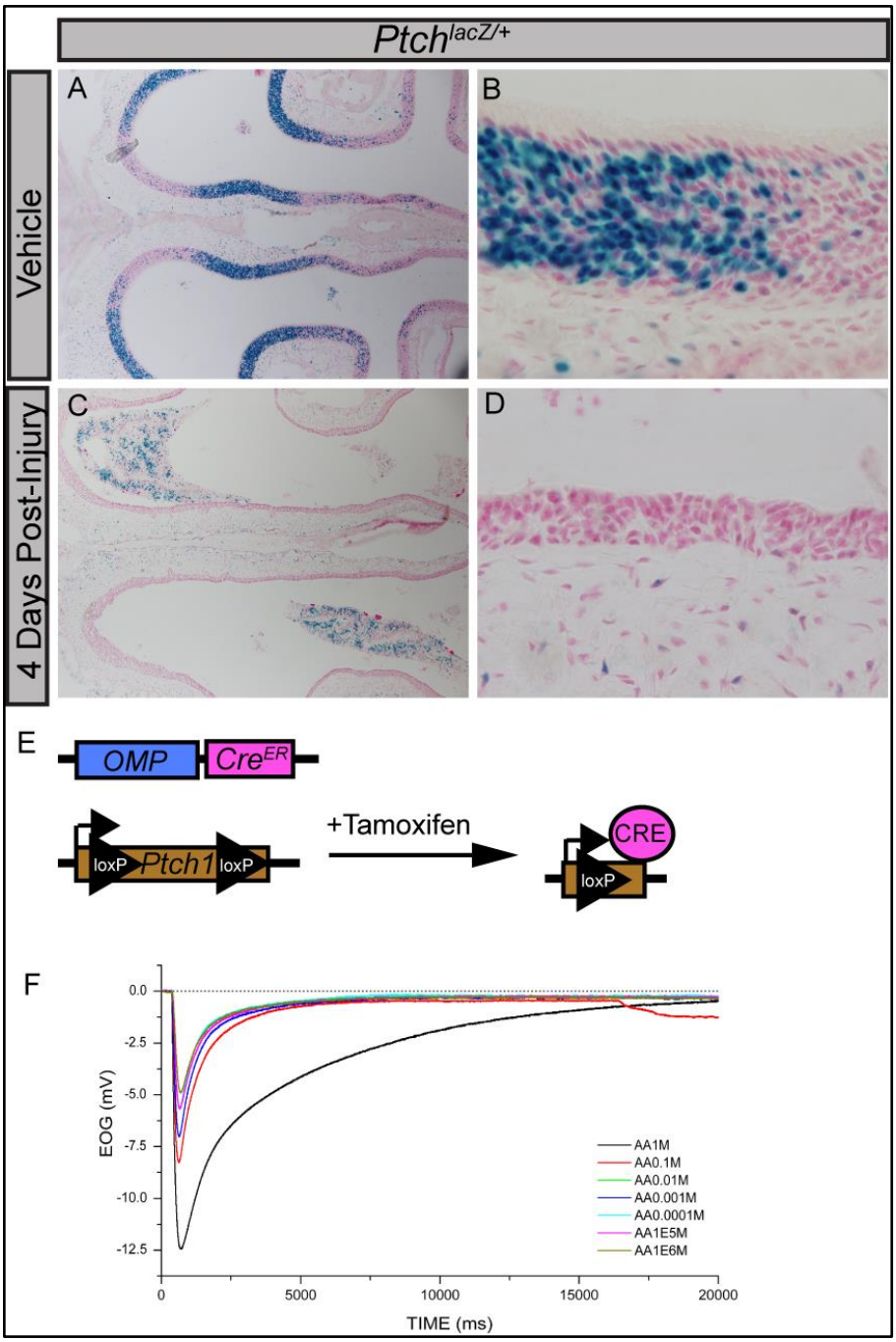

Figure 3.3 *Ptch* Expression in the Adult Olfactory Epithelium

(A-D) Adult *Ptch1*$^{lacZ/+}$ mice were either collected at 6-8 weeks of age (A-B) or injured with a 75mg/kg IP injection of methimazole (C-D). Coronal sections were treated with XGAL overnight at 37 °C. Blue staining indicates XGAL^{+} cells (A-D). Proposed scheme for conditional deletion of *Ptch* in OSNs (E). Example electroolfactogram (EOG), collected in collaboration with Dr. Robert Bradely and Dr. Hajime Sato in the Bradley lab (F).

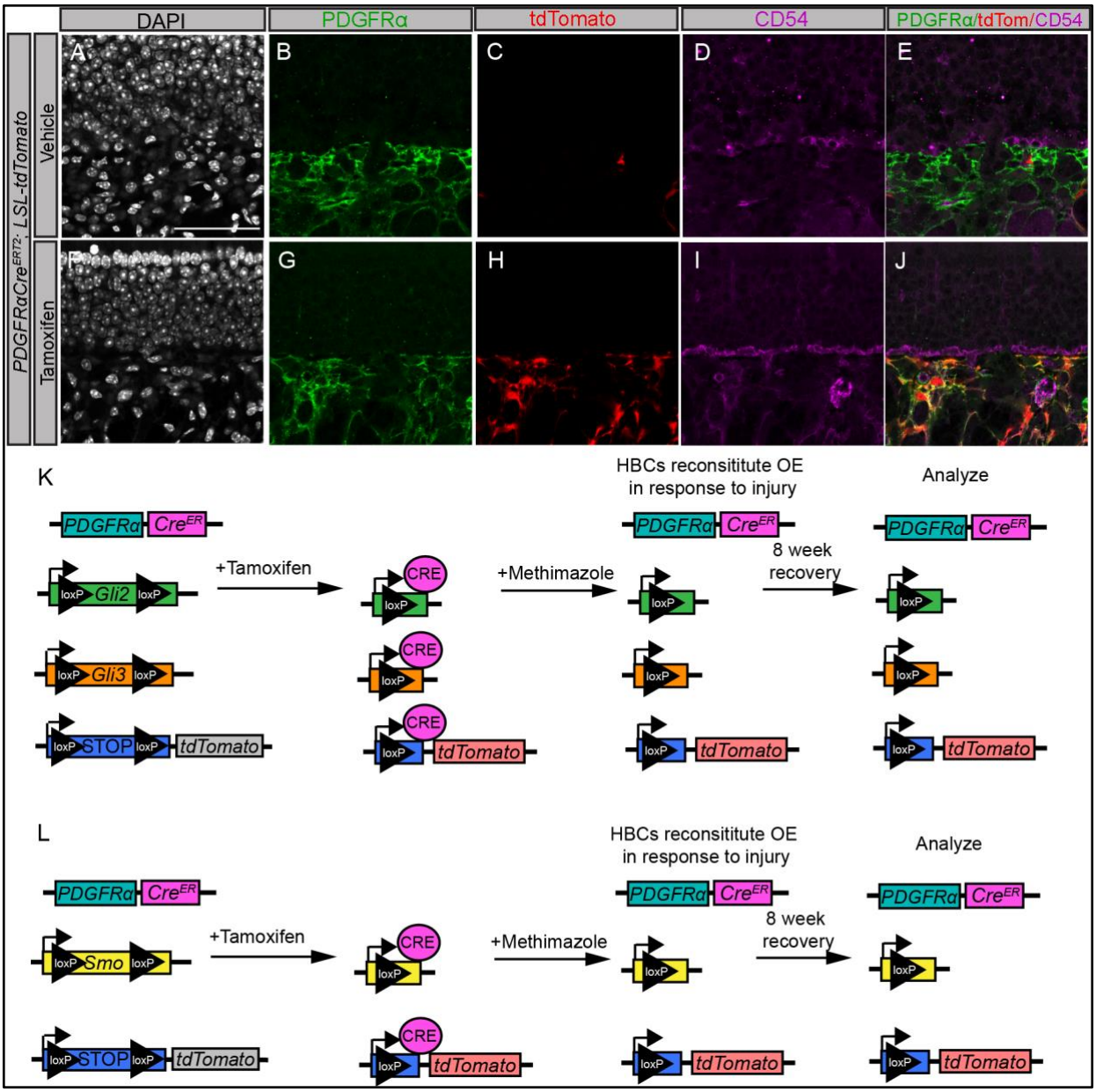

Figure 3.4 Using *PdgfrαCre^{ER}* to Target Stromal Cells in the Nose.

Adult *PdgfrαCre^{ER}*; *tdTomato*/+ mice were collected at 6-8 weeks of age after 5 days of either corn oil injections (A-E, vehicle) or 100mg/kg tamoxifen injections (P-J). Coronal sections were treated with antibodies against PDGFRα (B, G; green) marking fibroblasts and CD54 (D, I; magenta) marking HBCs. Scale bar=50μm. Cartoon depicting experimental scheme for targeted GLI2 and GLI3 deletion in stroma (K) and SMO deletion in stroma (L).

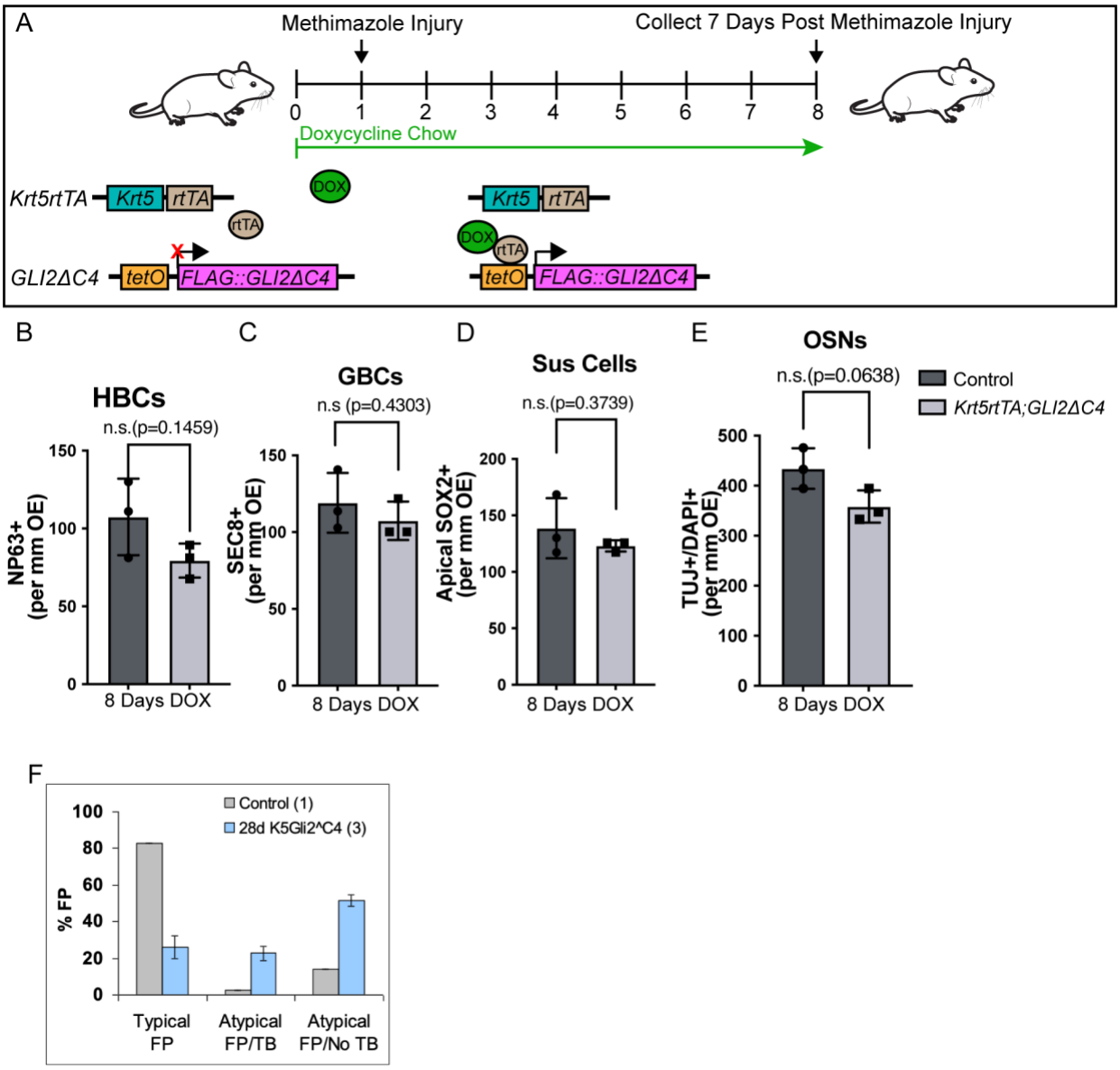

Figure 3.5 Expression of a Constitutive GLI repressor in HBCs does not alter OE regeneration.

A) Cartoon of *Gli2ΔC4* transgene activation using a doxycycline-inducible mouse model. Upon doxycycline (DOX, green) administration, mice carrying a Keratin 5 reverse tetracycline transactivator (Krt5-rtTA, blue) transgene and a tet-regulated FLAG-tagged GLI2ΔC4 transgene (pink) express constitutively active GLI2ΔC4 specifically in HBCs of the OE. 1 day following doxycycline induction, mice are injured with a 75mg/kg intraperitoneal (IP) injection of methimazole. Following methimazole injury, mice are kept on doxycycline and collected 7 days following injury. Quantitation of HBCs (B), GBCs (C), Sus cells (D), and OSNs (E) in mice at 7 days following injury. n=3 control and n=3 *Krt5rtTA*; *Gli2ΔC4* animals analyzed. Control animals refers to mice containing either the *Krt5rtTA* or *Gli2ΔC4* transgene. Data are mean ± standard deviation. P-values were determined by a two-tailed unpaired t-test; n.s.= not significant

($p>0.05$). Tongues collected from *Krt5rtTA*; *GLI2ΔC4* mice treated with DOX for 3 weeks were analyzed by Dr. Archana Kumari (F).

3.4 References

Barber, P.C., and Lindsay, R.M. (1982). Schwann cells of the olfactory nerves contain glial fibrillary acidic protein and resemble astrocytes. Neuroscience *7*, 3077-3090.

Briscoe, J., and Therond, P.P. (2013). The mechanisms of Hedgehog signalling and its roles in development and disease. Nat Rev Mol Cell Biol *14*, 416-429.

Chen, M., Reed, R.R., and Lane, A.P. (2017). Acute inflammation regulates neuroregeneration through the NF-kappaB pathway in olfactory epithelium. Proc Natl Acad Sci U S A *114*, 8089-8094.

Chen, M., Reed, R.R., and Lane, A.P. (2019). Chronic Inflammation Directs an Olfactory Stem Cell Functional Switch from Neuroregeneration to Immune Defense. Cell Stem Cell *25*, 501-513 e505.

Chung, M.I., Bujnis, M., Barkauskas, C.E., Kobayashi, Y., and Hogan, B.L.M. (2018). Niche-mediated BMP/SMAD signaling regulates lung alveolar stem cell proliferation and differentiation. Development *145*.

Delorme, B., Nivet, E., Gaillard, J., Haupl, T., Ringe, J., Deveze, A., Magnan, J., Sohier, J., Khrestchatisky, M., Roman, F.S., et al. (2010). The human nose harbors a niche of olfactory ectomesenchymal stem cells displaying neurogenic and osteogenic properties. Stem Cells Dev *19*, 853-866.

Echelard, Y., Epstein, D.J., St-Jacques, B., Shen, L., Mohler, J., McMahon, J.A., and McMahon, A.P. (1993). Sonic hedgehog, a member of a family of putative signaling molecules, is implicated in the regulation of CNS polarity. Cell *75*, 1417-1430.

Ermilov, A.N., Kumari, A., Li, L., Joiner, A.M., Grachtchouk, M.A., Allen, B.L., Dlugosz, A.A., and Mistretta, C.M. (2016). Maintenance of Taste Organs Is Strictly Dependent on Epithelial Hedgehog/GLI Signaling. PLoS Genet *12*, e1006442.

Field, P., Li, Y., and Raisman, G. (2003). Ensheathment of the olfactory nerves in the adult rat. J Neurocytol *32*, 317-324.

Gong, Q., Chen, H., and Farbman, A.I. (2009). Olfactory sensory axon growth and branching is influenced by sonic hedgehog. Dev Dyn *238*, 1768-1776.

Graziadei, P.P. (1973). Cell dynamics in the olfactory mucosa. Tissue Cell *5*, 113-131.

Graziadei, P.P., and Graziadei, G.A. (1979). Neurogenesis and neuron regeneration in the olfactory system of mammals. I. Morphological aspects of differentiation and structural organization of the olfactory sensory neurons. J Neurocytol *8*, 1-18.

Harfe, B.D., Scherz, P.J., Nissim, S., Tian, H., McMahon, A.P., and Tabin, C.J. (2004). Evidence for an expansion-based temporal Shh gradient in specifying vertebrate digit identities. Cell *118*, 517-528.

Herrick, D.B., Guo, Z., Jang, W., Schnittke, N., and Schwob, J.E. (2018). Canonical Notch Signaling Directs the Fate of Differentiating Neurocompetent Progenitors in the Mammalian Olfactory Epithelium. J Neurosci *38*, 5022-5037.

Herrick, D.B., Lin, B., Peterson, J., Schnittke, N., and Schwob, J.E. (2017). Notch1 maintains dormancy of olfactory horizontal basal cells, a reserve neural stem cell. Proc Natl Acad Sci U S A *114*, E5589-E5598.

Holl, A.M. (2018). Survival of mature mouse olfactory sensory neurons labeled genetically perinatally. Mol Cell Neurosci *88*, 258-269.

Imamura, F., and Hasegawa-Ishii, S. (2016). Environmental Toxicants-Induced Immune Responses in the Olfactory Mucosa. Front Immunol *7*, 475.

Kern, R.C. (2000). Chronic sinusitis and anosmia: pathologic changes in the olfactory mucosa. Laryngoscope *110*, 1071-1077.

Kong, J.H., Yang, L., Dessaud, E., Chuang, K., Moore, D.M., Rohatgi, R., Briscoe, J., and Novitch, B.G. (2015). Notch activity modulates the responsiveness of neural progenitors to sonic hedgehog signaling. Dev Cell *33*, 373-387.

Kumari, A., Ermilov, A.N., Allen, B.L., Bradley, R.M., Dlugosz, A.A., and Mistretta, C.M. (2015). Hedgehog pathway blockade with the cancer drug LDE225 disrupts taste organs and taste sensation. J Neurophysiol *113*, 1034-1040.

Kumari, A., Ermilov, A.N., Grachtchouk, M., Dlugosz, A.A., Allen, B.L., Bradley, R.M., and Mistretta, C.M. (2017). Recovery of taste organs and sensory function after severe loss from Hedgehog/Smoothened inhibition with cancer drug sonidegib. Proc Natl Acad Sci U S A *114*, E10369-E10378.

Miura, H., and Barlow, L.A. (2010). Taste bud regeneration and the search for taste progenitor cells. Arch Ital Biol *148*, 107-118.

Mirsky, R., Parmantier, E., McMahon, A.P., and Jessen, K.R. (1999). Schwann Cell-Derived Desert Hedgehog Signals Nerve Sheath Formation. Ann N Y Acad Sci *883*, 196-202.

Pan, S., Wu, X., Jiang, J., Gao, W., Wan, Y., Cheng, D., Han, D., Liu, J., Englund, N.P., Wang, Y., et al. (2010). Discovery of NVP-LDE225, a Potent and Selective Smoothened Antagonist. ACS Med Chem Lett *1*, 130-134.

Parmantier, E., Lynn, B., Lawson, D., Turmaine, M., Namini, S.S., Chakrabarti, L., McMahon, A.P., Jessen, K.R., and Mirsky, R. (1999). Schwann cell-derived Desert hedgehog controls the development of peripheral nerve sheaths. Neuron *23*, 713-724.

Rui, K., Zhang, Z., Tian, J., Lin, X., Wang, X., Ma, J., Tang, X., Xu, H., Lu, L., and Wang, S. (2016). Olfactory ecto-mesenchymal stem cells possess immunoregulatory function and suppress autoimmune arthritis. Cell Mol Immunol *13*, 401-408.

Scales, M.K., Velez-Delgado, A., Steele, N.G., Schrader, H.E., Stabnick, A.M., Yan, W., Mercado Soto, N.M., Nwosu, Z.C., Johnson, C., Zhang, Y., et al. (2022). Combinatorial Gli activity directs immune infiltration and tumor growth in pancreatic cancer. PLoS Genet *18*, e1010315.

Schwob, J.E., Szumowski, K.E., and Stasky, A.A. (1992). Olfactory sensory neurons are trophically dependent on the olfactory bulb for their prolonged survival. J Neurosci *12*, 3896-3919.

Schwob, J.E., Jang, W., Holbrook, E.H., Lin, B., Herrick, D.B., Peterson, J.N., and Hewitt Coleman, J. (2017). Stem and progenitor cells of the mammalian olfactory epithelium: Taking poietic license. J Comp Neurol *525*, 1034-1054.

Scott, J.W., and Scott-Johnson, P.E. (2002). The electroolfactogram: a review of its history and uses. Microsc Res Tech *58*, 152-160.

Spence, C. (2015). Just how much of what we taste derives from the sense of smell? Flavour *4*, 30.

St-Jacques, B., Hammerschmidt, M., and McMahon, A.P. (1999). Indian hedgehog signaling regulates proliferation and differentiation of chondrocytes and is essential for bone formation. Genes Dev *13*, 2072-2086.

Stott, W.T., Dryzga, M.D., and Ramsey, J.C. (1983). Blood-flow distribution in the mouse. J Appl Toxicol *3*, 310-312.

Uhmann, A., Dittmann, K., Nitzki, F., Dressel, R., Koleva, M., Frommhold, A., Zibat, A., Binder, C., Adham, I., Nitsche, M., et al. (2007). The Hedgehog receptor Patched controls lymphoid lineage commitment. Blood *110*, 1814-1823.

Wang, B.Y., Gil, J., Kaufman, D., Gan, L., Kohtz, D.S., and Burstein, D.E. (2002). P63 in pulmonary epithelium, pulmonary squamous neoplasms, and other pulmonary tumors. Hum Pathol *33*, 921-926.